ECONOMICS OF ENVIRONMENTAL AND PUBLIC HEALTH POLICIES

by

SHAN ZHANG

A DISSERTATION

Presented to the Department of Economics
and the Division of Graduate Studies of the University of Oregon
in partial fulfillment of the requirements
for the degree of
Doctor of Philosophy

June 2023

DISSERTATION APPROVAL PAGE

Student: Shan Zhang

Title: Economics of Recycling and Public Health Policies

This dissertation has been accepted and approved in partial fulfillment of the requirements for the Doctor of Philosophy degree in the Department of Economics by:

Eric Zou	Chair
Trudy Ann Cameron	Core Member
Grant McDermott	Core Member
Kory Russel	Institutional Representative

and

Krista Chronister	Vice Provost for Graduate Studies

Original approval signatures are on file with the University of Oregon Division of Graduate Studies.

Degree awarded June 2023

DISSERTATION ABSTRACT

Shan Zhang

Doctor of Philosophy

Department of Economics

June 2023

Title: Economics of Recycling and Public Health Policies

This dissertation is comprised of three papers that investigate the effects of recycling policy, pollution, and public health policy. The first paper examines the impact of China's waste import ban on U.S. polltion emissions at the national and state level. The second paper studies the distributional effect of China's waste import policy on waste transfers across local communities in California. The third paper investigates people's willingness to pay for public health policies to protect the health of a community during the COVID-19 pandemic. Chapter 1 provides a comprehensive overview of each dissertation chapter.

Chapter 2 analyzes the effect of China's Green Sword policy (waste import ban) on U.S. emissions at the national and state level. Using the synthetic control method, the study finds that many states experienced significant increases in methane emissions after the policy took effect, with the total U.S. methane emissions from the waste industry increasing by 10%. The study also finds a positive correlation between the waste trade each state had with China before the ban and the increase in emissions after the policy, suggesting that the states that relied more on trading recyclable wastes with China were more affected by the policy.

Chapter 3 examines the effects of the Green Sword policy on the relocation of solid waste pollution across local communities in California. Using detailed waste transfer data from California, the study finds that Black communities received more waste transfers before the policy, but after the policy, relatively more waste pollution relocated to lower-income White communities. The study identifies land costs as the primary explanation for this distributional effect.

Chapter 4 (co-authored with Trudy Ann Cameron) utilizes a choice-experiment survey of U.S. residents to determine people's willingness to pay for public policies to reduce illnesses and premature deaths in their communities. The study estimates people's ex-ante willingness to pay to avoid the actual monthly totals of COVID-19 cases and deaths from March 2020 to April 2021 by county and month. The estimated aggregate willingness to pay across the U.S. adult population during this period is about 3 trillion dollars.

CURRICULUM VITAE

NAME OF AUTHOR: Shan Zhang

GRADUATE AND UNDERGRADUATE SCHOOLS ATTENDED:

     University of Oregon, Eugene, OR, USA
     University of Florida, Gainesville, FL, USA
     Dalian Nationalities University, Dalian, Liaoning, China

DEGREES AWARDED:

     Doctor of Philosophy, Economics, 2023, University of Oregon
     Master of Business, International Business, 2018, University of Florida
     Bachelor of Science, Economics, 2015, Dalian Nationalities University

AREAS OF SPECIAL INTEREST:

     Environmental Economics
     Health Economics

PROFESSIONAL EXPERIENCE:

     Economic Consultant, World Bank, 2023
     Research Economist, Resources for the Future, 2022
     Research Assistant to Dr. Scott Kostyshak, University of Florida, 2017

GRANTS, AWARDS AND HONORS:

     Graduate Teaching Award, University of Oregon, 2022
     Gary E. Smith Professional Development Award, University of Oregon, 2022
     Kleinsorge Summer Research Award, University of Oregon, 2022
     Sloan Summer School Diversity Fellowship, UC Berkeley, 2021
     Kleinsorge Summer Research Award, University of Oregon, 2021
     Qualification Exam Scholarship Award, University of Oregon, 2019

ACKNOWLEDGEMENTS

I wish to extend my deepest appreciation to my committee chair—Eric Zou, and Trudy Cameron, who have consistently offered their unwavering support and invaluable guidance during my journey through graduate school. I am also indebted to Grant McDermott and Kory Russel, whose insightful feedback has significantly contributed to different sections of this dissertation. I must also express my heartfelt gratitude to my family and friends for their limitless support. Above all, my husband, Ryan Buttacavoli, deserves my special thanks for his relentless encouragement and support.

For my parents, who inspired and taught me the value of education, and my future children, to whom I hope to impart the same knowledge.

TABLE OF CONTENTS

LIST OF FIGURES

LIST OF TABLES

CHAPTER I

INTRODUCTION

The goal of my dissertation is to shed light on important policy questions related to recycling and their impact on emissions and pollution transfer, as well as people's willingness to pay for public health measures. This study examines heterogeneity in responses to a set of environmental and health policies, utilizing various methods including machine learning, spatial analysis, and causal inference analysis. Chapters 2 and 3 are the author's original work, while Chapter 4 is a collaborative effort with Trudy Ann Cameron.

Chapter 2 of this study examines the impact of China's waste import ban on U.S. pollution at both the national and state levels. To estimate the policy's effects on emissions from the waste industry in specific states, the study uses the U.S. EPA Greenhouse Gas Reporting Program (GHGRP), which records annual methane emissions at the facility level for all industries. Emissions from other industries that emit methane, but are not affected by the waste import ban, are used as controls in the identification strategy. For instance, emissions from the waste industry in California are used as the treatment, while emissions from other non-waste industries, such as oil and gas, mining, and refining industries, from California and all other states are used as the control group. The synthetic control method is applied to all states in the U.S. resulting in a map showing the various changes in emissions across states. The study finds that larger states, in particular, experience a greater increase in emissions following China's waste ban. To validate state-specific estimates, the study examines exposure, which refers to the amount of waste trade a state has had with China historically. The results indicate that states

more exposed to China's policy shock tend to experience larger pollution increases, on average, after the shock.

In addition to the synthetic control method, the study employs a second method, the Bartik instrument. In this part of analysis, waste export data from sources like USA Trade Online and UN Comtrade are utilized. The method instruments for the current shocks in waste exports by using historical state-level export shares multiplied by the national shock component. The study estimates that for every metric ton of waste exported, domestic methane emissions from the waste industry decrease by 0.89 metric tons. Overall, after the implementation of China's waste ban, there was a reduction of 12 million metric tons in U.S. waste exports to China. Consequently, the U.S. methane emissions is estimated to experienced an increase of 11 million metric tons.

In Chapter 3, I move beyond state-level analysis to examine the distributional effects of China's waste import ban on local communities. I investigate which communities were previously receiving more waste treatment and how the policy impacted them. With the ban in place, more recyclable waste remains in the U.S., but which communities are now bearing greater pollution costs due to the policy? Specifically, I examine which facilities are handling more waste treatment and their proximity to White and Black communities. To achieve this, I collect detailed demographic and socioeconomic data at the census block level, as well as California waste transfer records. These data allow me to construct a fixed-effects model and identify which communities are most affected by the policy. Before the policy, I replicate the standard result that minority communities were more likely to receive waste transfers from outside, which is consistent with much of the existing Environmental Justice literature. However, after the policy, I find

that White communities experience a relatively greater increase in waste flows compared to Black communities, which is a novel finding. The racial gap in waste transfers narrowed after China's policy shock. To understand what is driving this narrowing of the gap, I propose three mechanisms: land costs, transportation costs, and political costs. I proxy for land costs and transportation costs using population density and distance, and use the degree of polarization in political views between a community and its county as a proxy for the political costs of the destination communities. I find that, prior to the waste import ban, transportation costs and political costs were the primary drivers of waste transfers across communities. However, after the policy shock, low land costs of a community became a significant determinant of the communities to which the waste was relocated to.

In Chapter 4, my co-author Trudy Cameron and I utilize a 2003 general-population choice-experiment survey of U.S. residents to assess people's willingness to pay for public policies that aim to reduce illnesses and avoid premature deaths in their communities. We refine earlier models by excluding all respondent-specific individual characteristics and incorporating county-level data on various contextual variables from 2003. We then adapt our re-estimated model to the 2020-21 COVID-19 pandemic, using updated contextual variables such as household incomes and unemployment rates. We compute the model's implied values of ex-ante willingness to pay (WTP) to prevent the actual monthly numbers of cases and deaths from March 2020 to April 2021, by county and month, across the contiguous U.S. Our estimated total WTP by the U.S. adult population during this period is approximately 3 trillion dollars, although these estimates are conservative as the original choice scenarios did not involve infectious illnesses or pandemics. Our analysis indicates that people from counties with a higher proportion of working

3

adults and Black residents tend to have a greater WTP for public health policies that mitigate the risks of illness and death. Individuals from counties with higher incomes and better health access also tend to exhibit higher WTP. If preferences for public health programs remain relatively stable over time, our findings may be useful for predicting contemporary WTP for public health measures, both retrospectively for the current pandemic and prospectively for future pandemics.

CHAPTER II

THE IMPACT OF CHINA'S WASTE IMPORT BAN ON POLLUTION

EMISSIONS IN THE UNITED STATES

2.1 Introduction

As of 2016, half of the world's scrap intended for recycling was traded internationally, with more than one billion metric tons of waste transferred from developed to developing countries over the prior two decades.[1] China has been the largest recipient of this waste, accounting for 45% of the world's total since 1992, and 70% when including Hong Kong, which returned to Chinese sovereignty in 1997. This pattern has enabled China's factories to access inexpensive materials and has thus supported its emerging economy, but recycling has resulted in increased pollution from energy-intensive processes and contaminated imported wastes (Kellenberg, 2012; Kellenberg, 2015; Higashida & Managi, 2014; Gregson & Crang, 2015; Lee, Wei, & Xu, 2020).

In 2017, China enacted its "Green Sword" (GS) policy, which prohibited the import of most plastics, papers, and other materials for recycling processors, effectively shutting down the world's largest market for recyclable waste. According to the Institute of Scrap Recycling Industries, as of October 2019, U.S. scrap exports of plastic to mainland China had decreased by 89% since early 2017, while mixed paper exports had fallen by 96%. The Chinese government implemented this policy to address local environmental concerns such as air and water pollution, as well as to safeguard public health. Studies have shown that since the policy's implementation, Chinese cities connected to waste importation and reprocessing

---

[1]Statistics according to the UN Comtrade data

have significantly improved their air quality (J. Li & Takeuchi, 2021; Unfried & Wang, 2022).

China's GS policy has significantly affected the recycling industry in the United States, formerly the leading exporter of recyclable waste to China.[2] After China implemented the waste ban, several lower-income countries in Southeast Asia, despite having a lack of the necessary infrastructure to handle recyclables correctly, have attempted to take on some of the load. However, these countries were quickly overwhelmed by the volume of waste and most have since enforced their own limitations on paper or plastic imports.[3] Thus far, no single nation has completely replaced China as the world's primary market for recyclable waste. Consequently, the United States had to confront its own waste issues, uncovering fundamental flaws in its domestic recycling procedures. The escalating costs of transporting recyclable materials have rendered the practice unprofitable, causing an increase in the quantities of plastics and paper waste that end up in landfills and incinerators, polluting the environment.

This paper quantitatively studies the impact of China's waste import ban on the quantity and distribution of methane emissions from the waste industry, particularly landfill facilities, in the United States. I provide empirical evidence necessary to answer the following questions: (1) How has the GS policy affected domestic methane emissions at the national level in the U.S.? (2) How do changes in methane emissions relate to recyclable waste exports at the state level in the U.S.?

---

[2]In 2016, China imported about 17 billion tons of recyclable waste from the U.S., which made up 72.9% of the total U.S. waste exported.

[3]For example, in May 2018, Indonesia required 100 percent inspection of scrap paper and plastic imports. In March 2019, India announced a ban on scrap plastic imports.

The paper uses the EPA Greenhouse Gas Reporting Program to study the causal effect of China's GS policy on U.S. domestic methane emissions. The synthetic control method is used to estimate the effect of the waste ban on methane emissions from the waste industry in each state of the U.S. The study finds that 11 states, particularly larger states, have experienced a statistically significant increase in methane emissions from their waste industry after the waste ban, with California seeing a 9% increase in methane emissions. Aggregating the changes in methane emissions from all states, the study finds that the overall U.S. methane emissions from the waste industry increased by almost 10 million metric tons of CO_2 equivalent (mmt CO_2 eq.), accounting for 10% of total U.S. methane emissions from the waste industry in 2016.[4] The study also finds that the more waste a state exported before China's waste ban, the greater the impact of the waste ban on the state's methane emissions.

In the second part of my analysis, I delve deeper into the connection between U.S. emissions and exports of recyclable waste. If states with a history of high waste exports experienced a greater increase in methane emissions after the GS policy, then exports of recyclable waste must have been reducing emissions successfully in those states prior to the policy's implementation. For this analysis, I use data on recyclable waste exports by state and year from *U.S.A. Trade Online*, as well as methane emissions data from the waste industry by state and year from the *U.S. EPA Greenhouse Gas Inventory*. To estimate the causal relationship between exports and emissions, I must account for the fact that U.S. waste exports are endogenous to U.S. economic activities and emissions. To address this issue, I employ a Bartik shift-share instrumental variable. This instrument

---

[4]This number is calculated by aggregating the changes in emissions of all states whose synthetic control estimates can be judged to be statistically significant.

starts with the initial-year shares of recyclable waste exports by state and shifts these over time using annual aggregated recyclable waste exports from the U.S. to China. The underlying assumption is that the initial-year shares of recyclable waste exports by state are not related to future waste exports from the U.S. to China. As a result, recyclable waste exports weighted by the initial-year state - level shares are exogenous to future emissions and economic activities. Using this method, I discover that prior to China's GS policy, for each additional metric ton of recyclable waste exported, U.S. domestic emissions were lower by 0.83 metric tons of CO_2 eq. This finding supports the hypothesis that U.S. recyclable waste exports directly reduced domestic emissions from the waste industry. After China's GS policy was enacted, U.S. exports of recyclable waste to China declined by 12 million metric tons, accompanied by a corresponding increase of approximately 11 million metric tons of CO_2 eq. in methane emissions from the U.S. waste industry. This figure is comparable to the result obtained using the synthetic control method, thus cross-validating my findings from the two different approaches.

My research makes several significant contributions. Firstly, mine is the first study to investigate quantitatively the effects of China's groundbreaking GS policy on U.S. environmental quality at the national and state levels. The recycling sector is an essential but under-researched area in environmental economics, and China's GS policy, as a significant shock in this context, has received relatively little attention. Previously, most research focused on the efficiency of recycling programs in developed countries and their impact on social welfare, revealing low efficiency and low social welfare (Aadland & Caplan, 2006; Bohm, Folz, Kinnaman, & Podolsky, 2010; Kinnaman, 2014; Kinnaman, Shinkuma, & Yamamoto, 2014). In contrast, my research demonstrates that under China's exogenous policy shock,

recycling in the U.S. not only has low efficiency but also negatively and unevenly affects the domestic environment.

Second, my paper is the first to study the causal relationship between trade volume and emissions in the context of a high-pollution industry, the recycling industry, and a specific trade policy change. In recent years, more papers have begun to focus on the relationship between international trade policies and emissions (J. S. Shapiro, 2016; R. Shapiro Joseph S.and Walker, 2018). Copeland, Shapiro, and Taylor (2021) show that nearly one-fourth to one-third of global pollution emissions stem from industrial processes related to international trade. With increasing exposure to trade, dirty industries in rich countries tend to relocate their production to developing countries with more-lenient environmental policies. Many international trade policies, such as tariffs, have tended to impose more costs on "clean" industries than on industries with pollution (J. S. Shapiro, 2021). My research also sheds light on the pollution haven hypothesis, which posits that developed countries tend to relocate their pollution elsewhere through trade, typically to developing countries. Before China's GS policy, my research indicates that recyclable waste exports directly reduced domestic emissions in the U.S., supporting this hypothesis. My findings thus differ from those in the previous trade and environment literature, which has focused mainly on the impact of trade policies on general industries versus polluting industries.

My research demonstrates that many states in the U.S. are impacted to varying degrees by international environmental policy changes. Therefore, my research findings have important implications for domestic recycling policies. Given the rapidly changing international markets, these policies must be regularly updated. Ignoring the international context for domestic recycling policies is no

longer an option. Notably, recent legislative developments, such as the RECYCLE Act of 2021, the Recycling Infrastructure and Accessibility Act of 2022, the Plastic Waste Reduction and Recycling Research Act, and the $350 million solid waste and recycling grant from the Infrastructure Bill 2021 passed by the U.S. EPA, indicate that recycling is receiving greater attention at the national level.[5]

The rest of this chpater is organized as follows. Section 2 provides a brief background concerning international trade in recyclable waste and methane emissions in the United States and outlines my data sources. Section 3 identifies the impact of China's GS policy on domestic emissions in the U.S. Section 4 concludes with a few caveats and suggestions for future research.

2.2   Background and Data

2.2.1   Background.

Methane Emissions from Recyclables.   According to the U.S. EPA, methane emissions from landfills rank as the third largest source of human-related methane emissions in the U.S. Anaerobic decomposition of organic food, wood, and paper scraps are the primary sources of methane emissions from landfills. The GS policy affects the most-recycled products and materials in the U.S., particularly "mixed paper and paperboard" and plastic scrap, which account for 85 percent and 14 percent of total recyclable waste exports from the U.S., respectively before 2017.

---

[5]While recycling regulations are typically enforced by states or counties, various recycling bills are currently being proposed by legislators across different states. These bills may propose conflicting regulations due to the diverse needs and circumstances of each state. Some bills suggest creating grant programs to educate people on recycling and improve recycling accessibility in communities, while others propose expanding producer responsibility for material use and reducing existing residential recycling programs.

After the GS policy, most of these recyclable paper products end up in landfills, contributing to methane emissions.[6]

Aside from emissions and pollution from the degradation of recyclable materials themselves, organic food residues on recyclables can also contribute to methane emissions from landfills. Before China's GS policy, recyclable materials were separated and cleaned for export, resulting in less associated food waste contamination. However, after the GS policy, these recyclable materials are often merely thrown into the trash without being cleaned, likely contributing to an increase in landfill methane emissions.

I choose methane emissions as the main environmental outcome in this paper due to a number of reasons. First, methane emissions have been the most consistently recorded emissions at U.S. waste industry facilities by the U.S. EPA over time.[7] This makes it the most suitable choice for the empirical design of this paper. I employ methane emissions as an indicator for overall pollution emissions originating from the waste industry.[8] Second, as a greenhouse gas, methane is 85 times more potent than carbon dioxide in trapping heat, and it stays in the atmosphere for a shorter period of time than carbon dioxide. Thus, curbing methane emissions will have a more immediate impact on reducing global warming in the near future. U.S. Regulators are beginning to acknowledge the significance of reducing methane emissions as the EPA is currently reassessing its regulations

---

[6]Royer, Ferron, Wilson, and Karl (2018) find that the degradation of plastic in landfills can also emit methane, and the longer it remains, the more methane it emits.

[7]Due to inadequate oversight, methane emissions are the only emissions that the waste industry regularly monitors. Furthermore, local pollutant monitoring around landfill facilities is lacking when compared to other types of plants.

[8]It is understood that an increase in waste treatment activities at a facility results in a proportional rise in general pollution emissions, which consequently leads to greater methane emissions.

on methane pollution in the oil and gas industry under the Clean Air Act (CAA).[9] At some point, regulations concerning landfills, which constitute the third-biggest source of methane pollution, will need to be reassessed. Third, methane emissions can serve as a proxy for other types of pollution caused by recyclable wastes, such as soil and water pollution, as well as air pollution. These types of pollution are generally difficult to track around landfills, but they often co-occur with wastes that generate methane emissions. In the case of air pollution, although methane and carbon dioxide make up 90 to 98% of total landfill gases, the remaining 2 to 10% of other gases from potentially recyclable wastes include volatile organic compounds (VOCs), nitrogen, oxygen, ammonia, hydrogen sulfides, and surface ozone for which even small amounts can affect the health of people living nearby (Abernethy, O'Connor, Jones, & Jackson, 2021).[10]

It is noteworthy that methane emissions from landfills can be captured, converted, and utilized as a source of energy for electricity, renewable natural gas, and direct use. Nevertheless, according to the Landfill Methane Outreach Program (LMOP) National Map, only around 20 percent of all landfill facilities in the United States have implemented landfill gas (LFG) energy projects as of 2022.

China's Green Sword Policy. China's Green Sword Policy was implemented in response to a significant increase in U.S. recyclable waste exports to China within a decade of China joining the WTO in 2001. The increase was due to several factors, including China serving as an international pollution haven, China's economic growth and expanding manufacturing industry, and excess capacity

---

[9]https://www.epa.gov/newsreleases/us-sharply-cut-methane-pollution-threatens-climate-and-public-health

[10]Abernethy et al. (2021) shows that methane removal can reduce surface ozone, a local pollutant, and temperature.

on ships returning to China from the U.S. (Kellenberg, 2012; Kellenberg, 2015; Bransetter & Lardy, 2006; Brandt, Biesebroeck, & Zhang, 2012; Higashida & Managi, 2014; Palma, Lindsey, Quinet, & Vickerman, 2011; Olivia, 2014) As China's policies concerning environmental quality, regulation, and pollution evolved between 2010 and 2019, the government introduced the Green Fence (GF) policy in 2013, which had minimal effects on the total quantity of recyclable wastes being imported (Greenstone, He, Li, & Zou, 2021).[11] In 2017, however the much more stringent Green Sword (GS) policy was launched, which imposed much stricter contamination limits and banned many types of recyclables.[12] This policy caused a significant decrease in U.S. exports of all affected recyclable materials to China, but a significant increase in U.S. waste exports to other developing countries in South and Southeast Asia. In response, many South and Southeast Asian countries enacted similar stringent policies to restrict waste inflows and control illegal processing facilities. Additionally, in 2019, the Basel Convention (to which the U.S. is not a party) was revised to limit the cross-border transfer of plastic waste from developed nations to developing nations, and this agreement has been signed by 192 countries. Consequently, markets for U.S. recyclable wastes are much more limited than in the past.[13]

---

[11]The Green Fence policy imposed strict quality standards on imported recyclable materials, rejecting shipments that were contaminated or mixed with non-recyclable waste.

[12]According to the WTO Committee on Technical Barriers to Trade Notification, China forbade the importation of 24 kinds of solid waste, including plastic waste, vanadium slag, unsorted paper, cotton, and textile materials.

[13]Due to the GS policy, mixed paper and paperboard exports dropped from 15.1 billion tons in 2016 to just 5.4 billion tons in 2019 (a 64.24% decrease). Plastic scrap exports dropped from 2.89 billion tons in 2016 to 0.18 billion tons in 2019 (a 93.8% decrease). Other exports of recyclable wastes, such as cotton waste, man-made fibers, and textiles, decreased by 96.4%, 69.8%, and 99.5%, respectively.

2.2.2 Data.

Trade Data.   The data I utilize for trade in recyclable materials trade comes
from *U.S.A. Trade Online* and covers the period from 2002 to 2020. This dataset
provides annual information on the source state, destination countries, weight, and
value of exports for commodities categorized by HS4 and HS6 codes.[14] Total export
weight is calculated by aggregating vessel and air weights. I limit my analysis to
scrap commodities at both HS4 and HS6 levels that have been directly affected by
China's waste ban. Additionally, I use trade data from *U.N. Comtrade* for country-
level exports of recyclable waste. To examine trade in recyclable waste between
China and other countries besides the U.S., I gather data for 11 countries that have
regularly traded in substantial quantities of recyclable waste materials.

Emissions Data.   To examine the correlation between trade in recyclable
wastes and pollution emissions, I rely on data from the *EPA Inventory of U.S.*
Greenhouse Gas Emissions and Sinks. The data covers state-level greenhouse
gas (GHG) emissions from the waste industry annually from 2002 to 2020. It is
important to note that the dataset estimates state-level emissions prior to 2010
by using national-level emissions weighted by the proportion of waste sent to
landfills by each state. For the years 1990-2009, the methodology utilized the state
percentage of waste going to landfills reported by landfills under subpart H.H. of
the Greenhouse Gas Reporting Program (GHGRP) to calculate national methane
(CH_4) emissions estimates. However, the U.S. EPA improved the accuracy of state-
level methane emission calculations after 2010 by aggregating emissions reported

---

[14]HS codes are standard industry classifications used for goods exports, and HS6 codes are more
detailed than HS4 codes with six and four digits, respectively.

by individual waste industry facilities. To account for this measurement change, all estimating specifications include time fixed effects.

To examine the relationship between trade in recyclable waste and pollution emissions in more detail, I utilized methane emissions data from individual landfill facilities reported under the *U.S. EPA Greenhouse Gas Reporting Program (GHGRP)* from 2010 to 2020. This program requires large greenhouse gas emission sources, fuel and industrial gas suppliers, and CO_2 injection sites in the United States to report their greenhouse gas data annually. The GHGRP includes various industries, such as power plants, petroleum and natural gas systems, minerals, chemicals, pulp and paper, refineries, and, crucially for my analysis, the waste industry. Approximately 8,000 facilities are required to report their emissions each year, and the GHGRP has a high compliance rate due to the absence of a quantity-based penalty for emissions from landfill owners, and because non-compliant owners are issued warning notices by the U.S. EPA. Appendix Figure A3 displays the distribution of landfill facilities in the U.S. according to the EPA GHGRP. In my analysis of statistical identification, I also used data from various other industries in the GHGRP dataset, not including the waste industry, as control industries.

In this paper, Table 1 presents a concise overview of all the data sources used. The primary datasets constructed for the three main analyses are as follows: (1) annual state-level panel data from 2010 to 2020 for U.S. GHG emissions by industry; (2) annual state-level panel data from 2002 to 2020 for GHG emissions from the waste industry and recyclable exports.[15]

---

[15]Both export and emission data are at the state level since there is no smaller geographic unit for exports that can be easily matched to emissions. Although export data exist at the departure-port level, it is challenging to track whether the waste arriving at each port originates from within the state or other states, making it difficult to establish a correlation between port-level exports and local emissions.

2.2.3 Summary Statistics. The summary statistics for the export of recyclable waste by the U.S. and other major waste-exporting countries are presented in Table 2. In panel A, columns 1 and 2 display the total *value* of U.S. recyclable waste exports to China and the rest of the world between 2010 and 2020, while columns 3 and 4 show the corresponding values for 11 other countries that regularly trade recyclable waste with China, including Australia, Austria, Canada, France, Germany, Portugal, New Zealand, the United Kingdom, Japan, Spain, and Finland. Panel B shows the total *weight* of recyclable waste exports from the U.S., and from these 11 other countries, to China and to the rest of the world.

Before 2017, U.S. recyclable waste exports to China accounted for over half of the total value of U.S. recyclable waste exports to non-U.S. countries, and over 70% of total U.S. recyclable waste exports by weight. However, following China's 2017 waste ban, U.S. recyclable waste exports to China decreased significantly, while exports to the rest of the world initially increased but then eventually decreased as well.

Further information about the data can be found in Appendix Tables A.1 through A.8. Appendix Table A1 provides more detailed information about the composition of recyclable waste exports by value and weight, showing that from 2002 to 2020, the U.S. exported mixed paper/paperboard and plastic scrap with a total value of 31,521 million USD and 15,464 million USD, which account for 66% and 32% of the total value of recyclable waste exports. The next most-exported recyclables, in order, were metal, fibers, cotton, iron/steel, and wool scrap.

Details regarding the composition of greenhouse gas (GHG) emissions by industry in the U.S. can be found in Appendix Table A2. The waste, metal, and refinery industries primarily emit methane (CH_4) as their main GHG, while the

power plants, minerals, chemicals, and petroleum and natural gas industries emit more carbon dioxide (CO_2) than methane. The pulp and paper industry emits approximately equal amounts of methane and carbon dioxide, while nitrogen dioxide (NO_2) emissions are relatively low across all industries, at least in comparison to methane and CO_2 emissions.

Appendix Table A3 displays changes in the overall emissions levels for the waste industry over the years, as well as the varying numbers of facilities from 2010 to 2020. The dataset used excludes small facilities, focusing only on large emitters in the EPA GHGRP. While total GHG emissions from the waste industry have increased after 2017, the total number of facilities has gradually decreased, indicating that the average emissions per facility have risen over time. On the other hand, other industries such as power plants, metals, pulp and paper, and refineries have experienced a reduction in their GHG emissions between 2010 and 2019. Appendix Table A4 documents the overall GHG emissions from various industries in the U.S., with a focus on the nine main industries out of the 72 sectors listed in the GHGRP. This data reveals that the waste industry's emissions have increased both in total and on average after China's GS policy.

2.3 The impact of China's GS policy on Emissions in the U.S.

2.3.1 Raw Trends.

Export Trends. Figure 1 displays the trends in exports of recyclable waste from the U.S. to China and the rest of the world. After China's accession to the WTO in 2001, the value of recyclable waste exports to China increased and remained stable between 2013 and 2016. However, when China introduced its GS policy in 2017, the value of these exports plummeted. Meanwhile, the value of exports to the rest of the world remained stable from 2002 to 2016, but increased

temporarily after the waste ban diverted China's former recyclable waste inflows to other countries. Nevertheless, this increase was short-lived due to similar policy changes in those other countries. The trend in the net weight of recyclable waste exports shows an even more significant and direct impact of China's GS policy on U.S. exports to China and the rest of the world after 2017. These trends demonstrate that the waste ban has decreased recyclable waste exports from the U.S. to China and has temporarily increased exports to the rest of the world. However, this increase lasted for only a year, and thus many recyclable wastes that were previously exported overseas are now being processed within the U.S.

Figure 2 illustrates the composition of total recyclable waste exports from the U.S. Paper/paperboard and plastic scrap are the most-exported materials, accounting for about 76% and 22% of total exports by value, respectively, and 90% and 10% of total exports by weight, respectively. Figure 3 displays the trends in relative values of plastic scrap exports from the U.S. and six other OECD countries—Canada, France, Germany, Japan, the Netherlands, and the United Kingdom—over time. After China's waste ban, exports of plastic scrap to China by the U.S. and the six other OECD countries declined by about 99 percent compared to their 2010 trade values. Nevertheless, the U.S. plastic manufacturing industry's GDP has gradually increased over time. The exports of U.S. plastic scrap to the rest of the world were stable from 2010 to 2016. However, after China's GS policy, these flows increased temporarily but then decreased again. Similar patterns emerged in the plastic scrap exports of the other six OECD countries to the rest of the world.

Emissions Trends.   Trends in total greenhouse gas (GHG) emissions from the U.S. waste industry are displayed in Figure 4 using data from the EPA GHGRP

from 2010 to 2020. Prior to 2017, total GHG emissions from the waste industry had decreased over time. However, after China's GS policy was implemented in 2017, the trend in total GHG emissions from the waste industry reversed and began to increase. Methane emissions account for over 80% of the waste industry's total GHG emissions, followed by carbon dioxide and nitrous oxide. Although total emissions have increased since 2017, the number of waste industry facilities has gradually decreased over the past few decades, indicating that the average emissions per facility have also increased over time.

In Figure 5, the total GHG emissions from the waste industry and several other U.S. manufacturing industries are shown from 2010 to 2020. The raw trends indicate that most industries have seen decreasing GHG emissions over the years, including power plants, metals, pulp and paper, and refineries. However, a few industries, such as chemicals, minerals, and petroleum and natural gas, have seen increasing GHG emissions. Comparing the emissions changes of all industries with the timing of China's waste ban, it appears that the changes in GHG emissions for industries other than the waste industry are not influenced by the waste ban.

2.3.2   State-level Emissions.

Synthetic Control Method.   To identify the effect of China's GS policy on state-level methane emissions in the U.S., I use the synthetic control method. This strategy relies on exogenous variation in methane emissions across all other industries in the EPA GHGRP (such as power plants, petroleum and natural gas systems, minerals, chemicals, refineries, etc.). Appendix Table A2 shows the average emissions from industries across states by type of GHG. This identification strategy takes advantage of the fact that other industries in the GHGRP, which

19

also emit GHGs, were negligibly affected by China's waste ban. To exclude the possibility that the exports of these other industries may have changed in the year of 2017 (when the U.S. started its "trade war" with China) and thus contaminate the control industries for emissions, I plot the exports (by weight/kg) of control industries in Appendix Figure A5. The figure shows that the exports of the control industries, such as oil and gas, minerals, and chemicals, did not discernibly shift as of 2017.[16]

Given that waste industries from all states in the U.S. are affected to varying degrees by China's GS policy, data from the waste industry in other U.S. states (shown in Appendix Figure A4b) cannot be assumed to represent an entirely uncontaminated control pool for the waste industry in any given U.S. state of interest. Appendix Figure A4a plots the time trends for methane emissions from all industries (including the waste industry, in blue) using California as an example. As this figure suggests, simply using the other industries in the same state likewise may not provide a suitable control pool. Thus, I use all other industries from all states to greatly enlarge my control pool. For each U.S. state, separately, I use these other state-level industries as my control pool for the recyclable waste industry in the state in question. For my synthetic control approach, I fit a separate synthetic pre-policy trend that is as close as possible to the actual pre-policy trend for each state's landfill methane emissions (Abadie, Diamond, & Hainmueller, 2012). The "model training" process seeks to minimize the prediction error over the period prior to China's GS policy:

---

[16]Exports by industry can be obtained from the U.S.A Trade Online data by Standard International Trade Classification (SITC) code.

$$Y_{11t}^{\hat{N}} = \sum_{j=2}^{J} \sum_{s=2}^{50} w_{js} Y_{jst} \qquad (2.1)$$

Where $Y_{11t}^{\hat{N}}$ is the emissions from the waste industry for a given state (i.e. the industry "treated" by China's GS policy, indexed as industry $j = 1$) that would have been expected in the absence of China's GS policy, t is the year of these emissions, $j = 2, ..., J$ is a collection of untreated industries not affected by China's GS policy, and $s = 1, ..., 50$ are all states in the U.S.[17] Y_{jst} is observed emissions from the untreated control industries from all states. The synthetic control is defined as a weighted average across state-industry pairs in the "donor pool" of untreated controls. The weights on the emissions of industry j in state s are w_{js}.[18]

I use the trained model based on data for the pre-policy period to predict post-policy-date synthetic emissions in the absence of the GS policy for the waste industry in a given state. The difference between the synthetic post-policy landfill emissions trend and the actual landfill emissions trend, $\hat{\tau}_{1t}$, is the estimated causal effect of China's waste ban on U.S. state-level methane emissions from landfills:

$$\hat{\tau}_{1t} = Y_{11t} - Y_{11t}^{\hat{N}} \qquad (2.2)$$

I use the same process, separately, for the waste industry in each of the 50 U.S. states (excluding Washington DC) and calculate the estimated causal effects of China's GS policy on methane emissions for each state.

Figure 6 displays emissions from 2010 to 2020 from the waste industry for four selected states—California, Virginia, Texas, and New York—compared to

---

[17]Alaska is excluded from this analysis.

[18]For example, in the synthetic control for California, the donor pool includes state-industry pairs such as California oil and gas industry, Indiana mining manufacturing industry, etc.

their synthetic-control counterparts. The synthetic emissions for each state track very closely with the trajectory of actual emissions for the pre-GS policy period. This suggests that the synthetic trend for each state likely provides a reasonable approximation to the amount of methane that would have been emitted in each state from 2018 to 2020 in the absence of China's policy. Figure 7 suggests that China's waste ban has had a discernible effect on methane emissions from the waste industry in these four states, and these effects have increased over time.

Placebo Tests. To evaluate the robustness of my results and calculate effective p-values for my estimates, I run placebo tests by applying the synthetic control method to all state-industry pairs that were not affected by China's GS policy during the sample period of my study. If the placebo study shows that the marked change estimated for California's waste industry, for example, is unusually large relative to the emission changes for other state-industries that were not affected by China's waste ban, then my analysis can be assumed to provide statistically significant evidence that the waste ban causally increased domestic methane emissions from the waste industry in California.

Figure 8 shows my placebo test results for the four example states. The bright blue lines reveal causal estimates of the effects of China's waste ban on methane emissions in California, Virginia, Texas, and New York. The muted grey lines are the analogous causal estimates of the GS policy for other (non-waste) state-industry combinations that can be assumed not to be affected by the GS policy. The plots in Figure 8 show that the synthetic control estimates for the four states are above the 90th percentile of all placebo estimates, which proxies for a test of the statistical significance of the causal estimates for these four states.

I then apply the same placebo-test strategy to all other states in the U.S. Appendix Table A5 shows the causal estimates of China's GS policy on state-level methane emissions and the implied p-values calculated from the placebo tests for each state. Figure 9 shows the causal estimates of the GS policy on GHG emissions from the waste industry by state. States such as Nevada, Montana, Virginia, and New York show statistically significant percentage increases in GHG emissions after China's policy. Figure 9 also shows the net change in state-level emissions from landfills for each state in the U.S. after the GS policy. Larger states, such as California, New York, Texas, and Virginia have seen the largest absolute increases in methane emissions from landfills after the waste ban.

2.3.3 Emission Changes and Waste Export Exposure.

To further explore potential factors that may correlate with the heterogeneous effects of China's GS policy on the U.S., I plot emission changes for each state against both total (historical) recyclable waste exports, and the percentage of paper as a share of waste exports. Autor, Dorn, and Hanson (2013) find that the regions (community zones) which have a higher trade exposure with China in manufacturing industries experienced larger decreases in manufacturing employment in the U.S. from 1995 to 2010. In the present paper, I explore whether a state with higher trade exposure with China, specifically in terms of recyclable wastes, has lower domestic emissions before the GS policy but increased emissions after the GS policy is implemented. Given that mixed paper/paperboard account for more than 80% of exported recyclable wastes and that these materials generate methane in landfills, I also explore whether states with a higher percentage of waste paper exports experience greater increases in methane emissions after the GS policy. Historical recyclable waste exports and the percentage of paper exports

are calculated using annual trade data from *U.S.A. Trade Online.* Figure 10 shows that the increase in emissions due to the waste ban is positively correlated with historical recyclable waste exports. The more of its recyclable wastes a state exported overseas before the GS policy, the greater the increase in emissions it experienced after the GS policy. Given that waste paper/paperboard is the largest contributor to methane emissions from landfills among all recyclable wastes, I also try to link the heterogeneous effects by states with the percentage of recyclable paper/paperboard waste a state exported. However, I find the relatively weak correlation shown in Figure 11. The GS policy had an effect on how much a state exported, and not how much of the export was paper/paperboard.

The next step is to verify statistically the apparent finding that the greater a state's exposure to trade in recyclable wastes with China before the GS policy, the greater the increase in emissions the state experiences after the GS policy. I plot the raw trends of waste exports and domestic emissions from 2002 to 2019. Figure 12 shows that waste exports are negatively correlated with domestic emissions from the waste industry. Before China's waste ban, the more recyclable wastes the U.S. exported, the less methane emitted domestically in the U.S. waste industry. After China's waste ban, waste exports decreased dramatically and domestically methane emissions increased. To identify the general causal effect of recyclable waste exports on domestic emissions from the waste industry, I start with a simple OLS regression in levels as follows:

$$Methane_{it} = \alpha_0 + \alpha t + \beta_0 Export_{it} + \nu_i + \eta_i t + \mu_t + e_{it} \tag{2.3}$$

$Methane_{it}$ is the level of emissions in state i in year t. $Export_{it}$ is the level of recyclable exports from state i to China in year t. I then take the first difference of emissions and exports:

$$\Delta Methane_{it} = Methane_{i,t} - Methane_{i,t-1}$$
$$\Delta Export_{it} = Export_{i,t} - Export_{i,t-1}$$

$$(2.4)$$

After replacing equation (2.4) with equation (2.3), and taking the difference (subtracting the values in the previous year $t-1$ from the values in year t), I get the first difference model:

$$\underbrace{Methane_{i,t} - Methane_{i,t-1}}_{\Delta Methane_{it}} = \underbrace{\alpha_0 - \alpha_0}_{0} + \underbrace{\alpha(t-(t-1))}_{\alpha} + \beta_0 \underbrace{(Export_{i,t} - Export_{i,t-1})}_{\Delta Export_{it}}$$
$$+ \underbrace{\nu_i - \nu_i}_{\text{0 for each } i} + \underbrace{\mu_t - \mu_{t-1}}_{\Delta \mu_t} + \underbrace{\epsilon_{i,t} - e_{i,t-1}}_{\Delta \epsilon_{it}}$$

$$(2.5)$$

$$\Delta Methane_{it} = a + \beta \Delta Export_{it} + u_t + e_{it} \qquad (2.6)$$

where $\Delta Methane_{it}$ is the change in methane emissions in the waste industry for state i in year t, compared to the previous year. $\Delta Export_{it}$ is the change in recyclable waste exports to China from state i in year t, compared to the previous year. In differencing, any constant term in the model in levels drops out. The α in equation (2.6) is therefore the linear time trend in the levels data. Year fixed effects u_t control every time pattern other than the linear time trend. State fixed effect ν_i drops out for each state i after taking the first difference. I choose the first difference model in equation (2.6) over the fixed effect model in levels for the following reasons: (1) although the first difference model works just as

a fixed effects model, it relies on no serial correlation in the differenced errors (a weaker assumption); and (2) the first difference model controls for variations in differences across states, which is a stronger control.[19] There are still several concerns regarding first difference OLS identification in this context:

1. On the one hand, GHG emissions from most industries are monitored by the U.S. EPA. For the waste industry, it is difficult for landfills to get permits because they need to meet many environmental requirements. Given that the U.S. has relatively stringent environmental regulations on local pollution (such as the Clean Air and Clean Water Acts), it can be harder for recyclers to find facilities to process recyclable materials. As a result, emissions from the waste industry may be inversely related to the amount of recyclables being exported to China, reflecting the stringent domestic environmental regulation in the U.S.

2. Omitted variables (e.g. economic development) may increase both recyclable exports and domestic emissions. Thus there is a potential problem of endogeneity for the variable that measures the change of recyclable waste exports.

3. Instead of the observed demand policy shock from China (the waste ban), technological development—such as an increasing ability to reprocess recyclables cleanly and safely—could also decrease the supply of recyclable wastes to be exported.

To identify the causal effects of changes in U.S. recyclable waste exports on U.S. domestic methane emissions from the waste industry, I employ an instrumental

---

[19]The fixed effects model builds on the assumption of no serial correlation prior to demeaning.

variable that accounts for the potential endogeneity of U.S. recyclable exports. I use a Bartik shift-share instrument from the literature on international trade and labor economics, adapted to an environmental context (Bartik, 1991; Wong, 2021). The main IV is defined as follows:

$$IV_{it}^{Bartik} = \sum_j \left\{ \frac{E_{ijt_0}}{E_{jt_0}} \Delta Export_{ucjt} \right\} \tag{2.7}$$

where $\Delta Export_{ucjt}$ is the change in exports from the U.S. (u) to China (c) for recyclable waste of type j, in year t compared to the previous year. $\frac{E_{ijt_0}}{E_{jt_0}}$ is state i's share of exports to China for recyclable waste j in the initial year t_0. The product of the initial share term and the current change in exports is then summed across all recyclable wastes j. In other words, the shift-share instrument is a data-regenerating process that shifts the initial export share of each state to the trajectory of the change in total recyclable waste exports from the U.S. to China over time. The initial year I use is 2004, the earliest year for which complete data is available for recyclable waste exports from the U.S. to China for recyclable materials affected by China's policy. Given that the construction of IV_{it}^{Bartik} excludes state i's current-period recyclable waste exports to China, the initial distribution of export shares of state i for waste j is exogenous (or at least predetermined), relative to the subsequent changes in methane emissions for state i.

One concern for my upcoming estimation is that changes in recyclable waste exports from the U.S. may be correlated with U.S. technological improvements and thus the supply of recyclable materials. In that way, U.S. recyclable exports may be jointly endogenous with domestic emissions. Naive OLS estimates may overstate the true impact on domestic methane emissions of restrictions on recyclable waste exports from the U.S. to China. I thus employ a second alternative instrument that

accounts for this potential endogeneity as follows:

$$IV_{it,others}^{Bartik} = \sum_j \left\{ \frac{E_{ijt_0}}{E_{jt_0}} \Delta Export_{ocjt} \right\} \tag{2.8}$$

Instead of using the change in exports from the U.S. to China, I exclude the U.S. and instead construct the IV using the contemporaneous changes in export of recyclable wastes to China from 11 other developed countries. Specifically, I instrument for the measured change in U.S. exports of recyclable wastes with a non-U.S. analog $\Delta Export_{ocjt}$, where the o subscript, for "others" replaces the u subscript for "U.S." This variable is constructed using data for changes in recyclable exports (at the commodity level) from the 11 other high-income countries to China. These 11 countries are all OECD countries which have engaged in extensive trade in recyclable wastes with China during the past few decades.[20] This instrument is valid because: (1) the instrument constructed by other OECD countries is highly correlated with the U.S. waste exports (relevance); (2) this instrument affects the U.S. methane emissions only through the U.S. waste exports (exclusion restriction); and (3) this instrument does not have a direct effect on the U.S. methane emissions (exogeneity).

After constructing the main and alternative Bartik-type instruments, I fit models of the following form:

$$\text{First stage:} \quad \Delta \widehat{Export}_{it} = \alpha + \beta \Delta IV_{it}^{Bartik} + \mu_t + v_{it} \tag{2.9}$$

Where IV_{it}^{Bartik} is either the U.S. or the other-country version of the instrument. Then the fitted value for the first stage is employed in the second stage:

---

[20]The 11 selected countries are: Australia, Austria, Canada, France, Germany, Portugal, New Zealand, United Kingdom, Japan, Spain, and Finland.

$$\text{Second stage:} \quad \Delta Methane_{it} = \alpha + \beta \Delta \widehat{Export}_{it} + \mu_t + e_{it} \qquad (2.10)$$

In the second-stage equation, $\Delta Methane_{it}$ is the annual change in methane emissions from the waste industry in state i.[21] The key coefficient of interest is β, the average annual change in methane emissions across U.S. states caused by a one-unit change in U.S. recyclable waste exports to China. I then use this average estimate to calculate the cumulative aggregate impact of China's GS policy on U.S. methane emissions from the waste industry for 2016 through 2019. The calculation is as follows:

$$\Delta \widehat{Methane}_{total} = \sum_{t=2016}^{2019} \beta \left[\sum_{state=i}^{I} \Delta Export_t^i \right] \qquad (2.11)$$

I begin my analysis by estimating the naive OLS specification in equation (2.1). The coefficient β is interpreted as the change in methane emissions from the waste industry for a 1 metric ton change in recyclable waste exports. For the simple OLS specification, model 1 in Table 3 suggests that for every 1 metric ton reduction in recyclable waste exports, methane emissions from the waste industry in the U.S. increase by 0.49 metric tons per year. To address concerns about potential reverse causality and/or endogeneity, I then estimate 2SLS equations (4) and (5) using my basic Bartik shift-share instrument. Model 2 in Table 3 suggests that for every one metric ton reduction in recyclable waste exports, methane emissions increase by 0.722 metric tons of CO_2 equivalent per year. This shows that the estimation bias from reverse causality tends to attenuate the point estimate of interest toward zero. The logic here is that the point estimate shows

---

[21]I use a first-differenced estimator to address the problem of omitted variables that may bias the estimate.

that the more recyclable waste was exported from the country, the less methane pollution was emitted domestically. However, the reverse causality is that the higher are domestic methane emissions, the more new recyclable waste is likely to be exported due to the stringent environmental regulations of the U.S., such as emissions caps. Thus, without accounting for this reverse causality, the OLS specification tends to underestimate the true negative effect of waste exports on domestic emissions. However, there is still a possibility that these may have been nontrivial supply shocks in the recyclable waste industry instead of just China's GS policy, which could also bias these estimates. Thus I estimate equations (2.3) and (2.4) again, but this time I use my alternative Bartik shift-share instrument constructed with the recyclable waste exports from a set of 11 non-U.S. countries to China. Model 3 in Table 3 suggests that for every 1 metric ton reduction in U.S. exports of recyclable wastes to China, methane emissions increased by 0.893 metric tons of CO_2 equivalents per year. This even-larger estimate reinforces my finding that the decrease in U.S. recyclable waste exports to China has increased the U.S. domestic methane emissions in general. This could be due to U.S. supply-side shocks such as technology improvement. Technology that processes wastes more efficiently could decrease both exports of waste and methane emissions. Thus, without accounting for such supply-side shocks, the effect of "exposure" to waste exports to China and domestic emissions could be underestimated.

There are still several possible threats to identification in my strategy. One is that supply-side shocks like technology improvement may be correlated across high-income countries. In this event, my IV estimates may be contaminated by correlations between changes in waste exports and unobserved components of export supply, making the impact of waste export exposure on domestic emissions

30

appear smaller than it truly is. After estimating β—the average effect across all U.S. states annually, I then calculate the implied cumulative effect of (a) the total reduction in recyclable waste exports due to China's waste ban on (b) overall U.S. national increases in methane emissions from 2016 to 2019.[22] Over this time period, the total weight of recyclable waste exports decreased from nearly 18,000,000 metric tons to just 5,500,000 metric tons. Applying equation (2.6), the U.S. total methane emissions from the waste industry increased by approximately 8-11 million metric tons of CO_2 equivalents., which (for comparison) is about 9.68% of total methane emissions from the U.S. waste industry in 2016, or about 5.23% of total methane emissions from the U.S. petroleum and natural gas system in 2016.[23]

2.4 Conclusion

This paper examines the effects of China's Green Sword Policy (a comprehensive waste import ban) on environmental outcomes in the U.S. The waste ban, designed to reduce China's waste imports from the U.S., has resulted in far-reaching consequences for the U.S. environment at the national and state levels. Following the implementation of China's waste import ban, policy-makers have been concerned about its effects on the U.S. recycling industry, but few researchers have studied these effects in a quantitatively rigorous fashion. My paper is the first empirical analysis of the impact of China's GS policy on the U.S. I use methane emissions as an available and consistent measure of pollution outcomes from wastes, and find that the U.S. has seen a significant increase in landfill-related methane emissions after the GS policy, especially in larger states such as California, New York, Virginia, and Texas. Furthermore, the observed heterogeneous changes in

---

[22]I exclude 2020 exports and emissions because of the COVID disruption in international trade and domestic emissions.

[23]U.S. EPA: 1990-2020 National-level U.S. Greenhouse Gas Inventory Fast Facts

state-level methane emissions have been positively correlated with the amount of waste previously exported to China by each state. This positive correlation suggests a potential causal relationship between waste exports and domestic emissions. In my analysis of U.S. waste export and emissions, I find that recyclable waste exports are inversely related to domestic methane emissions in the U.S. This result is consistent with the "pollution haven" hypothesis, namely that developed countries tend to relocate their wastes and associated negative externalities to developing countries in order to reduce domestic pollution levels.

Other questions for further study include what kind of spillover effects the GS policy might have had on international policies regarding pollution. Despite there being many new destination countries for U.S. recyclable wastes in Southeast Asia, Africa, and the Middle East, only some countries reacted to the GS policy by adjusting their domestic regulations to control the altered flow of waste imports, while others did not have a prompt change in policy to control the inflow of wastes. Another point of investigation would be waste transfers across states: my analysis finds that among 11 states that have experienced statistically significant increases, some are smaller states such as Nevada, North Dakota, Alabama, Kentucky, and New Hampshire. It is difficult to connect their significant increases in methane emissions with their own waste generation. It is worth noting that these relatively small states might have experienced significant methane emission increases because they are often neighbors of larger states. There is the possibility that larger states have transferred their newly surplus amounts of recyclable wastes to neighboring states for processing and disposal. Additionally, within the states that have seen significant increase in emissions from wastes, it would be worth exploring which local communities are bearing the burden of the increased amounts of waste due to

China's waste ban and what are the demographics of these communities. Finally, a caveat concerning my research is that the methane emission data I use is from a self reporting database. Although the EPA has emphasized the high reporting compliance rate, it would be more accurate to test the effect of the policy using some type of ground-monitored emissions data or satellite data to verify the significance of the policy effect. Another potential caveat lies in the identification strategy I employed. I assume that industries not experiencing emission changes during the implementation of China's GS policy were unaffected by this policy. However, this assumption might overlook potential general equilibrium effects that could influence the outcomes. The GS policy's breadth and impact could potentially alter the overall demand and supply dynamics for numerous goods, thereby indirectly affecting units in the control group.

2.5   Figures
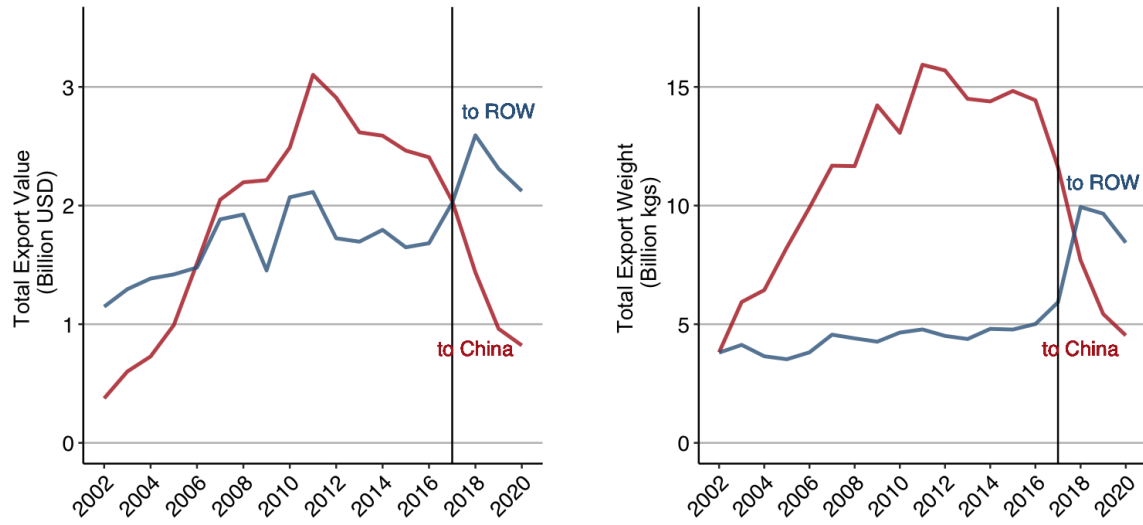
Figure 1. U.S. Recyclable Waste Exports to China and the Rest Of the World (ROW). This figure shows that U.S. recyclable waste exports to China dropped dramatically after 2017 when China's Green Sword (GS) policy was announced and implemented. Meanwhile, U.S. exports in recyclable wastes to the rest of the world increased temporarily but decreased after 2018.
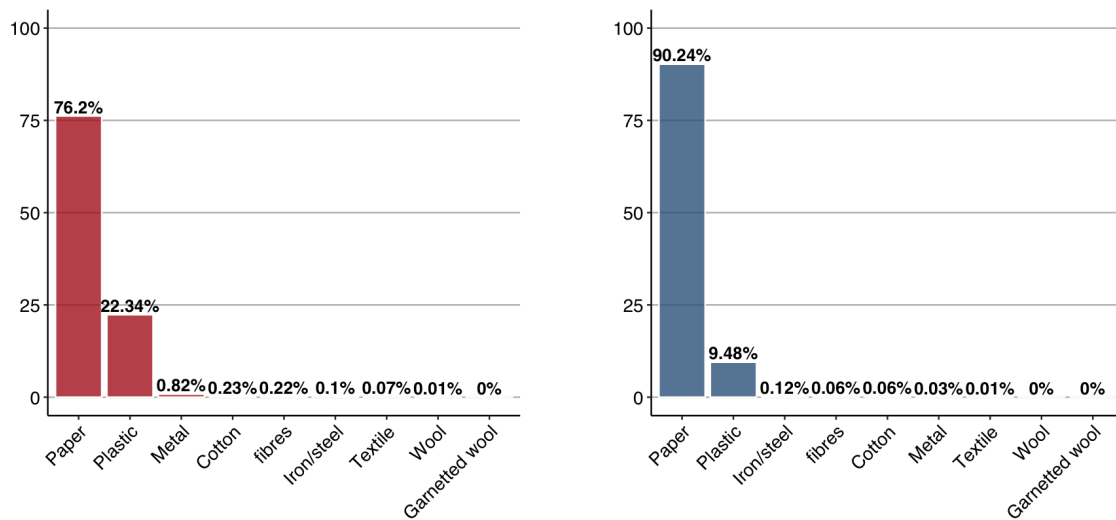
Figure 2. Composition of U.S. Recyclable Waste Exports to China. This figure shows the composition of recyclable wastes that were exported in the past two decades. The listed waste materials are all wastes that are directly affected by China's GS policy. The left panel shows the types and percentages of waste materials exported by value ($ USD). The right panel shows the types and percentages of waste materials exported by weight (kg). Paper and paperboard and plastic scraps are the most exported recyclable wastes by value and weight, followed by metal, iron/steel, fibre, cotton, etc.
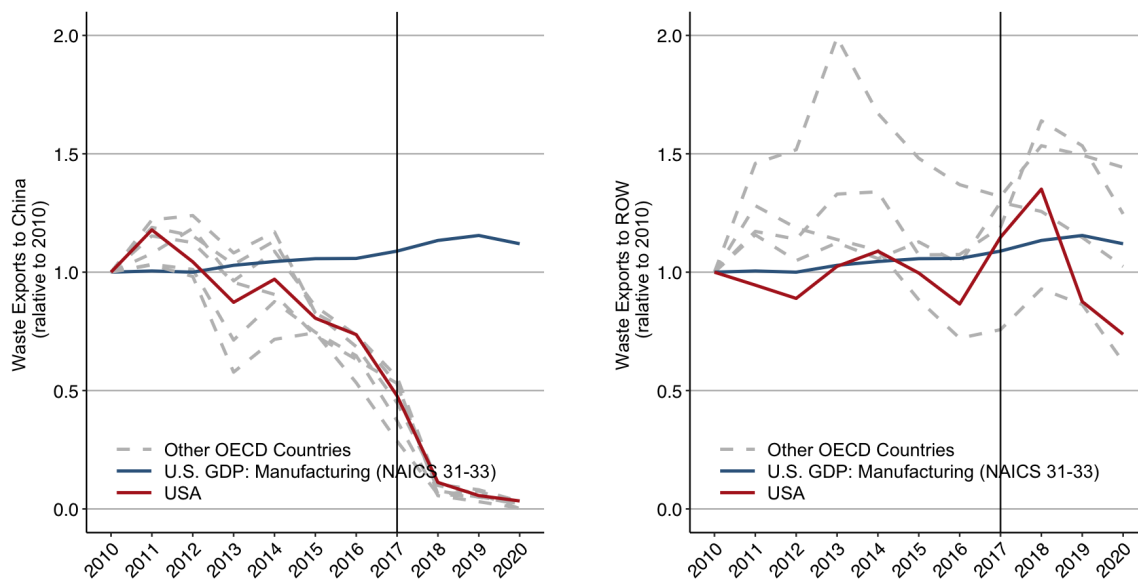
Figure 3. Plastic Waste Exports from the U.S. and Other OECD Countries to China. This figure shows recyclable waste exports (taking plastic scrap as an example) for the U.S. (red line), as well as for a set of six other OECD countries (grey lines) to China and to the rest of the world from 2010 to 2020. All of the export values are normalized by the 2010 export values for each country. The blue line represents the U.S. manufacturing GDP—NAICS 31-33 (the industry code) that includes the plastics industry. Although the plastic-manufacturing GDP of the U.S. increased gradually over time, the U.S. plastic scrap exports to China dropped by almost 99 percent, especially after China's GS policy. Similar patterns are found in other OECD countries. After China's GS policy, plastic scrap exports by the U.S. and by the set of six other OECD countries increased temporarily to the rest of the world but then decreased.

36
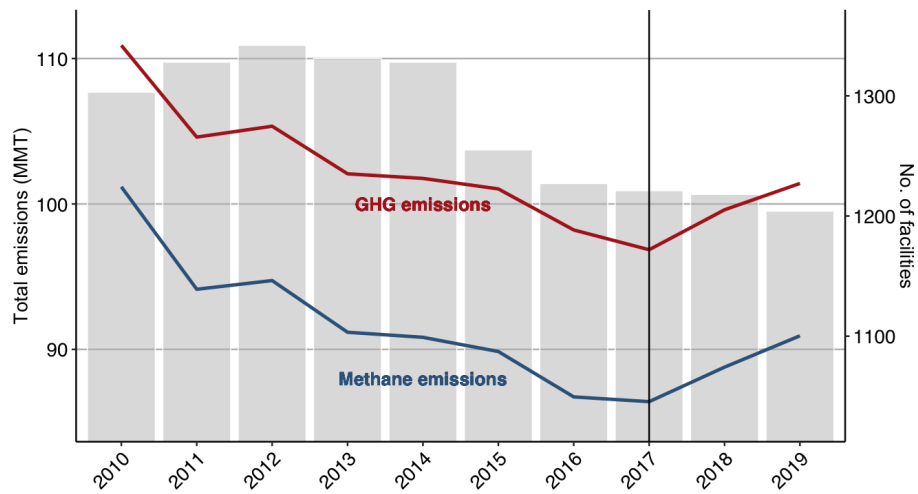
Figure 4. U.S. Waste Industry GHG Emissions. Total emissions from the waste industry based on the aggregated reporting records from facilities for each year between 2010 and 2020. In the waste industry, total emissions are from methane (CH_4), carbon dioxide (CO_2), and Nitrous oxide (N_2O). However, the amount of CO_2 and N_2O are too small compared to CH_4. Thus, more than 80% of total emissions from the waste industry are CH_4. Although the number of facilities has decreased gradually over the years, the total emissions and methane emissions of facilities have increased since 2017.
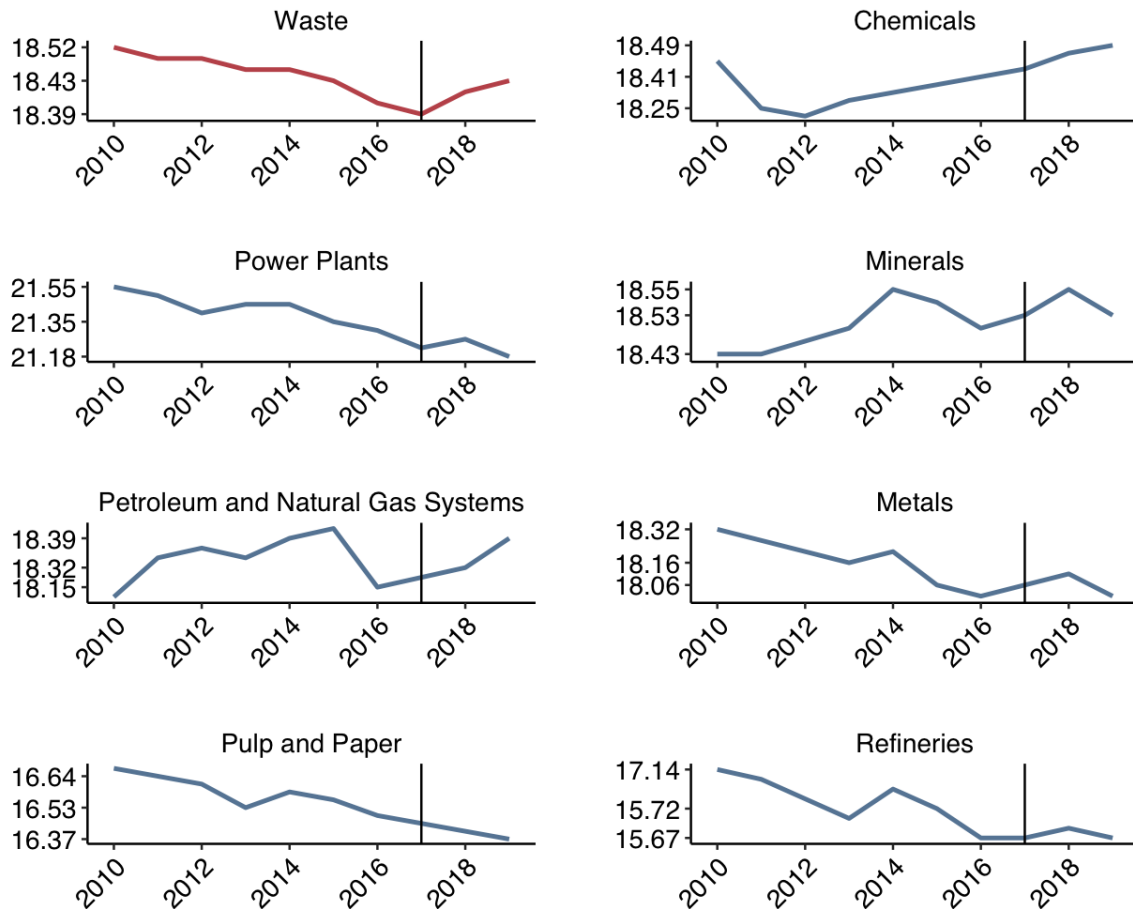
Figure 5. U.S. Greenhouse Gas Emissions (log.MMT) by Industry. This figure shows the GHG emissions from the eight main industries in the EPA GHGRP data. Waste, power plants, and petroleum and natural gas are the industries that have the highest emissions in the U.S. on average from 2010 to 2020. The waste industry (in red) has seen a decrease in methane emissions from 2010 to 2017 and an increase in methane emissions afterwards, both in total and on average. Changes in GHG emissions of other industries are exogenous to China's GS policy.

Actual Methame Emissions (solid) vs. Synthetic Methane Emissions (dashed)
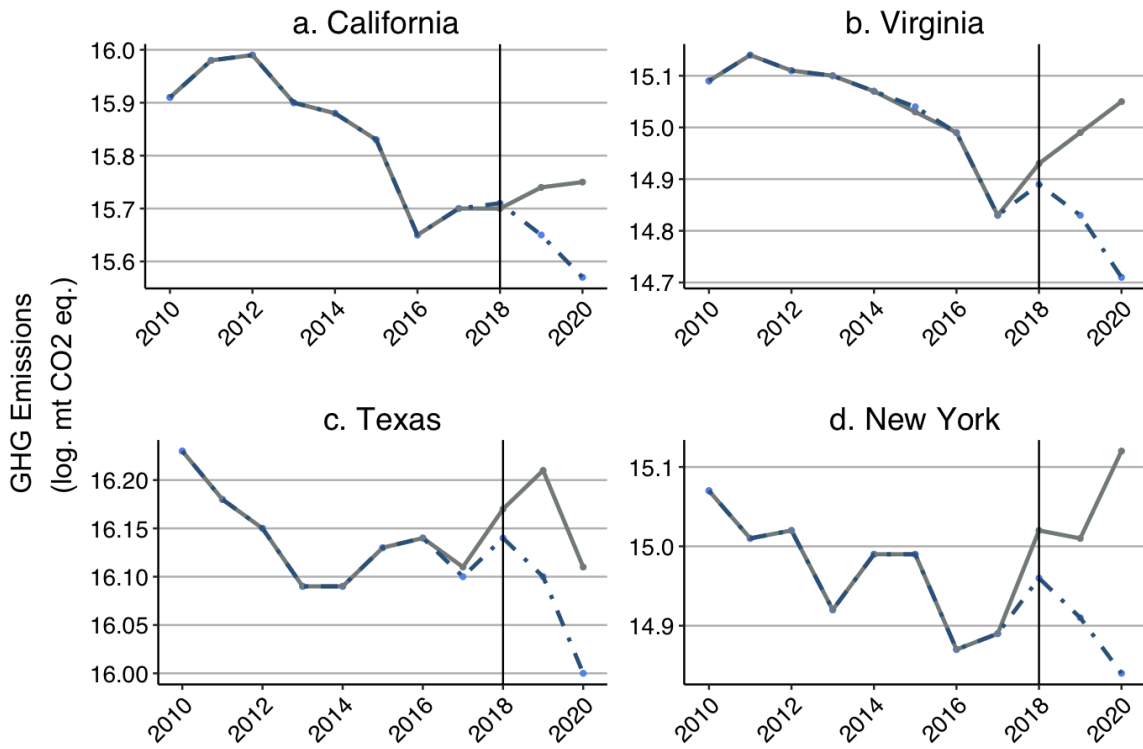
Figure 6. State-level Synthetic Control Results. This plot shows the synthetic control results from four selected states. The solid grey lines are the actual methane emissions from the waste industry in four states. The blue dashed lines are the synthetic methane emissions estimated by a function of other state-industries (controls) with different weights. The differences between the actual methane emissions and synthetic emissions are the causal effects of China's GS policy on the U.S. domestic methane emissions from the waste industry at state level. California, Virginia, Texas, and New York have all seen an increase in methane emissions after China's GS policy. Texas's methane emissions from the waste industry dropped in 2020. This may be caused by a variety of reasons due to the 2020 Covid-19 pandemic.

Causal Estimates (Differences between Actual and Synthetic Emissions)
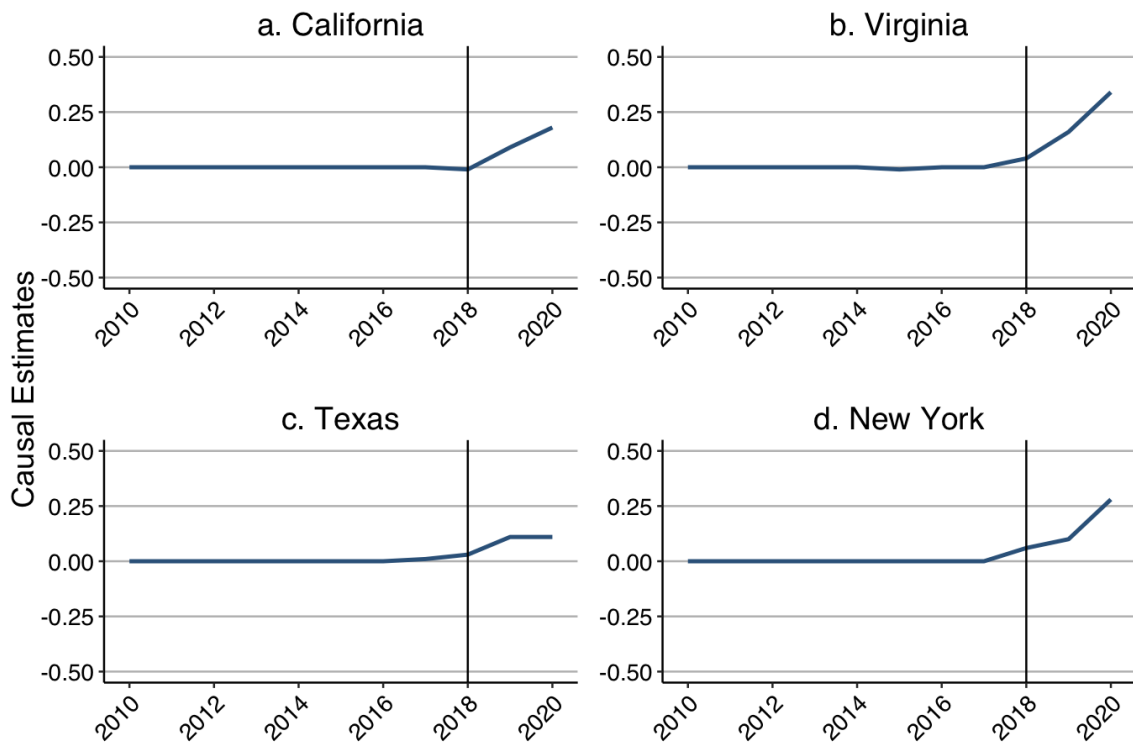
Figure 7. State-level Synthetic Control Results: Four States. The causal estimates are calculated by subtracting the synthetic emissions from the actual emissions. Since the synthetic emissions are predicted in the absence of China's GS policy, the difference between actual and synthetic emissions is the causal effect of the GS policy on emissions from the waste industry for each state. All of the four example states have seen increasingly positive effects on methane emissions from the waste industry.
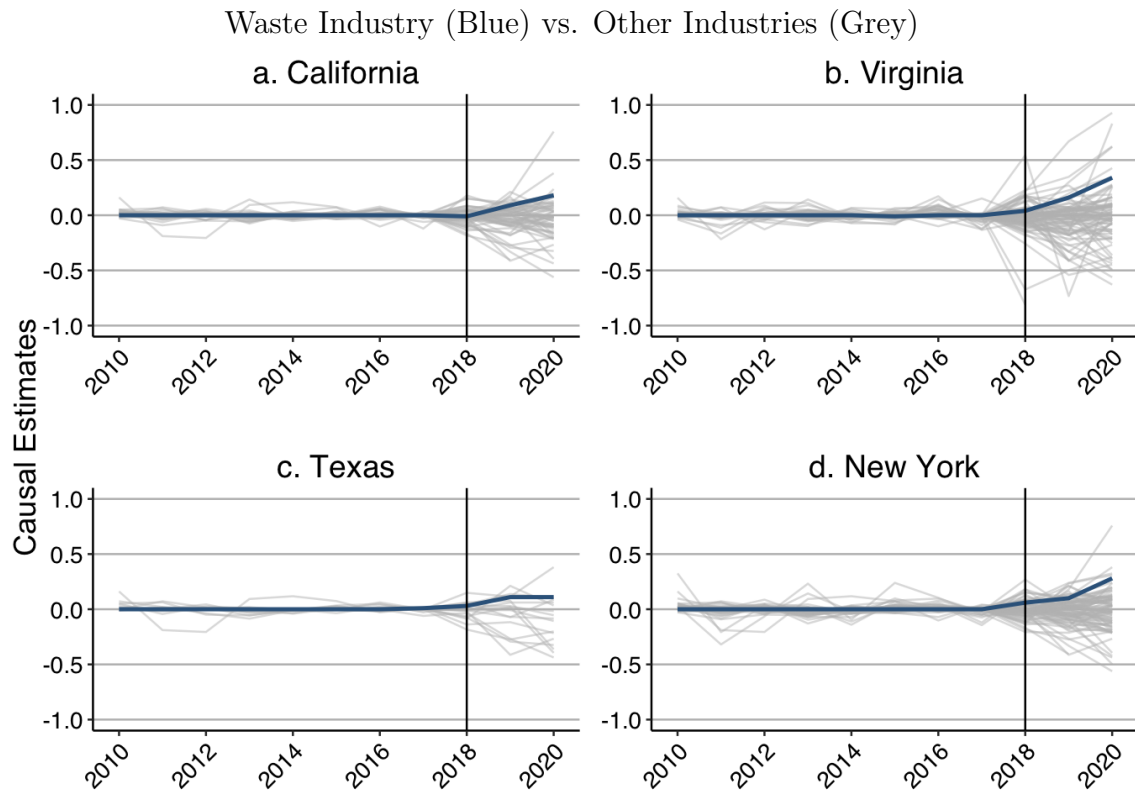
Figure 8. State-level Synthetic Control Results: Placebo Tests. This figure shows results from placebo tests associated with the synthetic control method for the four states. The blue lines are the causal effects of China's GS policy on the waste industry of each state. The grey lines are the causal effects of China's GS policy on other industries of different states. The p-value is calculated by the distribution of the post/pre-GS policy ratios of the MSPE for treatment industry of a state and all other control state-industry pairs.
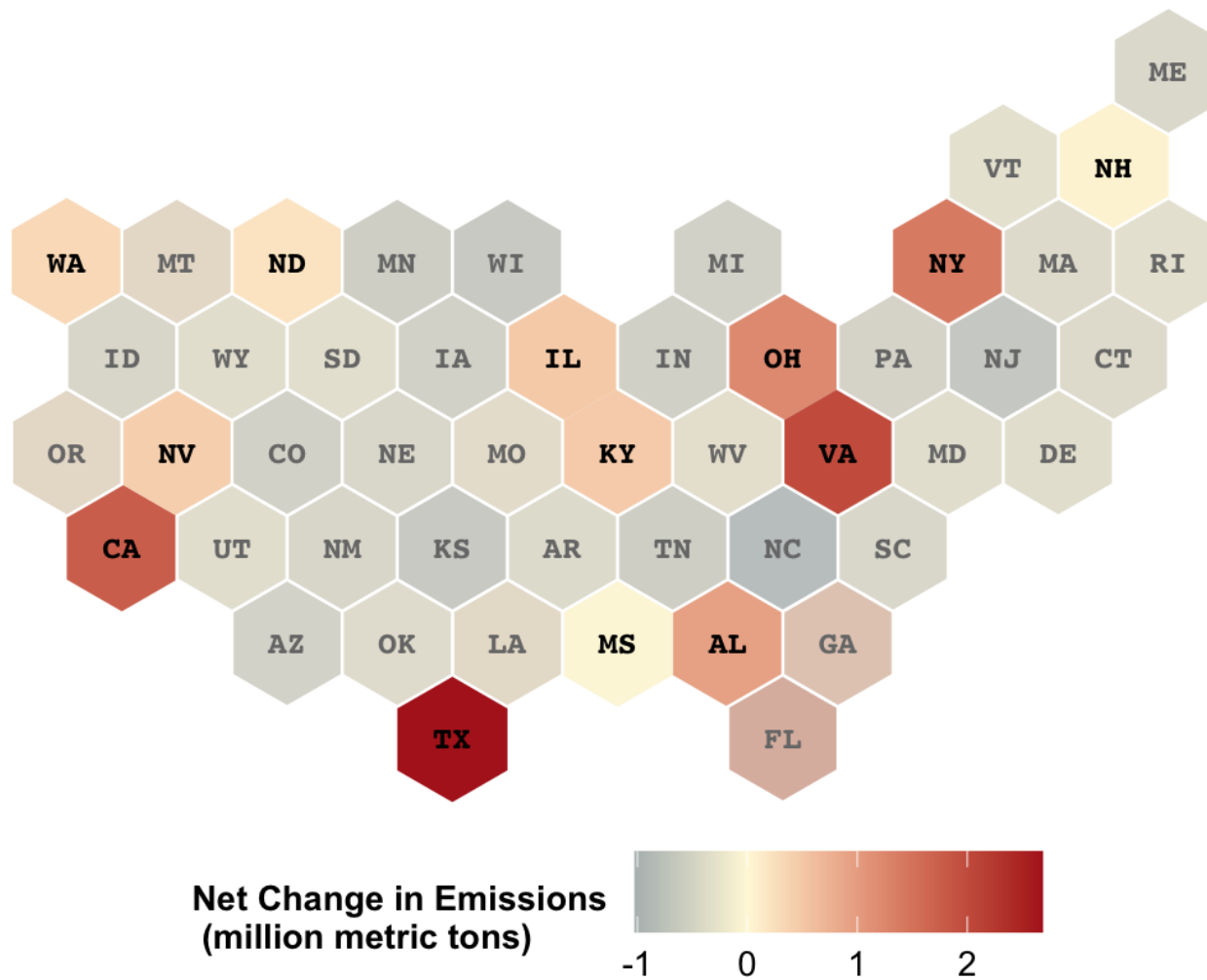
Figure 9. State-level Synthetic Control Results—Estimates of the Percentage and Net Change in GHG Emissions from the Waste Industry. Red-colored states represent state-level estimates that can be considered statistically significant at the 10% level. Grey states represent state-level estimates that are statistically insignificant.
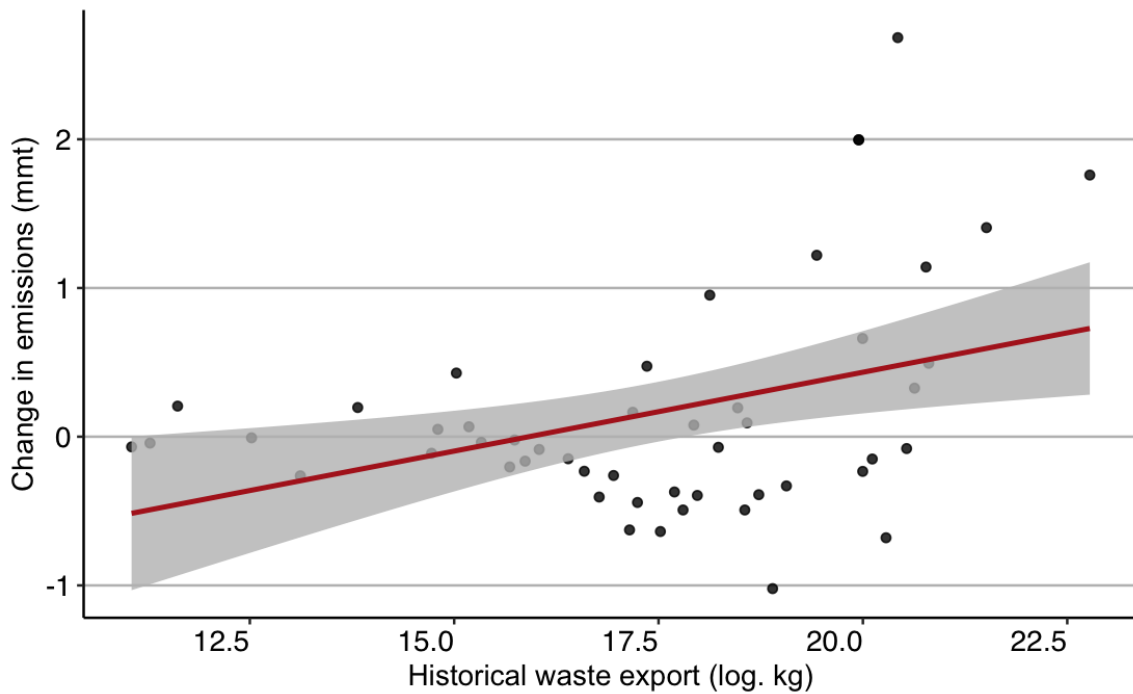
Figure 10. Pairwise Correlations: State-level Emission Changes and Waste Trade Exposures. Methane emission increases for states are calculated by multiplying the state's methane emissions in 2016 by the percentage increases in emissions estimated by the synthetic control method. The dots (observations) are the net methane emission increases by state. The log of total recyclable waste exports (before China's GS policy) is used as a measurement of the "export exposure" of a given state to China. The red line is the fitted line for a regression that regress the net change in methane emission on the log of total recyclable exports at the state level.
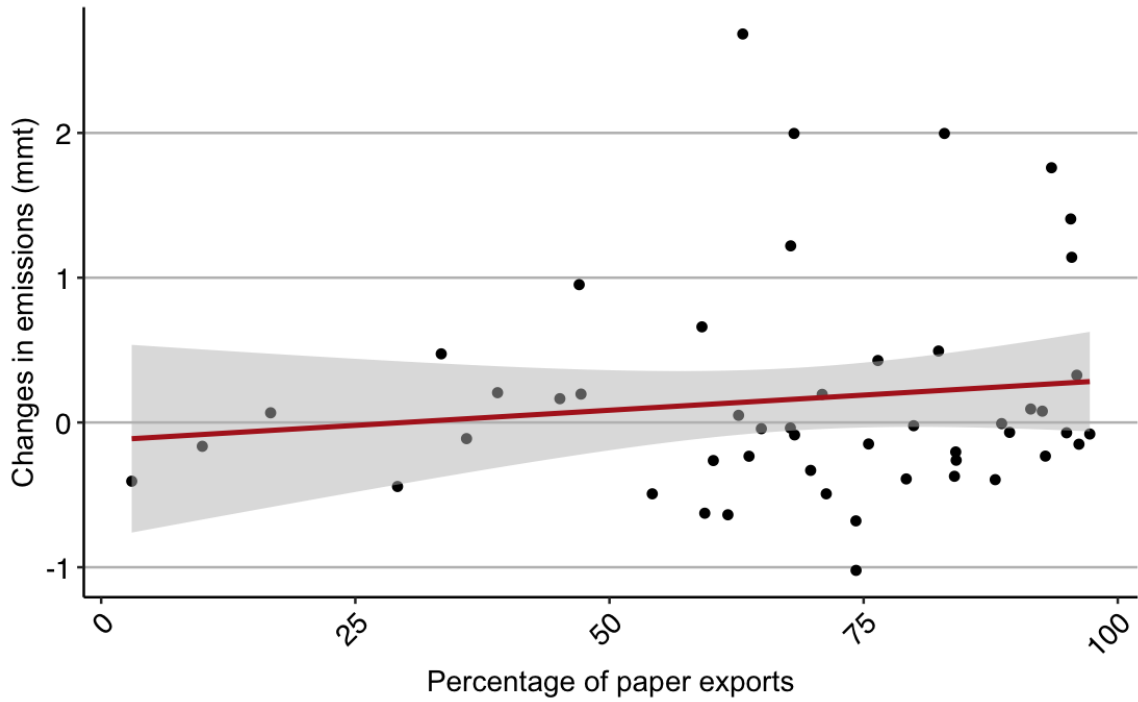
Figure 11. Pairwise Correlations: State-level Emission Changes and Paper/paperboard Exports. Methane emission increases for states are calculated by multiplying the methane emissions in 2016 with the percentage increases in emissions estimated by the synthetic control method. The dots (observations) are the net methane emission increases by state. The red line is the fitted line for regression that regress the net change in methane emissions on paper/paperboard exports at the state level.
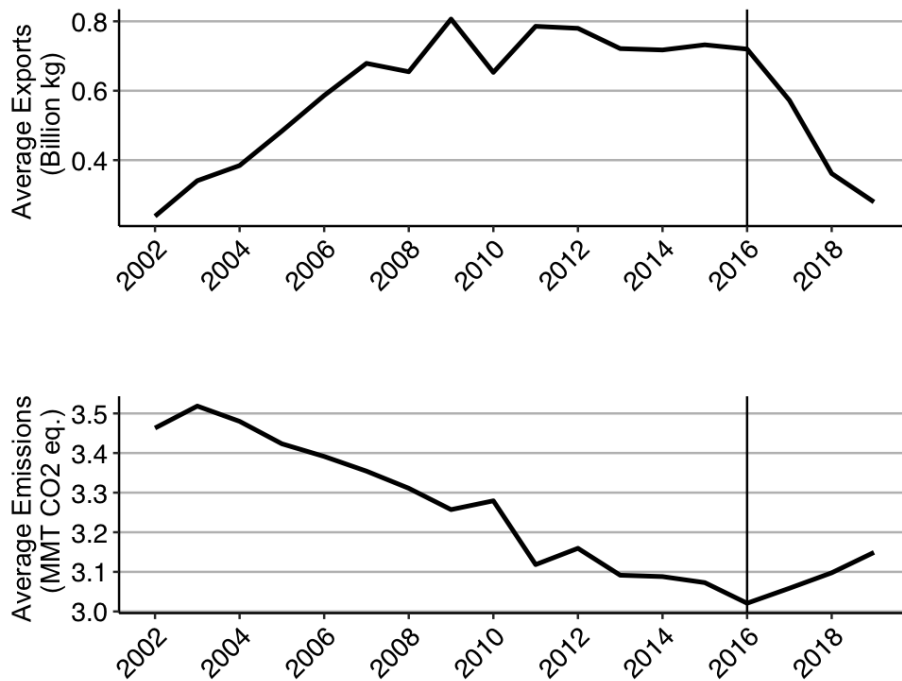
Figure 12. U.S. Waste Exports and Methane Emissions from the Waste Sector. The average emissions of the waste industry in the United States are derived from the aggregated reports submitted by states from 2010 to 2020. Meanwhile, the average waste exports from the industry are determined based on state-level waste export data. The plots demonstrate an inverse correlation between waste exports and domestic emissions from the waste industry in the U.S.

45

2.6 Tables

	Spatial Unit	Years available	Frequency
UN Comtrade Data	country level	2002-2020	yearly
U.S.A Trade Online Data	state level	2002-2020	yearly
EPA GHG Inventory Data	state level	2002-2020	yearly
EPA GHG Reporting Program Data	facility level	2010-2020	yearly

Table 1. Data Sources Summary: State-level Analysis. This table summarises all of the data sources that are used in this paper. Export and emission data are tracked by state and year.

	I. U.S.		II. Other countries	
	Exports to China (1)	Exports to rest of world (2)	Exports to China (3)	Exports to rest of world (4)

Panel A. Total value ($ U.S. billion) over all U.S. states

Year	(1)	(2)	(3)	(4)
2010	3.54	2.85	3.30	4.05
2011	4.29	2.95	3.16	4.59
2012	3.96	2.41	3.76	4.89
2013	3.54	2.41	3.28	4.28
2014	3.57	2.51	3.13	4.52
2015	3.33	2.31	2.82	3.69
2016	3.16	2.29	2.62	3.55
2017	2.59	2.75	2.33	4.64
2018	1.53	3.49	1.36	5.14
2019	1.01	3.09	0.68	4.64
2020	0.86	2.78	0.33	4.33

Panel B. Total weight (billion kg) over all U.S. states

Year	(1)	(2)	(3)	(4)
2010	17.30	6.59	13.74	14.01
2011	20.03	6.58	14.11	15.58
2012	19.88	6.15	15.33	16.09
2013	18.39	6.05	14.03	12.85
2014	18.65	6.56	13.64	16.49
2015	19.04	6.50	14.24	9.39
2016	17.99	6.69	14.26	10.67
2017	14.31	8.08	11.19	6.29
2018	7.95	12.95	6.81	9.66
2019	5.59	12.21	4.23	11.85
2020	4.71	10.38	2.19	10.78

Table 2. Summary Statistics: Recyclable Waste Exports by the U.S. and Other Countries. "Other countries" refers to 11 selected OECD countries—Australia, Austria, Canada, France, Germany, Portugal, New Zealand, United Kingdom, Japan, Spain, and Finland. They all have regular trade with China in recyclable wastes.

Dependent Variable: Change in Methane Emissions			
	Naive OLS	2SLS Bartik shift-share IV	2SLS Bartik shift-share IV Other countries
	(1)	(2)	(3)
2003-2019 first differences			
Change in Exports	-0.492***	-0.722***	-0.893***
	(0.122)	(0.114)	(0.124)
2SLS first stage estimates:	Change in Exports regressed on IV		
IV^{Bartik}		1.11***	9.55***
		(0.038)	((0.465)
First stage F-statistics		50	34
Year FE	✓	✓	✓
Observations	897	897	897

Table 3. Models to Explain the Changes in Methane Emissions as a Function of the Changes in Recyclable Waste Exports. Each column reports a separate regression. *$p < 0.1$, **$p < 0.05$, ***$p < 0.01$. The first-differenced model is like the fixed effect model but with a less restrictive assumption. The intercept in this first-differenced model captures all unobserved factors that may affect the emissions but are constant over time. It also captures the linear time trend. The year-fixed effects capture every time pattern other than the linear time trend.

CHAPTER III

THE EFFECTS OF CHINA'S WASTE IMPORT BAN ON LOCAL

COMMUNITIES: A CASE STUDY OF CALIFORNIA

3.1 Introduction

Each year, the United States produces over 200 million tons of solid waste, with a substantial portion being transported beyond the borders of the originating county or state.[1] This practice is expected to continue as waste generation rates have nearly doubled in recent years.[2] However, the extra jurisdictional transfer of waste can result in unequal exposure to waste facilities and shipments among various demographic groups. Low-income and minority communities are often disproportionately impacted, as these groups are more likely to live near landfills and other polluting facilities (GAO, 1983; Chavis & Lee, 1987). In fact, people of color are more likely to inhale contaminated air or consume water with harmful contaminants due to their proximity to these facilities.[3] This exposure can lead to various adverse health outcomes, including respiratory diseases and cancers, and it can also harm ecosystems, agriculture, and fisheries that are relied upon by the affected communities. To reduce this inequality, it is important to address these disparities and take action to minimize the impact of waste shipments on vulnerable communities.

---

[1] The blue whale is the largest animal on Earth. 200 million tons of waste generated annually equals 1 million blue whales.

[2] In 2017, 70% of hazardous waste processed in commercial facilities in Michigan originated outside of that state, according to data from the Environmental Protection Agency. Massachusetts is a significant exporter of materials such as wood, brick, and asphalt, for which disposal is prohibited in their own landfills. These materials are thus transported to other states like Maine, where they account for a significant proportion of the receiving state's landfill.

[3] For example, the population of Uniontown, the second-largest city in Perry County, Alabama, is over 90% Black, but the city permitted a large landfill to open in 2005, which eventually accepted waste from 33 states, including toxic coal ash from one of the worst environmental disasters in the country.

China's "Green Sword" policy, which was announced in 2017, prohibited imports into China of most recyclable waste from around the world, including the United States. The impact of this policy on local waste transfers in the U.S. has been significant. Prior to the policy, the U.S. was the largest exporter of solid waste to China. However, after the policy was enacted, U.S. solid waste exports to China decreased by almost 90%. As a result, many waste products that were previously exported by the U.S. are now being processed domestically, putting greater pressure on the country's land capacity for waste management. This has led to an increased need to transfer waste from densely populated areas to other locations, and haulers and municipalities are facing new decisions about where to send waste and whether to expand existing landfills or to open new landfill facilities.

In this paper, I describe a case study using the west coast U.S. state of California to investigate the distributional impact of China's waste ban on waste transfers at the local community level. California is selected as a case study because it is the largest state that exported recyclable waste and has comprehensive data at the facility level, allowing a more rigorous analysis. Prior to the GS policy, waste from California tended to be relocated to pollution havens like China, but after the policy, new local or original pollution havens emerged as destinations for excess recyclable waste. To study the distributional effects of the GS policy on local communities, I utilize the *CalRecycle Recycling and Disposal Reporting System (RDRS)*, which contains detailed waste transfer records from origin jurisdictions to destination facilities in California from 2002 to 2020. This dataset includes over 400 origin jurisdictions and nearly 150 destination facilities, with almost 800,000 tons of waste transferred across local communities in California over the past 20 years.

To examine the change in patterns on waste relocation, I use China's waste ban as a natural experiment. I collecte local characteristics of destination communities, such as racial composition, median income, economies of scale, and political vote shares, and compare how these characteristics affecte waste transfers across communities before and after the GS policy. The results indicate that before the waste ban, communities with higher minority population shares, higher median income, greater economies of scale, and higher Republican registration shares tend to receive more waste transfers from other jurisdictions. However, after the waste ban, communities with higher White population shares, lower median income, fewer economies of scale, and lower Republican registration shares experience a greater relative increase in waste inflows. These findings suggest that, perhaps counter-intuitively, racial disparities in arriving waste transfers appears to be narrowing after the exogenous GS policy shock.

I then utilize a simple theoretical model to investigate the mechanisms behind the narrowing of racial disparities related to waste transfers after China's policy shock. I propose several cost metrics to explain the phenomenon. In my model, the amount of waste pollution received by the destination community is negatively associated with land costs, transportation costs, and political costs for the destination community. To proxy for the costs of land and transportation, I use population density and distance between origin and destination. For political costs, I use the absolute difference between the Republican voting registration share of the destination community and the Republican voting registration share of the county where the destination facility is located. Communities with lower political costs are likely to have less political voice and thus lower resistance to waste pollution inflows.

To investigate which mechanisms have led to an increase in the relocation of waste to lower-income White communities, I use a simple OLS model with policy dummy interactions. The results show that before the GS policy, destination communities located within a shorter distance and with lower political costs receive more waste pollution transfers. However, after the exogenous GS policy shock, communities with lower land costs appear to experience relatively greater increases in waste inflows, and political costs associated with these flows seem to have become lower. As a result, rural White communities with lower land costs appear to have been relatively more likely to experience increased waste transfers after China's GS policy.

My paper makes several important contributions to the literature. First, I contribute to the growing literature on racial inequities in pollution exposure, specifically with respect to waste transfer. Previous studies have examined residential proximity to industrial facilities and found that racial and ethnic minority groups and/or lower socioeconomic status groups tend to live closer to these facilities compared to other groups, and this trend persists over time. Examples of such studies include research by Abel and White (2011) for Seattle from 1990 to 2007, research by Hipp and Lakon (2010) for southern California from 1990 to 2000, and research by Pais, Crowder, and Downey (2013) using a national cohort sample from 1990 to 2007. In contrast to these studies, my research examines how waste is relocated to different landfill facilities, taking into account whether these facilities are situated in areas with higher minority populations. Specifically, I investigate whether patterns in waste transfers, conditioned on the location of the destination facilities, is systematically related to the socioeconomic and demographic characteristics of the communities where these

destination facilities are located. To address challenges associated with drawing causal inferences from this literature, such as the ecological fallacy that can affect analysis using aggregate data, I define destination communities as those within a 3km radius of each destination facilities, which corresponds to only a few blocks of neighborhoods.[4]

Second, my paper describes a novel examination of the impact of China's GS policy as a natural experiment for assessing racial disparity in waste transfers. Prior research has demonstrated that minority communities in the United States are disproportionately exposed to hazardous waste and pollution, and the affected groups are less able to relocate to avoid such exposure (S. H. Banzhaf & Walsh, 1994; Baden & Coursey, 2002; S. H. Banzhaf & Walsh, 2008; Depro, Timmins, & O'Neil, 2015; S. Banzhaf, Ma, & Timmins, 2019). Moreover, remediation of contaminated sites may primarily benefit home-owning households and wealthier households who subsequently move into the area and bring about gentrification (Cameron & McConnaha, 2006; Depro, Timmins, & O'Neil, 2011; S. H. Banzhaf & Walsh, 2013). In this study, I explore how China's GS policy affects racial disparity in waste transfers based on existing environmental disparities in the United States. I first confirm that, prior to the policy's implementation, minority communities experienced greater waste pollution, in line with prior research. However, my research highlights a new finding that, following the GS policy, lower-income White communities have experienced relatively more waste pollution. This shift in racial disparity suggests that one impact of the GS policy has been to narrow racial disparities in waste transfers. My analysis of the underlying mechanisms suggests

---

[4]To guarantee that landfill facilities are in close proximity to residential areas, I have selected a 3km radius, considering that most landfills in the United States span a land area of several hundred acres.

that, in the wake of this policy change, land costs (rather than transportation or political costs) played a more significant role in determining the destinations of waste flows.

Third, my paper addresses the issue of "pollution displacement." Previous research has shown that pollution is displaced from the global North to South (Copeland, Shapiro, & Taylor, 1994; Cherniwchan, 2017). Additionally, Tanaka, Teshima, and Verhoogen (2021) examines how a 2009 tightening of U.S. air-quality standards for lead pollution led to relocation of battery recycling facilities to Mexico and concomitant changes in infant health in Mexico. Pollution can also relocate from highly polluted regions to less polluted regions within the same country (Henderson, 1996; Becker & Henderson, 2000; Greenstone, 2002; J. S. Shapiro & Walker, 2021). This relocation can be either unintentional or strategic. For example, Ho (2023) shows how NIMBY regulations, which restrict waste transfers between states, can unintentionally induce waste relocation among local communities within a state. Meanwhile, Morehouse and Rubin (2021) demonstrate how decision-makers strategically sited coal-fired power plants at the border of their counties to comply with the Clean Air Act, thereby exporting emissions to neighboring counties via prevailing winds. Most of the pollution displacement studies focus on endogenous environmental regulations within the U.S. (Hernandez-Cortes & Meng, 2020; J. S. Shapiro & Walker, 2021). Currie, Voorheis, and Walker (2023) find that a significant proportion of the decrease in Black-White disparities in pollution exposure can be attributed to differential effects of the Clean Air Act (CAA) in communities with different relative populations of Black and White individuals. In contrast, my study emphasizes the exogenous impact of a foreign policy shock on local pollution relocation in the U.S.

and finds that land costs became the most critical determinant of the narrowing racial disparity regarding waste transfers after the policy.

The rest of this chapter is structured as follows: Section 2 provides a brief overview of California's waste transfer system and China's policy on restricting waste imports from the United States, along with a description of the data sources used. The impact of China's GS policy on pollution relocation in California is analyzed in Section 3. Section 4 investigates the potential mechanisms behind changes in the pattern of waste transfers between Black and White communities. Finally, Section 5 concludes with some limitations and recommendations for future research.

3.2 Background and Data

3.2.1 Background.

Local communities and waste transfers. Historically, small, local dumps were the primary places for disposing solid waste before the practice evolved to transporting waste to larger, regional facilities. However, the 1990s brought about more rigorous government regulations aimed at safeguarding public health and the environment. These new measures prompted significant improvements in waste management technologies and necessitated the closure of many landfills that fell short of the prescribed standards. In the wake of this, contemporary, large-scale landfill facilities were established, leading to a considerable rise in the transportation of solid waste across counties and states. Between 1989 and 1999, the movement of waste between states soared by 300%, escalating from 10 million tons to 30 million tons (Repa, 2005). Trucks are still the main vehicles used for transporting waste between facilities, though some landfills have begun using trains to haul trash from urban centers, with the aim of reducing truck traffic and

its associated emissions. Nowadays, waste continues to be transported between communities. For example, New York City dispatches its waste to locations in upstate New York, New Jersey, and even Virginia, while Los Angeles sends its waste to northern California, Oregon, and Nevada. Presently, Uniontown, Alabama, is a recipient of waste, including hazardous coal ash, from as many as 33 different states.

The international transportation of waste is influenced by a variety of factors, including environmental regulations, labor costs, and trade imbalances. One example of this has been the trade in recyclable waste between the United States and China. In the ten years following China's accession to the WTO in 2001, U.S. exports of recyclable waste to China increased from 5 billion tons to 20 billion tons, representing an increase from 27.2% to 59.8% of total recyclable waste exports from the U.S. This increase can be attributed to several factors. First, China was initially viewed as a "pollution haven" where recycling processes that generated pollution could still be used because of the lack of stringent environmental regulations in the country. Second, China experienced significant economic development and demand for raw materials, particularly in manufacturing industries, and as a result, the import of recyclable waste from developed countries tended to increase alongside expanding domestic industrial activity and economic growth. Lastly, because China frequently had a trade surplus with the United States, ships returning to China from the U.S. often had excess capacity and could therefore transport recyclable waste at relatively low marginal costs.

In contrast, the transportation of waste within a nation or among local communities can be attributed to factors such as disposal fees, land expenses, transport costs, biased landfill location decisions, and uneven enforcement of

environmental regulations. In certain uncommon instances, evidence suggests that communities with limited political influence have been indirectly selected as sites for industries or sources of pollution, including waste disposal. These communities are more susceptible to environmental pollution due to a lack of political representation, limited resources for challenging polluting industries, and biased zoning and regulatory practices. For instance, an indigenous community near the Standing Rock Sioux reservation, with arguably less voting power and political clout, has been contesting the pipeline's rerouting from a predominantly White community due to concerns over water pollution and the disturbance of sacred lands.[5]

This paper reports upon an investigation of the impact of China's recyclable waste import ban on waste shipments at the local level within the U.S. state of California. Specifically, I analyze a dramatic policy change affecting in international waste shipments and its effects on intranational waste shipments. China had been the largest importer from the U.S. until 2016, when revisions to its environmental regulations and policies led to the implementation of stricter inspection and contamination limits under the Green Fence and then Green Sword policies. China's ban on imports of many types of recyclables has resulted in a shift from international waste relocation to domestic waste relocation, which has differentially affected local communities. This research examines the distributional consequences of an international trade-related policy on waste shipments received by local communities in California, which is home to roughly 10% of the population in the U.S.

---

[5]Standing Rock Sioux and Dakota Access Pipeline: https://americanindian.si.edu/nk360/plains-treaties/dapl

Environmental Equity.   Over the past four decades, a significant body of research has thoroughly documented the prevalence of environmental injustice, highlighting that pollution and environmental degradation disproportionately affect minority communities. This field of research emerged in the late 1970s when a middle-class Black neighborhood in Houston, Texas, discovered a solid waste facility was planned for their area. In 1987, a national study, spearheaded by United Church of Christ minister Benjamin Chavis, validated that race was the primary determinant of whether a person would live near a hazardous waste site, even after adjusting for geographical location and income. The most pronounced disparities in hazardous environmental exposure occur in communities that are both economically disadvantaged and belong to minority groups (Bullard, 1983; GAO, 1983; Chavis & Lee, 1987).

The issue of unequal pollution exposure in minority communities is a significant concern, as it can result in disparities in health, education, and other outcomes. Research by Hoek et al. (2013) demonstrated a negative association between air pollution and health outcomes, while accounting for race and income. Various studies have utilized quasi-experimental designs to establish a robust causal link between pollution exposure and health consequences for both children and adults (Chay & Greenstone, 2003; Currie & Neidell, 2007; Currie & Walker, 2011; Currie, Davis, Greenstone, & Walker, 2015; Schlenker & Walker, 2016; Currie, Greenstone, & Moretti, 2011; Persico, Figlio, & Roth, 2016).

Furthermore, long-lasting effects of pollution exposure on health, education, and economic outcomes have been observed, including human capital accumulation, labor market performance, family structure, and welfare reliance (Black, Devereux, & Salvanes, 2007; Currie & Moretti, 2007; Oreopoulos, Stabile, Walld, & Roos,

2008; Sanders, 2012; Figlio, Guryan, Karbownik, & Roth, 2014). Studies by Aizer, Currie, Simon, and Vivier (2018) and Persico et al. (2016) found that lead exposure and proximity to Superfund sites can influence test scores and other educational outcomes. By reducing such exposure, the gap in educational outcomes between disadvantaged children and their peers can be significantly narrowed.

Addressing environmental inequality requires understanding the underlying mechanisms contributing to such disparities. S. Banzhaf et al. (2019) highlights several key factors: 1) discriminatory siting of harmful facilities, 2) low-income households prioritizing basic needs over environmental quality, leading to higher pollution exposure, 3) Coasean bargaining, where firms and households negotiate pollution compensation, but unclear environmental property rights leave communities vulnerable, and 4) the government's role in distributing pollution through legislation, monitoring, enforcement, and regulatory decisions, which can be influenced by various factors and interest groups, potentially resulting in inequitable exposure to environmental hazards.

Building on the previous environmental inequality mechanisms, I suggest three potential factors influencing local waste transfers. First, land cost and population density could directly impact waste disposal tipping fees, leading to low-density rural areas, often predominantly White in California, receiving excess waste. Second, transportation costs can influence waste haulers' decisions, with areas farther from cities possibly receiving less waste due to distance. Third, local political influence can affect waste transfers through the permitting process, as landfills in the United States, whether private or public, need permits from local or state government agencies to open or expand. This process, involving compliance with environmental regulations, zoning requirements, and public health and safety

standards, could result in unequal waste exposure. My paper aims to examine which mechanism dominates general waste transfer patterns and investigates if the dominant mechanism changes after an exogenous policy shock from China.

3.2.2 Data.

California Disposal Flow Data. To investigate the impact of China's GS policy on pollution relocation in California, I analyze data from CalRecycle's *Recycling and Disposal Reporting System (RDRS)* from 2002 to 2021. The RDRS provides facility-level information on disposal flows, including waste flows (in disposal tons), for each origin jurisdiction and destination facility. These data are collected quarterly and cover more than 450 origin jurisdictions and over 250 destination disposal facilities over the 2002 to 2021 time period.

Socioeconomic and Demographic Data. To capture the characteristics of destination communities, I collected data from various sources. To measure racial composition, I utilize census-block level data from the *U.S. Census*. Median income data is drawn from the *U.S. 5-year ACS* at the census-block-group level. For economies of scale, I rely on data from the *Waste Business Journal*, which includes geographic coordinates for all recycling-related facilities across the United States, such as landfills, composters, recycling centers, and transfer stations. Lastly, I obtain data on political ideologies from California's *Statewide Database (SWDB) for Elections*, specifically, presidential election data at the precinct level. The summary of all data sources utilized in this paper is displayed in Table 4.

3.2.3 Summary Statistics.
Appendix Table B1 provides summary statistics for CalRecycle RDRS disposal flows from 2002 to 2020. The dataset covers of approximately 464 origin jurisdictions and 263 disposal facilities, on

average, over time. Columns 2 and 4 of Appendix Table B1 show that the average disposal quantities shipped from the origin jurisdictions have increased since 2013, as have the disposal quantities received by the destination facilities. In contrast, columns 1 and 3 indicate that the numbers of origin jurisdictions and destination facilities have decreased over time. Appendix Table B2 presents summary statistics for community characteristics around each destination facility in the CalRecycle RDRS data. These community characteristics are calculated for different buffers around each destination facility to ensure the model's robustness.

3.3 Determinants of Pollution Relocation: Evidence from California

My state-level analysis described in chapter 2 of this dissertation constitute a first step towards understanding the causal effect of China's waste ban on aggregate emission levels in the U.S. Among my state-level analyses in last chapter, I find that California's methane emissions from the waste industry increased by an average of 9.4 percent per year following China's GS policy.[6] To gain a more detailed understanding of the disaggregated local environmental effects of the GS policy, I use facility-level data on disposal flows within California to explore some distributional effects of China's GS policy and propose some potential mechanisms to explain these effects.[7]

3.3.1 Raw Patterns.

Waste Flows in California. To depict visually the distributional effects of China's GS policy on pollution relocation, I plot the spatial distribution of all

---

[6] The number is calculated using U.S. EPA GHGRP data.

[7] I compare the EPA GHGRP data with the CalRecycle RDRS data and find that the EPA data (in methane emissions) are highly correlated with CalRecycle disposal flow data (in tons). See Figure B1 in Appendix.

destination facilities in the CalRecycle RDRS dataset on the map of California. Appendix Figure B2 shows that most facilities in the CalRecycle data are located near urban areas (highlighted in yellow) in California, and fewer facilities are located in more-remote areas or agricultural regions. I then plot disposal flows on a California map using the coordinates of each origin jurisdiction and destination facility. To illustrate, I pick a specific city source (Los Angeles) and a destination facility (Covanta Stanisalaus Landfill) and show general patterns of pollution relocation in the state of California for this origin and this destination. Figure 13 shows four things: (1) the different destinations for waste pollution shipped outside the source city; (2) the different origins for waste pollution shipped into the destination community; (3) the size of the increase in waste shipments sent by each origin jurisdiction after China's GS policy; and (4) how much of an increase in waste shipments was received by each of the destination facilities after China's GS policy. The maps in Figure 13 show that most shipments of waste pollution are transported to destination facilities either in remote rural areas or in suburbs immediately outside urban areas (yellow areas) of California.[8] To explore further the characteristics of the destination communities where receiving facilities are located, I then plot an analogous spatial map based on the racial composition and political affiliation for California.[9] Figure 15 shows that for waste being shipped from Los Angeles, for example, most changes in pollution relocation have involved increased shipments to remote and light-shaded areas, with higher proportions of White residents, or to darker-shaded areas where larger shares of minority populations reside. Figure 16 shows that pollution relocation has also increased

---

[8]Figure 14 shows waste transfers from San Francisco and and into Potrero Hill Landfill.

[9]I use census-tract data for the racial composition map and precinct-level data for the political affiliation map.

shipments of waste going to more-remote Republican-leaning districts. Appendix Figure B3 and Appendix Figure B4 shows changes in disposal flows based on median income and pollution vulnerabilities of the destination communities in California after China's waste ban.[10] To address the concern that disposal facilities are more likely to be sited in minority communities, I plot all landfill facilities in the CalRecycle dataset in relation to the racial composition and political affiliation of the communities. Appendix Figure B4 shows that although many facilities are situated close to minority communities or Republican-leaning districts (darker green or red areas), some facilities are located in White communities or Democratic-leaning districts (lighter green or blue areas).

Altered Distributional Effects of Pollution Relocation. The maps that summarize disposal flows motivate my research questions concerning the distributional effects of China's GS policy: (1) How has China's GS policy, as a specific international trade policy shock, affected existing patterns of pollution relocation? (2) Are there environmental justice concerns with regard to changes in waste pollution relocation?[11]

3.3.2 Distributional Effects.

Correlation. To identify factors that potentially determine disposal flows and the relocation of waste pollution, I start with some simple scatter plots. I select six characteristics of destination communities that may correlate with

---

[10]Pollution vulnerability is reported by the Office of Environmental Health Hazard Assessment (OEHHA) CalEnvironScreen4.0. CalEnviroScreen is a screening methodology that can be used to help identify California communities that are disproportionately burdened by multiple sources of pollution.

[11]Pollution relocation refers to activities that transfer negative environmental externalities to places outside of the local community.

patterns of waste pollution relocation that create a net increase in disposal inflows. These characteristics include racial compositions (White and Black shares of the population), median income, economies of scale, and political affiliation. I define "economies of scale" for a community by counting the number of other related facilities/industries that are within a 15 km buffer around each destination facility[12]

Figure 17 shows that the White share of the population of the destination community is inversely related to net increases in disposal inflows. However, the Black share of the population is directly related to waste pollution inflows. These relationships suggest that the higher the share of Whites in the population of the destination community, the lesser the increase in disposal inflows.

Among other factors, the distances between origin jurisdiction and destination communities(facility) are inversely related to the net increase in waste inflows to destination communities. Nearby communities tend to receive greater net increases in waste inflows. The median income of the destination community is also negatively correlated with the net increase in waste inflows, which shows that the lower the median income for a community, the greater the increase in waste inflows it experiences after China's GS policy. Economies of scale for destination communities are negatively correlated with the waste inflows. The fewer similar facilities are located near the destination facility, the greater the increase in waste inflows to such communities. Finally, the Republican voting registration share of the destination community is positively correlated with net increases in waste flows.

---

[12]Racial composition measure is defined by the average population share by race within a 3-km buffer of the destination facility(see more details in Appendix Figure B6 and Figure B7). Political affiliation is defined by average registration share by party within a 3-km buffer of the destination facility (see more details in Figure B8 and Figure B9). The economies of scale measure is defined by the number of waste facilities that are within a 15-km buffer of the destination landfill facility for a disposal shipment. Waste facilities can be composting sites (CO), landfills (LF), recycling centers (MR and MW), and transfer stations (TS) (see more details in Appendix Figure B10 and Appendix Figure B11).

This shows that the greater the Republican share in the destination community, the greater the increase in waste inflows experienced by the destination community after China's waste ban.

Fix-effects model. Knowing that California has seen a significant increase in methane emissions and waste pollution after China's GS policy, I investigate the distributional effects of China's policy on waste flows for local communities (at the census-block level) in the state of California. I apply a fixed-effects model which includes the distances between the origins and destinations for inter-regional waste flows. For each destination community, the model also includes racial composition, median income, economies of scale in the waste industry, and the voting registration share of residents.[13] The model specification is as follows:

$$
\begin{aligned}
Y_{ijt} =& \alpha + \beta_1 log(Dist_{ij}) + \beta_2 log(R_j) + \beta_3 log(X_{jt}) \\
& + \beta_4 \left[log(Dist_{ij}) \times 1(post) \right] + \beta_5 \left[log(R_j) \times 1(post) \right] + \beta_6 \left[log(X_{jt}) \times 1(post) \right] \\
& + \zeta o + \theta_d + \mu_{od} + \eta_t + \epsilon_{ijt}
\end{aligned}
$$

$$(3.1)$$

The dependent variable Y_{ijt} is the tons of the waste transported from jurisdiction i to destination (facility) community j in year-quarter t.[14] $Dist_{ij}$ is the distance between origin jurisdiction i and destination community j. R_j is the racial composition of destination community j. $1(post)$ is an indicator variable, which takes the value of 1 for the year of China's waste ban and beyond. X_{jt} is a set of socioeconomic factors such as median income, economies of scale in the

---

[13]The voting registration data used here at the precinct level is from Statewide Database (SWDB) election data.

[14]I define the destination community as the areas that are within a 3km buffer of the destination facilities (S. Banzhaf et al. (2019)).

waste industry, and political affiliation for destination j.[15] To reveal any altered distributional effects caused by China's GS policy, I interact the characteristics of the destination communities with the policy indicator variable. In Appendix Table B3, I present results that are adjusted for different types of fixed effects, including origin-county fixed effects (ζ_o), destination-county fixed effects (θ_d), year-quarter fixed effects (η_t), and an error term (ϵ_t).

Figure 18 shows my estimates of the altered distributional effects caused by China's GS policy. Before China's waste ban, the estimates and their 90% and 95% CIs show that the sizes of waste flows are negatively correlated with distances between origin and destination communities. The greater the proportion of Black residents in the destination community, the more waste pollution the community receives from other places. The greater the proportion of White residents in the destination community, the less waste pollution the community receives. These coefficient estimates on the racial composition variables for the destination communities confirm that well-documented racial disparities in pollution exposure also exist with regard these patterns of waste pollution relocation. The median income and economies of scale for destination communities are both positively correlated with the amount of waste the destination communities receive.[16] The higher the percentage of registered Republican voters in a destination community, the more waste pollution is transported to that community on average, prior to China's waste ban.

---

[15]Economies of scale for community j are measured by counting how many waste-related facilities are within a 5km buffer of the destination facility.

[16]Comparing to all destination communities with a waste facility, communities with more economies of scale may provide more job opportunities to the community, which could account, in part, for a higher median income.

I then use the interaction terms in the model to compare pollution relocation patterns before and after China's GS policy. After China's waste ban, the positive coefficient on Black share of the population shows that the Black communities continue to receive more waste pollution from elsewhere. However, communities with higher White population shares now are more affected— communities with a higher White share of their population have seen a greater increase in their incoming shipments of wastes. Communities that are more remote, have fewer economies of scale, and lower Republican shares receive more waste pollution from elsewhere after China's GS policy takes effect, compared to before that event.

3.3.3   Mechanism.

Theory model.   In this section, I present a stylized model to illustrate the potential determinants of the observed altered waste shipments within California. The amount of waste being transported to other locations depends on the amount of waste generated by each origin jurisdiction and the cost of transporting this waste from that origin to each destination. The more waste the origin jurisdiction generates, the more waste can potentially be transported to other places. The lower the cost of transferring the waste, the more waste is likely to be transported to other locations. This relationship can be summarized as:

$$TranspWaste_{ijt} = f(\underset{+}{TotalWaste_{it}}, \underset{-}{Cost_{ijt}}) \tag{3.2}$$

$TranspWaste_{ijt}$ is the amount of waste transported from origin jurisdiction i to destination facility j at time t. $TotalWaste_{it}$ is the amount of waste generated in jurisdiction i at time t. $Cost_{ijt}$ is the monetary costs and non-monetary costs of

transporting this waste along with its negative externalities from origin jurisdiction i to destination facility j at time t.

My empirical analysis, in the previous section, suggests several factors that affect inter-regional pollution flows. Before China's waste ban, waste pollution tended to be transferred to communities with a higher percentage of Black residents. This is still the case after the GS policy. However, after China's GS policy, waste transfers shifted, to some extent, to lower-income White communities, and to less remote communities. The GS policy does not seem to have exacerbated the usual environmental disparity across communities with regard to waste pollution relocation. Instead, it has tended to narrow this relative disparity across communities. Black communities have continued to receive, in absolute terms, more waste shipments after the policy shock. However, White communities have experienced a greater increase in waste pollution, relative to the shipments they received before the GS policy.

There are three potential mechanisms to explain this altered distributional effect. The reason some White communities are receiving more waste after China's GS policy may be due to some of their characteristics. These increasingly used destinations are in California communities that tend to have (1) lower land costs; (2) lower transportation costs; (3) lower political costs. I assume the cost of waste relocation, in the case of recyclable waste transfers, depends on land values (LC_{jt}), transportation costs (TC_{ijt}), and political costs (PC_{ijt}) incurred in destination communities where the receiving facilities are located. I also assume that the amount of waste ($TotalWaste_i$) generated by an origin jurisdiction is relatively constant over time.

$$Cost_{ijt} = f(\underset{+}{LC_j}, \underset{+}{TC_{ij}}, \underset{+}{PC_{ij}}) \tag{3.3}$$

Three metrics. First, land costs tend to be lower in places where population densities are lower. Waste pollution tends to be transferred to places with lower land costs, where tipping rates (i.e., disposal fees) are lower. Based on this logic, I use population density (people/acre) as a proxy for land values.

$$LC_{jt} = f(\underset{+}{Population_{jt}}) \tag{3.4}$$

Second, waste pollution also tends to be transferred to closer locations to minimize transportation costs. I use distance (in kilometers) between the origin and destination as a proxy for transportation costs.

$$TC_{jt} = f(\underset{+}{Distance_{ijt}}) \tag{3.5}$$

Third, waste shipments to some communities (in this case, voting precincts) might be motivated by political cost. I define political cost as the deviation of the destination community's vote share from that of its county.[17] If the community's vote registration share by party is very different to the vote registration share by party of its county, then this community has a lower political cost.[18] The voting registration share of the community is the percentage of those who registered as Republican among all registered voters in the population of the voting precinct.

---

[17]Vote share is defined as the Democrats/Republican registrations among all all registered voters.

[18]The voting data is from Statewide Data Base (SWDB). SWDB collects the Statement of Vote and the Statement of Registration along with various geography files from each of the 58 counties for every statewide election. The Statement of Vote is a precinct-level dataset and precincts in California change frequently between elections. The goal of the SWDB is to make election data available that can be compared over time, on the same unit of analysis—a precinct, a census block or a census tract.

$$P_{jt} = f(\underbrace{Votes_{jt} - Votes_{ct}}_{-}) \qquad (3.6)$$

$Votes_{jt}$ is the Republican registration share of the community where destination facility j is located, calculated at time t. $Votes_{ct}$ is the Republican registration share of county c to which destination community j belongs at time t.[19] The difference between the community and county registration shares by party reflects the political cost of transporting waste and its externalities to community j. The greater the difference between the community and its county in terms of "political voting registration shares", the lower the political cost for waste inflows to that community. For example, a very Republican community in an overall Democratic county may have a high vote discrepancy and, thus, a lower resistance to increased waste shipments for various reasons: (1) such a community may have less political influence within the county; (2) its residents may also have a very different philosophy, relative to the county as a whole, concerning environmental issues; or (3) it may be harder to change the minds of such voters in such communities about their political affiliations. Consequently, waste haulers may hear fewer complaints from such communities if they increase their shipments to such places. For all three of these reasons, these communities may put up the least resistance to increased waste relocation after China's GS policy shock. Figure 19 shows the spatial distribution of voting registration discrepancies across communities (precincts) in California. The lighter the color, the more the destination community deviates from its county in political ideology, regardless of the dominant party in that county.

I estimate an ad hoc regression specification in order to examine which of these potential mechanisms best accounts for my finding that waste pollution has

---

[19]Here the vote shares are registrations votes.

relocated relatively more to poorer, more remote, and White communities after China's GS policy shock. The regression is as follows:

$$Y_{ijt} = \alpha + \beta_1 C_{ij} + \beta_2 \left[C_{ij} \times 1(post) \right] + \mu_{od} + \eta_t + \epsilon_{odt} \tag{3.7}$$

C_{ij} are the three cost metrics: land cost, transportation cost, and political cost—approximated by population density, distance between origin and destination, and discrepancy (absolute difference) of political vote shares between community and county. Population density is from the 2010 census data at the census-block level. Vote data at the precinct level is from the 2016 presidential election. I examine which of the three potential mechanisms appears to dominate as an explanation for the altered distributional patterns in waste pollution relocation.

Results. Table 5 shows that before China's waste ban, i.e., $1(post) = 0$, waste pollution tended to be relocated to remote places with low land values. Waste also tended to be transported to places with relatively low political costs. However, after the waste ban, more waste pollution has been relocated to destinations that are further away, with lower land costs but higher political costs. Furthermore, the effect of land costs on the altered distributional patterns is more statistically significant (at 5% level) than the effect of political costs (at 10% level). Although land costs and political costs both seem to influence waste pollution relocation, these estimates suggest that land costs may be more important than political costs as a determinant of the decisions about where to transport excess amounts of waste pollution in the event of an exogenous policy shock.

3.4   Conclusion

This paper investigates the far-reaching environmental consequences of China's waste import ban on local communities in the United States, particularly in California. The study examines changes in the burden of waste pollution on various communities before and after the policy is implementation. By utilizing detailed demographic, socioeconomic, and waste transfer data, the research also contributes to the Environmental Justice literature by shedding light on changes in pollution disparities between Black and White communities as a result of the policy shock.

My findings reveal that China's waste import ban has led to a counterintuitive decrease in the pollution gap between Black and White communities. Minority communities have a history of being exposed more to waste pollution. However, after the waste ban, lower-income White communities experienced a relatively greater increase in waste inflows. This unexpected outcome prompts an investigation into the mechanisms driving this change. I propose three explanations—land costs, transportation costs, and political costs—to determine which factors are responsible for the narrowing racial gap. My analysis shows that before the waste import ban, transportation and political costs were the main determinants of waste transfers across communities. However, after the policy shock, low land costs for a community have become a significant determinant for waste relocation. This research highlights the broader environmental implications of China's waste import policy for the US, beyond its immediate trade impacts, and emphasizes the importance of studying the domestic recycling industry and related policies in environmental economics.

This study still has several limitations, however. First, the waste data used in the local pollution relocation analysis cannot accurately track the amount or composition exclusively of recyclable wastes that are transferred locally, since disposal data incorporates both regular and recyclable wastes. Second, this paper has examined the effects of China's waste ban on emissions and pollution relocation related to landfill facilities only; data specifically for recycling facilities are not yet publicly available due to privacy issues. Finally, the GS policy might not be the only factor that has caused the observed narrowing of the racial disparity for waste-transfer destinations; other unobserved factors such as local policies or ideological changes in environmental equity might simultaneously have begun to have an effect on California's waste transfers around 2017.

While this study focuses on California, future research could potentially leverage satellite data to directly detect pollution caused by waste and evaluate the long-term effects of the policy on US communities. Additionally, further investigation into the distributional effects of the policy on waste facility siting and capacity expansions in minority or low-income communities is warranted, if we wish, to understand more completely how the waste ban has altered the landscape of waste transfers across local communities. This paper is the first to use empirical data from multiple sources and spatial scales, as well as a variety of econometric methods, to assess the policy's effects on the US environment at national, state, and local levels, providing valuable insights into its equity implications.

3.5 Figures
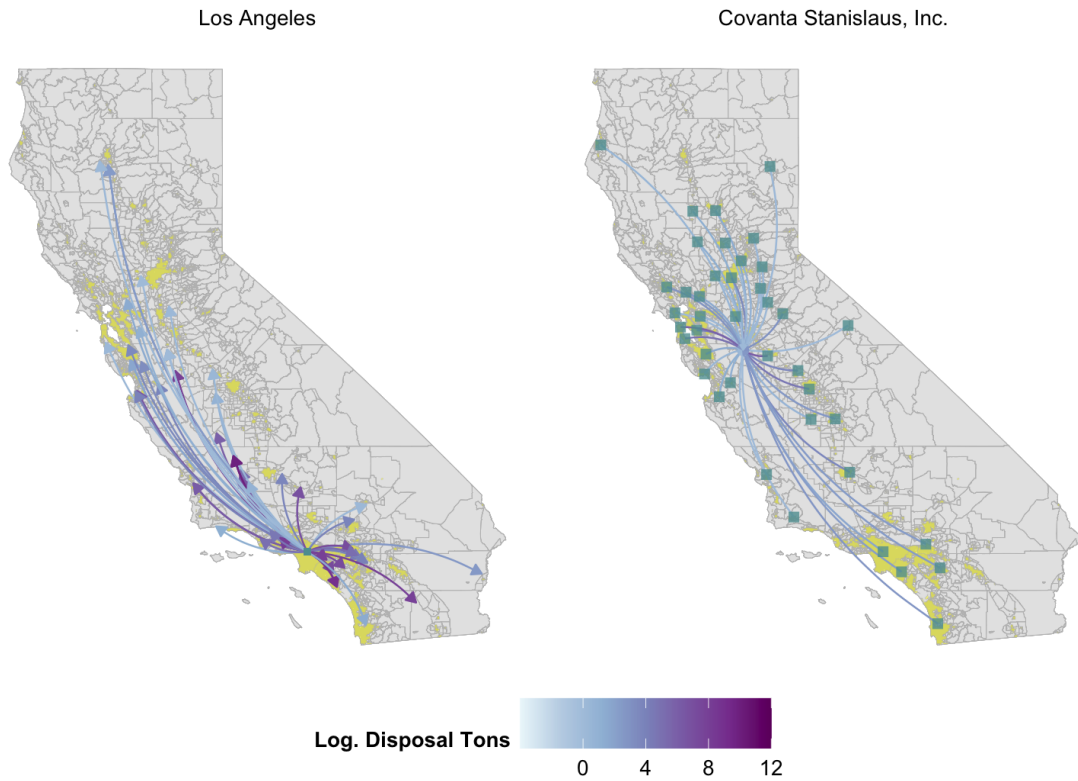
Figure 13. CalRecycle: Average Net Increase of Disposal Flow after China's GS Policy Los Angeles and Covanta Landfill. These maps show the disposal flows from source cities (Los Angeles) and disposal flows to destination facilities (Covanata Stanislaus, Inc.), as examples. They show (1) where the disposal goes from Los Angeles and (2) where disposals originate for the Covanata Stanislaus, Inc. The color of the arrows shows the increase in amount of disposal flows after China's GS policy. From the source city, most of the disposal has gone to rural or suburban areas outside the urban areas (yellow areas). Disposal that was transferred to closer rural areas increased more (represented by the darker color of curves with arrows) after China's GS policy.

San Francisco   Potrero Hills Landfill

Log. Disposal Tons
0   4   8   12
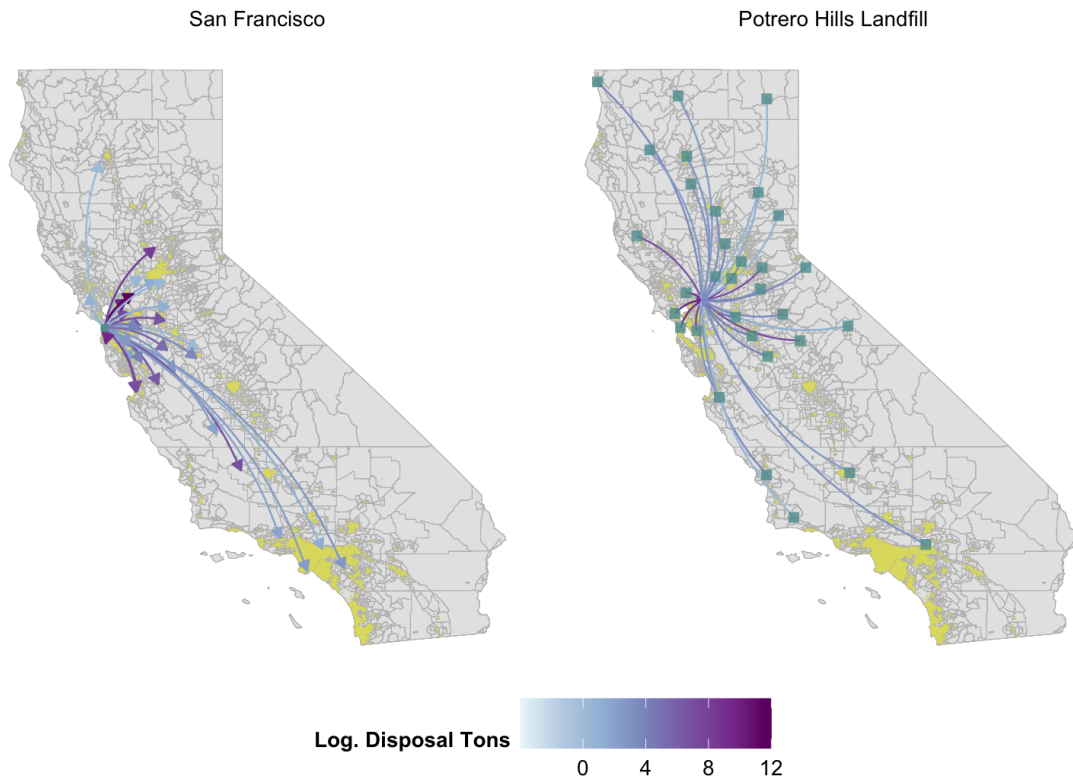
Figure 14. CalRecycle: Average Net Increase of Disposal Flow after China's GS
Policy San Francisco and Potrero Hills Landfill. These maps show the disposal
flows from source cities (San Francisco) and disposal flows to destination facilities
(Potrero Hills Landfill), as examples. They show (1) where the disposal goes from
San Francisco and (2) where disposals originate for the Potrero Hills Landfill. The
color of the arrows shows the increase in amount of disposal flows after China's GS
policy. From the source city, most of the disposal has gone to rural or suburban
areas outside the urban areas (yellow areas). Disposal that was transferred to closer
rural areas increased more (represented by the darker color of curves with arrows)
after China's GS policy.

75

Figure 15. CalRecycle: Average Net Increase of Disposal Flow by Racial Composition. This map shows the net increase in disposal flow after China's GS policy based on racial composition. The geographic unit for racial composition is the census tract. The color of the arrows shows the increase in amount of disposal flows after China's GS policy. The map shows that most of the destinations for disposal transfer are in "minority" areas (represented by darker blue/green). However, the "White" areas (represented by lighter green) have seen a greater increase (darker red arrows) in waste transfers after China's GS policy.
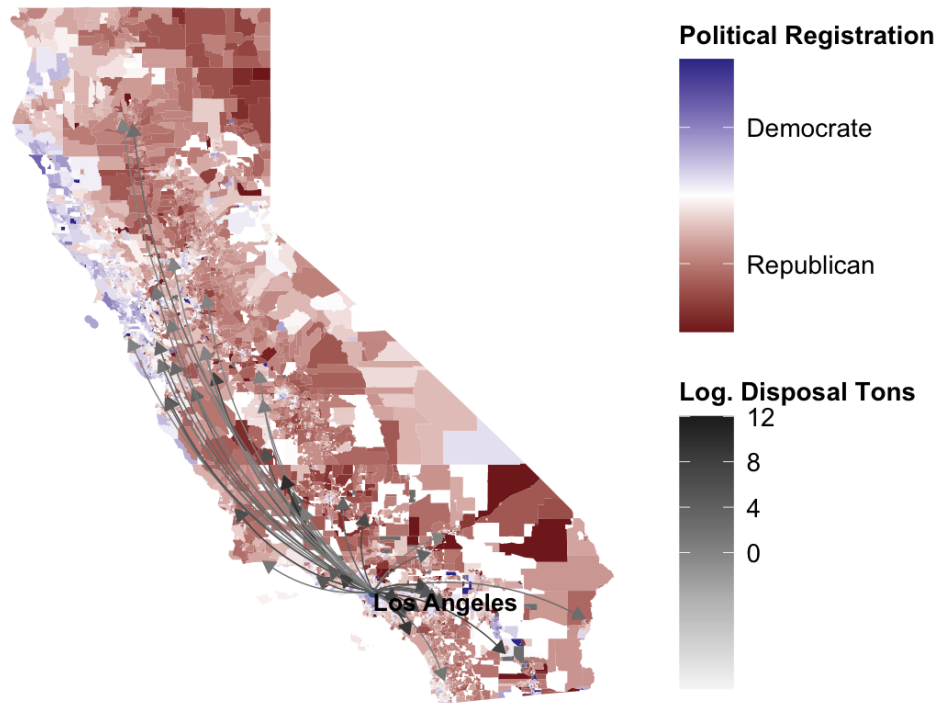
Figure 16. CalRecycle: Average Net Increase of Disposal Flow by Registered Voters. This map shows the net increase in disposal flows after China's GS policy based on voting registrations. The geographic unit for vote shares is the voting precinct. The map shows that more destinations of waste transfers are in Republican precincts (red) in California. The color of the arrows shows the increase in amount of disposal flows after China's GS policy.
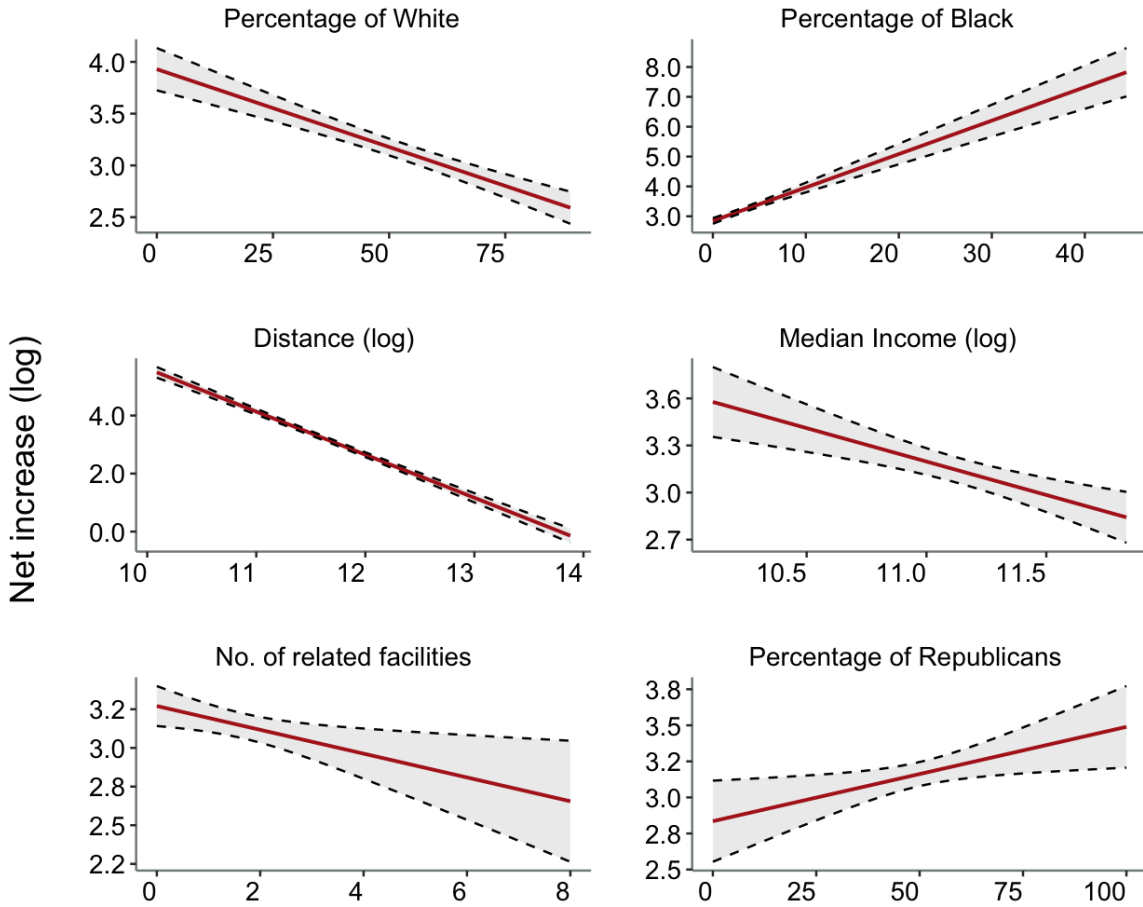
Figure 17. Correlations of Disposal Flow and Destination Community
Characteristics. These plots show potential factors determining the community-
level waste pollution relocation in California after China's GS policy. The
percentage of the White population, the distance between origin and destination,
median income, and the economies of scale of destination communities are
negatively correlated with the net increase in waste inflows. The percentage of
the Black population and the percentage of Republican voting registrations are
positively correlated with the net increase in waste pollution inflows.
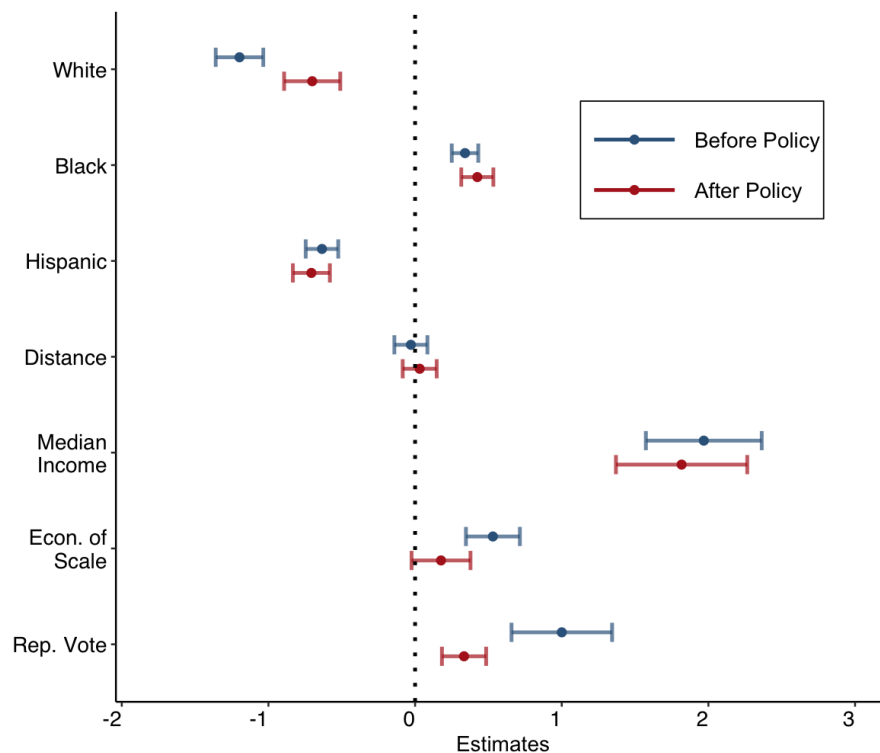
Figure 18. CalRecycle: Effect of Destination Community Characteristics on Waste Flows Before and After China's GS Policy. This plot shows the results of the fixed-effects model. Before the GS policy, the White share of the population in a community is *negatively* correlated with the amount of waste transported into the community. The Black share of the population is *positively* correlated with the amount of waste transported into the community. However, this pattern changed after the GS policy. The White communities have seen a greater increase in waste inflows than Black communities. The estimate (after the GS policy) that does not intersect with the CIs of estimates (before the GS policy) shows that the change is statistically significant.
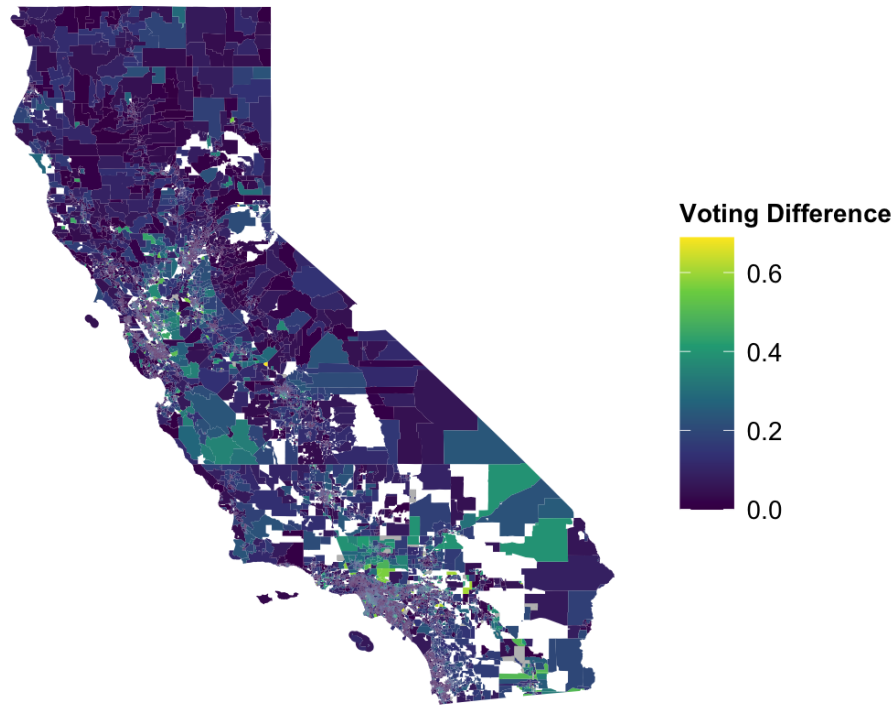
Figure 19. Potential Mechanism: Disposal Flow Map by Political Deviation.
Political deviation is one of the three potential mechanisms to explain waste
transfers across communities. Blue/green indicates the political deviation of a
community from its county in terms of Republican voting registration shares
(voting registration is the only data that is available at the precinct level in
Statewide Election Database.). White spaces indicate where no data was available.
Political deviation is calculated by the absolute difference between a community's
Republican voting registration share and its county's Republican voting registration
share. The higher political deviation a community has, the lower the political cost
such a community has for waste pollution inflows.

3.6 Tables

	Spatial Unit	Years available	Frequency
CalRecycle Disposal Flow Data	jurisdiction by facility level	2002-2020	quarterly
U.S. Census Data	census block level	2000-2020	decennial
ACS 5-year Data	census block group level	2002-2017	5-year
Waste Business Journal	facility level	1992-2020	yearly
Statewide Database Election Data	precinct level	2000-2020	4-year

Table 4. Data Sources Summary: Community-level Analysis. This table summarizes all of the data sources that are used in this paper. Disposal flow data is aggregated to origin jurisdiction, destination facility, and year. For the census data, since the geographic units are small and data frequency is low, I use 2010 census-block level data for racial composition, 2013 ACS 5-year data for median income, and 2016 precinct-level election data for vote share.

Dep.Variable: Disposal shipment (tons)	(1)	(2)	(3)	(4)
Transportation costs	-0.326***			-0.476***
	(0.113)			(0.112)
Transportation costs×1($post$)	0.031			0.0196
	(0.049)			(0.063)
Land costs		0.019		-0.063
		(0.052)		(0.060)
Land costs×1($post$)		-0.017		-0.057**
		(0.020)		(0.024)
Political costs			0.028	-0.011
			(0.041)	(0.032)
Political costs×1($post$)			-0.107*	0.101*
			(0.062)	(0.057)
County FE	✓	✓	✓	✓
Year FE	✓	✓	✓	✓
Quarter FE	✓	✓	✓	✓
R^2	0.642	0.638	0.654	0.664
Observations	293,238	291,016	210,767	209,647

Two-way clustered standard errors at the county-year level in all models. *$p < 0.1$, ** $p < 0.05$, *** $p < 0.01$.

Table 5. Potential Mechanisms: Model Estimates. Transportation costs are approximated by the distances between origin jurisdictions and destination facilities. Land costs are approximated by the population density of the communities where the destination facilities are located. Political costs are defined as the discrepancy (absolute difference) between the community Republican voting registration share (at the precinct level) and the county Republican voting registration share. For example, community A has 30 percent of Republican voters, and the county it resides in has 45 percent of Republican voters. The political cost of community A as a destination community for waste shipment is $|30 - 45| = |-5| = 5$, which is a "high" political cost. Because these communities, which have similar political ideologies as the county, are more likely to be resistant to the increased waste relocation due to the GS policy.

CHAPTER IV

WILLINGNESS TO BEAR THE COSTS OF PREVENTATIVE PUBLIC

HEALTH MEASURES

This chapter is co-authored with Trudy Ann Cameron. I had an essential role in developing the initial idea that led to this project. I also wrote a significant amount of code that generates the results in this paper. I wrote and edited many sections of the paper. I have also presented this paper at multiple seminars and conferences.

4.1 Introduction

Many policies and regulations are intended to protect human life and health. In the context of the recent global pandemic, given the externalities associated with infectious disease, public health policies have been essential. To analyze the benefits and costs of public health measures, policymakers must take into account the level of (and heterogeneity in) people's willingness to bear the costs of appropriate public health measures.

It is challenging to monetize the social benefit from costly policies to protect human life and health. Economists typically use a measure called the Value of a Statistical Life (VSL) to quantify society's willingness to bear the costs of small reduction in mortality risks for a large number of people. VSL can be interpreted as a marginal rate of substitution between individual private mortality risk and money. Mathematically, VSL is the marginal utility of a small reduction in mortality risk divided by the marginal utility of a small change in income. In 2006, for example, the U.S. Environmental Protection Agency (EPA) estimated that people in the U.S. are willing to pay about $7,000,000 for one "statistical" life.

This number means, for example, people are willing to pay about $70, on average, to reduce the probability of death by 1/100,000 for 100,000 people.[1]

For the COVID-19 pandemic, Echazu and Nocetti (2020) calculate society's overall willingness to pay for morbidity and mortality risk reductions. They estimate that the aggregate social WTP for a sizeable reduction in infection risk during a pandemic may be on the order of $3T to $7T. This dramatic estimate for WTP (for all statistical lives "lost") for risk reduction during an *infectious* pandemic likely reflects the fact that people are willing to pay not just for a reduction in their own risk of illness and death, but also to permit reductions in the stringency of pandemic restrictions. Cameron (2010) points out that VSL, as a "one-size-fits-all" measure, can hinder our ability to understand distributional effects of risk-reducing policies or interventions. A single VSL—where the majority of estimates of the VSL are derived from labor-market studies where the risk in question is sudden death in an industrial workplace accident—may also fail to reflect the particular features of COVID-19 as a specific health threat. Likewise, the populations for which wage-risk VSLs are typically estimated (prime-aged white male workers in hazardous occupations) may be a poor approximation to the characteristics of the populations most seriously affected by COVID-19.

The research described in this paper constitutes an exercise in "benefits function transfer" (Smith, Van Houtven, & Pattanayak, 2002), where the "study sample" is an existing survey-based choice experiment fielded to more that 1400 respondents in a representative probability sample of households in counties across the U.S. in 2003 (Bosworth, Cameron, & DeShazo, 2009). The goal in that

---

[1]EPA's estimates of the value of a mortality risk reduction were reviewed in a white paper called "Valuing Mortality Risk Reduction in Environmental Policy" included 33 studies between 1988 to 2009. See line 694 in this white paper.

original study was to determine the social benefits from public health policies to reduce illness and deaths from different types of health threats in the respondent's community. For the current benefits transfer task, the "policy samples" consist of the populations of all counties across the U.S. during the 2020-21 COVID-19 pandemic.

Benefits transfer has been widely used to in environmental economics to supply information for benefit-cost analyses to support policy decisions when a new study is not affordable or when no time is available to conduct a thorough new study (Richardson, Loomis, Kroeger, & Casey, 2015). Benefits *function* transfer exercises can involve study and policy samples at different points in time where conditions may be different. For example, Price, Dupont, and Adamowicz (2017) evaluate the temporal stability of willingness-to-pay values from two identical stated preference surveys undertaken in 2004 and 2012. The surveys were designed to capture the trade-offs between (a) risk reductions for two health endpoints related to tap water, and (b) monetary costs. Across these two time periods, their study found no significant differences in real-valued WTP, or in the structure of heterogeneous preferences.[2]

In the broader environmental benefits literature, it is also a common practice to estimate a benefits function for one country, and then to attempt to transfer this benefits function to another country. These efforts can be challenging, however, because there are often cultural differences between countries (especially between developed and developing countries) that can call into question whether the preferences estimated in one country should be *expected* to hold in another country

---

[2]Benefit function transfers maybe be derived from just one study, or they may combine the results for several related studies to "triangulate" the conditions for which a new benefits estimate is needed.

(Brander, Beukering, & Cesar, 2007; Lindhjelm & Navrud, 2008; Ready & Navrud, 2006). In this paper, fortunately, we seek to transfer a benefits function only between two different time periods in the U.S. This requires only that we assume that U.S. preferences over public health policies and net incomes be relatively stable across time, after controlling for changes over time in the variables that systematically affect these preferences. It also requires the assumption that *cross-sectional* differences among U.S. counties in 2003 have similar effects on public health policy preferences as do changes over time in the characteristics of these U.S. counties.

Instead of using a single one-size-fits-all VSL, our research estimates people's WTP for public health policies that reduce both illnesses and deaths, in light of both the relevant cost and the expected duration of such policies. Furthermore, rather than focusing on *private* WTP to reduce an individual's personal mortality risk, we emphasize a specifically *public* program, where people are asked their WTP for reduction in the risk of illness and deaths in their broader community. In our current analysis, we interpret *counties* as communities. Although counties are not the smallest geographic regions we might use, they are the most appropriate administrative units in the context of the original survey. During a public health crisis like the COVID-19 pandemic, publicly available data on cases and deaths are also commonly reported at the county level.

Assessing people's willingness to pay for community-level public health policies is essential for public health policymakers for four reasons. First, people from the same community often have more in common than do people from different communities, in terms of sociodemographics, ethnicities, economic status, and health characteristics. To the extent this is true, community characteristics

86

may systematically affect individuals' preferences for public health policies. Second, during an infectious pandemic like COVID-19, people's behaviors and actions are intimately related to the health and well-being of *others* who live in the same community. Third, pandemic policies have often been tailored to conditions in specific counties as authorities attempt to allocate public health resources more efficiently. Fourth, many communities struggle with specific types of health risks systematically. For example, Lincoln, Abdou, and Lloyd (2014) find that Black communities tend to suffer more from obesity and depression than do White communities. Yancy (2020) finds that, during COVID-19, infection rates within Black-dominated communities have sometimes been three times higher than that in White-dominated communities. Even more strikingly, the COVID-19 death rate for Black communities has been as much as six times higher than for White communities. With more-refined knowledge about their population's willingness to bear the costs of community-level health policies, county-level decision makers can implement public health measures with greater confidence that their strategies will deliver positive net social benefits for their constituents.

In this research, we re-analyze some high-quality stated-preference choice-experiment survey data from an original 2003 study reported in Bosworth et al. (2009) that reveals people's preferences for randomized public policies that benefit community-level health.[3] To permit out-of-sample forecasting, our re-analysis substitutes county-level explanatory variables for the individual-specific variables that were largely relied-upon to explain respondents' choices in the original study. We collect new data on county-level policy contexts with the requirement that our

---

[3]The 2003 survey was one of four surveys funded by research grants from the U.S. EPA and the National Science Foundation, and was fielded using Knowledge Networks, the leading research-quality representative consumer panel available in the U.S. at the time.

measures for all these county-level variables be available for both (a) the 2003 context and (b) the more-recent context of the 2020-21 pandemic. We need to control for differences, both across counties and between 2003 and 2020-21, in each county's mix of socio-demographic characteristics, incomes, political affiliations, health status, and access to medical care. If people's basic preferences for policies to reduce risks to public health have remained sufficiently stable between 2003 and 2020-2021, after controlling for shifts in all of these explanatory variables, lessons from our 2003 survey can illuminate people's likely policy preferences today. While we cannot identify a premium for infectious diseases, it will be helpful at least to understand what people would be willing to give up simply to avert illnesses and premature deaths at the scale of the recent pandemic.

We first estimate a latent class model and discern three classes of preferences. Within each class, people's preferences are driven by different combinations of policy attributes and community characteristics. There is evidence of considerable heterogeneity. Next, we use LASSO methods to help select the most important observable determinants of heterogeneity in preferences for public health policies using our 2003 data. Then, based on the updated community-level characteristics in counties across the U.S. in 2020-21, we use the fitted model to predict overall WTP for policies to reduce monthly generic cases and deaths on a scale commensurate with county-level casualties from the COVID-19 pandemic. For example, we find that people from Black-dominated counties have a higher WTP for public health policies than those from White-dominated counties. Residents of counties that have populations which are younger or more highly educated have lower WTP for public health interventions to reduce illnesses and deaths on a scale

such as the recent pandemic risks, compared to those who live in counties with older and less-educated populations.

Stated preference methods, such as those employed for this paper, are used frequently to quantify preferences in health economics, health technology assessment, risk-benefit analysis, and health services research (Mühlbacher & Johnson, 2016). A few contemporary survey-based discrete choice experiments have sought to understand public perceptions of COVID-19 pandemic interventions and to identify preference classes across individuals. Rees-Jones, Attoma, Piolatto, and Salvadori (2020) conduct a survey of 2,516 Americans concerning their preferences for both short- and long-term expansion to governmental-provided healthcare and unemployment insurance programs. That study finds that preferences for such programs are positively affected by the county's COVID-19 deaths, unemployment caused by COVID-19, and how respondents perceive the consequences of COVID-19. Chorus, Sandorf, and Mouter (2020) use survey-based choice experiments to infer people's preferences from the trade-offs they are willing to make among policy effects, including health-related effects, impacts on the economy, education, and personal income. They find that "the average citizen, to avoid one fatality directly or indirectly related to COVID-19, is willing to accept a lasting lag in the educational performance of 18 children, or a lasting (> 3 years) and substantial ($> 15\%$) reduction in net income of 77 households."

In an earlier, pre-COVID context, Cook, Zhao, Chen, and Finkelstein (2018) use a survey in Singapore regarding the trade-offs between risks of infectious diseases and the inconvenience of government interventions to prevent outbreaks of infectious disease. They find that respondents prefer more-intense interventions and prefer scenarios with fewer deaths and lower taxes. L. Li, Long, and Rad

(2020) use a survey-based choice experiment in three U.S. states and empirically quantify "willingness to stay home." They find broad support for statewide mask mandates. Their estimate of WTP to reduce new cases is large, and demographic and socioeconomic factors are the main drivers of the heterogeneity in individuals' willingness to stay home. Reed, Gonzalez, and Johnson (2020) also use a survey-based choice experiment in the U.S. to quantify Americans' acceptance of COVID-19 infection risks from lifting public health restrictions earlier and to reduce economic impact of the pandemic.[4]

Other recent papers focus on factors that affect people's responses to COVID-19. Cattapan, Ackerverney, Dobrowolsky, Findlay, and Mandrona (2020) find that the need for community engagement is pressing in a pandemic crisis. Engagement is essential to ensure that policy-making is built on equity, access, and inclusion. Adeel et al. (2020) find that the sub-national policies of U.S. states and Canadian provinces are more important than the national-level policies in each country.

Some studies focus on the benefit-cost analysis of restrictive public health policies during COVID-19. For example, Viscusi (2020) applies a standard Value of a Statistical Life (VSL) to monetize COVID-19 deaths for the first half of 2020 and produces a U.S. mortality cost estimate of $1.4 trillion. Miles, Stedman, and Heald (2020) conduct a benefit-cost analysis of U.K. public health policies during COVID and find that the costs of continuing severe restrictions are large compared to benefits. Dorantes, Kaushal, and Muchow (2020) use county-level data on COVID-19 mortality and infections, as well as the county-level information on

---

[4]They find four classes of people among all respondents: "risk-minimizers", "waiters", "recovery-supporters", and "openers". Political affiliation, race, household income, and employment status were all associated with class membership.

the adoption of non-pharmaceutical interventions (NPI) and find that NPIs slowed infection rates in counties where the healthcare system might otherwise have been overwhelmed by the pandemic. They also suggest that political ideology is a factor that may have limited the effectiveness of those measures in Republican-dominated counties.

4.2   Data

4.2.1   The Original 2003 Survey.   Our survey from 2003 was originally employed in an analysis that takes advantage of the characteristics of individual survey respondents to explain their policy preferences in that 2003 context. The original analysis is described in Bosworth et al. (2009). The 2003 survey produced 1,466 completed responses, and was designed specifically to elicit individuals' willingness to pay for *publicly* provided health policies.[5] Each respondent faces a choice between either of two different health policies and the status quo. For example, Policy A might be described as reducing air pollutants that cause heart disease; and Policy B might reduce pesticides in foods that cause adult leukemia. The status quo "Neither Policy" option would involve no change in community health risks, but also no cost to the respondents' household. Each policy is also described in terms of a set of attributes that includes cases and premature deaths prevented in this community, duration of the policy, and the cost of the policy. The randomized illness labels include respiratory disease, cancer, leukemia, colon/bladder cancer, asthma, lung cancer, heart disease, heart attack, and stroke. See Appendix Figure C1 for one instance of the randomized choice sets used in the survey.

---

[5]See Johnston et al. (2017) for an inventory of current best practices in SP research.

91

The original survey was fielded in June of 2003 and was distributed to members of a premium nationally representative consumer panel (Knowledge Networks) that produced a representative sample of respondents from counties throughout the conterminous U.S. The essentially national scope of the survey captured extensive geographic variation in sociodemographics, voting patterns, health status, and access to medical care. Figure 20 maps the geographic distribution across counties of our 1,466 respondents.
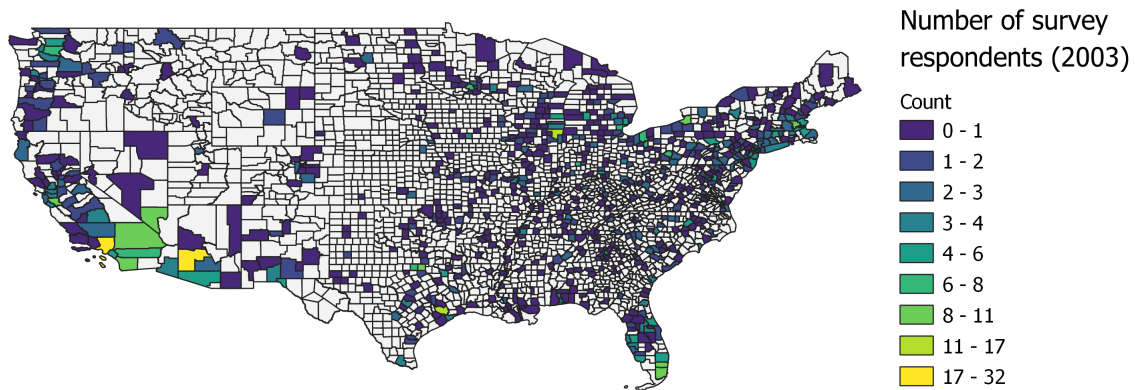
Figure 20. The map highlights every U.S. county containing one or more online survey respondents.

The main policy attributes described in each policy-choice task include monthly cost, policy duration, the size of the affected population, illnesses avoided and premature deaths averted. Our basic model allows for "status quo" effects, i.e., a discrete mass of utility, positive or negative, associated with the "Neither Policy" option, regardless of the specified attributes of either of the the two public health policies under consideration. Importantly, each policy choice was followed by a "self-interest" question about the degree to which the respondent or their family would personally benefit from that particular public health policy. Briefly, the relevant policy attributes for the present study were:

– **Affected population in thousands:** Across respondents, but not within a respondent's version of the survey, the original survey varies the size of the population affected by the policy. While it would have been ideal to describe this population as that of the respondent's own county, the anonymity of the survey prevented the tailoring of policy options specifically (in advance) to match each prospective respondents' county of residence. We asserted, about each pair of policies, that these two policies will be implemented for the "X thousand people living around you." We randomized X (among 1, 2, 3, 4, 5, 6, 7, 8, 9, 10, 15, 20 (2-3% in each case), 30 (4%), and 50, 100, 500, and 1,000 (8-15% each).

– **Policy duration:** Each prospective policy to reduce public health risks was described as a commitment to pay the cost of the policy for a specified time period.

– **Total illnesses avoided and deaths averted:** Over the specified time horizon, each policy is described as being expected to result in a specific number of cases avoided and a specific number of premature deaths averted. Preliminary models revealed that WTP for these public health policies is not simply linear in these policy attributes. Instead, people appear to derive diminishing marginal utility from additional avoided illnesses or averted premature deaths. Likewise, preferences are nonlinear in the policy's duration and in the size of the affected population.[6]

– **Status quo (or conversely, "Any policy") effects:** Respondents are allowed to choose "Neither policy" in every choice set, if they do not like either of the offered policies. Best practices in choice modeling include making an allowance for a status-quo effect. Equivalently, we use an indicator that equals one for "any policy (regardless of its effectiveness or duration)" and zero for the "Neither policy" alternative.

– **Monthly cost to your household:** Each prospective policy was associated with a specified private household cost, expressed both per month and annually, with a reminder of the duration of the commitment.

Given that we need a model that can be transferred to the 2020-21 COVID-19 context, we must forgo the use of any of the available individual-specific variables that were collected by the 2003 survey for those respondents. In place of these individual-specific variables, we recruit new county-level variables that are

---

[6]For the models in this paper, we employ logarithmic or shifted logarithmic transformations for these variables, since these functions seem best to explain people's choices.

both available and consistently measured both close to the time of the original 2003 survey and likewise close to the time of the recent pandemic.

Most of our 1,466 respondents made five policy choices each. For our estimating sample, then, the 14,466 non-status-quo policies described in our choice experiments have randomized levels of each attribute, with the attribute levels in each case designed to span a wide range of possible policy choice scenarios. Fortunately, the original design spans the potentially relevant ranges of attributes for the 2020-21 pandemic. The arbitrary randomized distribution of the program design attributes used in the 2003 survey is summarized in Table 6.

	mean	sd
Pop. affected/county pop.	2.706	8.341
Duration of policy (months)	167.9	116.6
Baseline illnesses	1004.7	2334.5
Number of illnesses avoided	606.9	13854.
Baseline deaths	96.16	472.0
Number of deaths avoided	102.1	467.9
Policies	14466	

Table 6. Descriptive Statistics, Public Health
Policy Design Variables, Choice Experiments
Posed within the 2003 Estimating Sample

4.2.2   County-level Sociodemographic and Contextual

Heterogeneity.   Respondents to the original survey considered an aggregate of 7,233 choice sets. The randomized design of the choice experiments permits the estimation of a set of homogeneous preferences without any risk of bias from

omitted policy attributes. In this paper, however, we seek to identify important dimensions of preference heterogeneity. We permit policy preferences to vary systematically with the characteristics of the community-of-residence (county) for each respondent. Models with adequate preference heterogeneity can potentially allow us to predict changes in demand for public health policies, over time, in response to changes in sociodemographics, political ideologies, and healthcare access.[7] The cross-sectional variation in the original sample can be exploited to accomodate differences in the composition of county populations across the 17-year interval between the original 2003 study period and the recent 2020-21 policy period.

4.3 Estimating Specification

We specify indirect utility as linear in net income. This is a common practice and is expedient because this functional form allows the individual's own household income level to drop out of the utility difference that drives the model. This leaves only the policy cost as a dollar-denominated measure that can be used to calculate the marginal rates of substitution that can be interpreted as marginal willingnesses to pay for avoided illnesses and avoided premature deaths.[8]

Preliminary exploration of the data has revealed that people tend to experience diminishing marginal utility from illnesses prevented and premature deaths averted. Given that microeconomic theory does not guide the functional form of utility beyond an expectation of diminishing marginal utility, we generalize our additively separable shifted-logarithmic form to a more flexible translog-type specification that is quadratic in these shifted log transformations. We include

---

[7]See data source in Appendix C1.

[8]This description of the model assumes a basic familiarity with utility-theoretic conditional logit choice models.

the square of each logged variable and the interaction between these logged terms to yield a translog-type specification in terms of the changes in the numbers of illnesses and deaths associated with policy A.[9]

$$
\begin{aligned}
V_i^A = {} & \alpha \left(Y_i - c_i^A \right) \\
& + \beta_1 log \left(\Delta illnesses^A + 1 \right) + \beta_2 log \left(\Delta illnesses^A + 1 \right)^2 \\
& + \beta_3 log \left(\Delta deaths^A + 1 \right) + \beta_4 log \left(\Delta deaths^A + 1 \right)^2 \\
& + \beta_5 \left[log \left(\Delta illnesses^A + 1 \right) \times log \left(\Delta deaths^A + 1 \right) \right] + \beta_6(0) + \epsilon^A
\end{aligned}
\tag{4.1}
$$

where β_6 is the lump of utility associated with the status-quo alternative, which involves no policy. For Policy A in equation (4.1), of course, there is no status-quo utility increment/decrement.[10] Under the status quo alternative, in the absence of the policy, there will be no cost, but also no changes in the baseline numbers of illnesses or deaths, so that indirect utility will be determined simply by the individual's income and any utility associated with the status quo:

$$
V_i^N = \alpha \left(Y_i \right) + \beta_6(1) + \epsilon^N
\tag{4.2}
$$

Thus, in a pairwise choice between just Policy A and No Policy (N), the utility-*difference* will depend on the cost of the policy, the expected cases of illness avoided, and the expected number of premature deaths averted under the chosen

---

[9]A shifted logarithmic transformation adds one to the argument of the log function, ensuring that the function takes a value of zero when the argument is zero. An alternative to our specification in equation (4.1 where utility is expressed in terms of *reductions* in illnesses and deaths (which should be "goods") would be to use *absolute* illnesses and deaths, with and without each policy (which would imply that each attribute was a "bad", likely to confer a negative marginal utility).

[10]If the interaction term in equation (4.1 does not have a statistically significant coefficient, the level curves of the indirect utility function would to be circular, rather than elliptical.

policy:

$$V_i^A - V_i^N = \alpha\left(-c_i^A\right)$$

$$+ \beta_1 log\left(illnesses^A + 1\right) + \beta_2 log\left(deaths^A + 1\right) \tag{4.3}$$

$$+ \beta_3 log\left(\Delta illnesses^A + 1\right) + \beta_4\left[log\left(\Delta illnesses^A + 1\right)\right]^2$$

$$+ \beta_5 log\left(\Delta deaths^A + 1\right) + \beta_6\left[log\left(\Delta deaths^A + 1\right)\right]^2 \tag{4.4}$$

$$+ \beta_7\left[log\left(\Delta illnesses^A + 1\right) \times log\left(\Delta deaths^A + 1\right)\right]$$

$$+ \beta_8(-1) + (\epsilon^A - \epsilon^N)$$

Note that if baseline levels of illness or death are to affect utility within this particular framework, they need to be interacted with the changes in the numbers of illnesses and deaths under each policy. To limit the complexity of the specification, we will allow baseline illnesses to shift only the marginal utility of reductions in the number of illnesses, and allow baseline deaths to shift only the marginal utility of reductions in the number of deaths. We also allow the baseline marginal utility parameters in the equation 4.3 to vary with selected sociodemographic variables for each respondent's county. The coefficients on these interactions capture the extent to which these county-level variables affect the underlying preference parameters $\beta_1, ..., \beta_6$. As is typical, we assume that the marginal utility of net income is approximately constant.[11]

4.4   Results

4.4.1   Identifying Dimensions of Heterogeneity: LASSO

Estimation.   Table 7 provides parameter estimates for a set of three increasingly complex specifications. After employing our shifted log transformations, Model 1 in

---

[11]This description of the basic model assumes pairwise choices between a single policy and the status quo. In the data, however, respondents are asked to choose between a pair of policies and the status quo alternative. The model in equation (4.3) can readily be generalized to accommodate three-way policy choices.

Table 7 is even simpler than equation (4.3), being linear and additively separable. Model 2 is a homogeneous-preferences model that is consistent with equation (4.3), involving some key interactions between the basic attributes. Model 3 permits the preferences in equation (4.3) to vary systematically with the characteristics of each respondent's county (circa the 2003 time period). To identify the subset of more-important sources of systematic heterogeneity in policy preferences across counties, we force the basic attributes into the model. We then interact each of the basic attributes with all of the available county-level data and subject just these interaction terms to LASSO variable selection.

characteristics and select the most important interactions using LASSO model estimation.[12] We use a LASSO model with 10-fold cross-validation to yield the variables and interactions in the model specification in section 3. We then use the LASSO-selected variables in a conditional logit model with individual fixed effects to produce both the parameter means and their asymptotic variance-covariance matrix for use in deriving WTP estimates for our 2020 WTP simulation.[13] Table 7 model 3 provides the preliminary results based on LASSO-selected variables and binary choice model estimation.

4.5 Benefit Transfer: 2020-21 WTP to Avoid COVID-19 Illnesses and Deaths in Each Month

In contrast to the wide variety of choice scenarios presented to respondents in our 2003 study sample, we wish to use our estimated model to simulate WTP in

---

[12]Packaged LASSO algorithms for logit models appear to be limited to binary choice specifications. We assume that the same set of preferences underlie our three-way choices as would drive the two pairwise choices that would be consistent with these three-way choices would remain the preferred alternatives if it was to be paired with either of the two non-chosen alternatives from the three way choice.

[13]Double Lasso: Use machine learning Lasso algorithm to select the variables. Then take the selected variables back into a maximum likelihood the conditioned logit model with individual fixed effects.

Table 7. WTP Estimation Model Results

	(1) Parsi- monious	(2) Homo- geneous	(3) Double Lasso
Preferred alternative in choice scenario			
Monthly cost	-0.01***	-0.01***	-
	(0.0007)	(0.0009)	0.015*** (0.004)
... × Unemployment (v last month)			0.0069** (0.0025)
Policy duration	-0.02***	-	-0.013**
	(0.002)	0.013*** (0.005)	(0.0048)
Log(base illnesses + 1)	-0.037. (0.02)	0.32* (0.13)	0.44** (0.15)
... × County prop. Hispanic			-0.77*** (0.14)
$[$Log(base illnesses + 1)$]^2$		-0.017* (0.0065)	-0.037** (0.011)
... × County log. median income			-0.082* (0.038)
... × County poverty rate			-0.297** (0.113)
... × County prop. obesity			-0.57* (0.238)
... × County prop. excessive-drinking			-0.143* (0.065)
... × Primary care physicians rate			-
			0.001*** (0.0003)

Table 7 (continued).

	(1) Parsi-monious	(2) Homo-geneous	(3) Double Lasso
Log(base illnesses + 1) × Log(duration)		-0.028 (0.021)	-0.061* (0.030)
... × County log. median income			0.178*** (0.043)
... × County prop. obesity			-1.182** (0.328)
... × PM2.5			0.008** (0.003)
... × Primary care physicians rate			0.002** (0.0008)
Log(base illnesses + 1) × (Affected pop/1000)$^{-1}$		-2.43* (1.33)	-3.67 (7.15)
... × County prop. Hispanic			69.49* (10.26)
... × PM2.5			0.58* (0.295)
Log(base deaths + 1)	0.039 (0.031)	-0.4 (0.19)	-0.23 (0.31)
... × County prop. aged 65-84			12.96 6.235
... × County prop. excess.-drink.	0.039 (0.031)	-0.4 (0.19)	-6.234 (2.167)
(Log(base deaths + 1))^2		0.011. (0.012)	-0.0016 (0.0056)
... × County prop. Black			0.198* (0.081)
Log(base deaths + 1) × Log(duration)		0.06. (0.035)	0.063 (0.042)
... × Primary care physicians rate			0.001** (0.0004)

Table 7 (continued).

	(1) Parsi-monious	(2) Homo-geneous	(3) Double Lasso
... × Preventable hospitalization rate			0.003* (0.001)
Log(base deaths + 1) × (Affected pop/1000)$^{-1}$		3.65. (1.96)	14.82 * (9.47)
... × County log. median income			-40.8* (9.57)
... × County prop. aged 65-84			-328.7* (122)
Log(Δ illness + 1)	0.068*** (0.0097)	0.039 (0.052)	-0.26*** (0.035)
... × Unemployment (v last month)			0.353* (0.151)
... × County prop. Asian			6.46*** (1.89)
... × County poverty Rate			-4.05* (1.85)
... × County avg. physical unhealthy days			0.278** (0.087)
(Log(Δ illness + 1))^2		0.0073 (0.0038)	-0.016. (0.009)
... × County prop. Republican			0.053*** (0.015)
... × Unemployment (v last month)			0.029** (0.011)
... × County prop. aged 0-17			-0.534* (0.219)
... × County prop. Black			0.097** (0.037)

Table 7 (continued).

	(1) Parsi-monious	(2) Homo-geneous	(3) Double Lasso
... × County prop. Asian			-0.304* (0.153)
... × County log. median income			0.04* (0.018)
... × County avg. physical unhealthy days			- 0.031*** (0.007)
... × County prop. obesity			-0.339* (0.171)
... × Primary care physicians rate			- 0.0004** (0.0001)
... × Preventable hospitalization rate			0.0006* (0.0002)
Log(Δ illness + 1) × Log(duration)		-0.0061 (0.0088)	-0.111** (0.038)
... × County log. median income			0.059* (0.029)
... × preventable hospitalization rate			-0.013* (- 0.0005)
Log(Δ illness + 1) × (Affected pop/1000)$^{-1}$		0.077 (0.052)	1.17* (0.50)
... × Unemployment (v last month)			0.37* (0.17)
... × County prop. Black			-3.48*** (0.84)
Log(Δ deaths + 1)	0.20*** (0.018)	0.45*** (0.091)	0.51*** (0.11)

Table 7 (continued).

	(1) Parsi-monious	(2) Homo-geneous	(3) Double Lasso
$(\text{Log}(\Delta \text{ deaths} + 1))^2$		-0.0083 (0.007)	-0.14* (0.061)
... × County prop. Black			0.198* (0.081)
... × Primary care physicians rate			-0.0005* (0.0002)
$\text{Log}(\Delta \text{ deaths} + 1) \times \text{Log(duration)}$		-0.034 (0.016)	0.23* (0.094)
... × County poverty rate			-1.51** (0.51)
... × County prop. excessive-drinking			-0.44* (0.23)
$\text{Log}(\Delta \text{ deaths} + 1) \times (\text{Affected pop}/1000)^{-1}$		-0.21* (0.085)	1.01 (0.7)
... × County prop. Asian			-8.97* (4.52)
... × County prop. obesity			-14.8* (5.85)
... × County excessive-drinking rate			-6.82* (3.17)
... × Primary Care Physicians Rate			-0.008* (0.003)
1=Status quo	0.68*** (0.071)	1.13*** (0.13)	2.53* (1.11)
... × Unemployment (v last month)			-0.88** (0.33)
... × County prop. Black			5.62*** (1.67)
... × County prop. Asian			8.78* (3.97)

Table 7 (continued).

	(1)	(2)	(3)
	Parsi-monious	Homo-geneous	Double Lasso
... × County prop. aged 65-84			-5.4* (2.2)
... × Primary care physicians rate			-0.0051. (0.0019)
1=Status quo × (Affected pop/1000)$^{-1}$		-2.75*** (0.62)	8.01. (4.57)
... × County prop. Republican			-10.77 ** (3.85)
... × County prop. Black			36 *** (6.82)
... × County log. median income			9.98 * (4.41)
... × County prop. college			-39.35 *** (11.81)
... × County prop. smoker			107.8*** (23.51)
... × County prop. excessive-drinking			39.6*** (19.6)
(1=Status quo × (Affected pop/1000)$^{-1}$)^2		2.04*** (0.60)	-11.78* (5.12)
... × Unemployment (v last month)			5.36** (1.96)
... × County prop. Black			-30.9*** (7.0)
... × County prop. aged 65-84			-81.36* (39.52)
... × County log. median income			-25.8** (7.24)

Table 7 (continued).

	(1) Parsi- monious	(2) Homo- geneous	(3) Double Lasso
… × County prop. Asian			75.1** (33.5)
… × County prop. college			40.84** (14.03)
… × County poverty rate			85.25*** (25.72)
… × County avg. physical unhealthy days			-7.08*** (1.88)
… × County prop. smoker			108.3** (24.82)
… × County prop. excessive-drinking			-55.1** (19.65)
… × Preventable hospitalization rate			0.11** (0.04)
Max. log-likelihood	-	-	-9935.82
No. respondents	11674.45 1518	11627.78 1518	1466
No. choices	7492	7492	7233
No. alternatives	22476	22476	21699

2020-21 by a representative individual in each U.S. county to prevent the numbers of COVID-19 cases and deaths recorded in each month for which data are available. We wish to simulate a measure of the household costs that people would have been willing bear, if a public health policy in 2020-21 could reduce new illnesses and baseline deaths to zero. COVID-19 is infectious, so until all of the cases are eliminated, people cannot return to a normal life. Table 8 shows the hundreds of

new COVID cases each month across the entire U.S., along with the thousands of the reported deaths. The policy we wish to simulate for 2020-21 is the reduction of these baseline cases and deaths to zero.

Month	03/2020 mean/sd	04/2020 mean/sd	05/2020 mean/sd	06/2020 mean/sd	07/2020 mean/sd
COVID-19 cases	0.58	2.74	2.24	2.62	5.97
	4.91	17.28	11.72	14.05	31.05
COVID-19 deaths	0.014	0.18	0.13	0.07	0.08
	0.16	1.61	0.79	0.39	0.44

Month	08/2020 mean/sd	9/2020 mean/sd	10/2020 mean/sd	11/2020 mean/sd	12/2020 mean/sd
COVID-19 cases	4.54	3.74	5.84	13.50	19.77
	28.01	12.01	16.50	40.97	83.00
COVID-19 deaths	0.09	0.07	0.07	0.11	0.23
	0.46	0.29	0.19	0.30	0.71

Month	1/2021 mean/sd	2/2021 mean/sd	3/2021 mean/sd	4/2021 mean/sd	5/2021 mean/sd
COVID-19 cases	19.11	7.33	5.51	6.05	2.82
	85.75	25.84	19.96	20.46	8.79
COVID-19 deaths	0.29	0.22	0.12	0.08	0.05
	1.42	1.06	0.57	0.36	0.21
Observations 3142	3142	3142	3142	3142	3142

Table 8. Descriptive Statistics, 2020-21 COVID-19 New Cases and Deaths (in hundreds), County-level.

4.5.1 Preferences for a Representative Individual in Each County, for Each County-Month of the 2020-21 Pandemic.

In lieu of each individual respondent's characteristics, our estimating specification explains the choices of individuals using only the characteristics of the county in which the individual resides. The distribution of characteristics of the U.S. counties used in simulating our WTP amount for 2020 are shown in Table 9.

4.5.2 Parametric Bootstrap Estimates of Predicted WTP in Each County-month.

We estimate our models in utility space, so the calculations of WTP involve dividing other coefficients by the estimated marginal utility of net income, where all the maximum likelihood parameters in the model are distributed asymptotically joint normal. We used a large number of draws from the joint distribution of the parameters to calculate the predicted distribution of WTP to reduce to zero all COVID cases and deaths in each county-month, with the distribution being determined by the noise in the parameters' estimates. Given that there were no opportunities for respondents to record a negative willingness to pay, we interpret negative calculated point values of WTP values as zero, using a Tobit-like interpretation. We calculate monthly average WTP to reduce to zero all cases and deaths attributed to COVID-19 from March 2020 to February 2021 across all counties in the U.S.

For March 2020 through February 2021, Table 10 shows for a representative county resident across all U.S. counties, the average monthly WTP to reduce to zero of the COVID-19 cases and deaths. These monthly estimates vary by the changes of monthly new cases, deaths, and unemployment rates at the county level. May, July, August, September, and October 2020 had relatively high WTP to reduce new COVID cases and deaths compared to other months. These monthly

Table 9. Descriptive Statistics, 2003 Estimating Sample vs 2020 Simulation Sample, County-level Heterogeneity(for candidate interaction terms considered in Lasso model, where not all interactions are retained.)

	Study Sample		Policy Sample	
	2003[a]		2020-2021[b]	
	mean	(sd)	mean	(sd)
County prop. aged 0-17	0.254	(0.0289)	0.22	(0.033)
County prop. aged 18-24	0.096	(0.029)	0.086	(0.033)
County prop. aged 65+	0.129	(0.038)	0.193	(0.046)
County prop. White	0.773	(0.168)	0.835	(0.161)
County prop. Black	0.114	(0.129)	0.091	(0.146)
County prop. Asian	0.029	(0.044)	0.013	(0.026)
County prop. Hispanic	0.105	(0.137)	0.093	(0.138)
County prop. Native American	0.008	(0.026)	0.015	(0.058)
County prop. uninsured	0.160	(0.057)	0.114	(0.050)

Table 9 (continued).

	Study Sample		Policy Sample	
	2003[a]		2020-2021[b]	
	mean	(sd)	mean	(sd)
County fractionalization (0-1)	0.383	(0.219)	0.280	(0.196)
Rep/(Dem+Rep), Pres. Election	0.511	(0.121)	0.667	(0.161)
County Med. Income	34766.67	(9392.89)	37219	(10592.8)
Hospitals per 10000 population	0.221	(0.338)	0.56	(0.876)
County prop. college degree	0.509	(0.104)	0.524	(0.107)
County overall Poverty	0.124	(0.0433)	0.144	(5.65)
County PM2.5	11.066	(2.623)	6.59	(1.47)
County prop. Fair or Poor Health	0.158	(0.043)	0.179	(0.047)
Avg. Num. Physically Unhealthy Days	3.566	(0.72)	3.99	(0.6.95)

Table 9 (continued).

	Study Sample		Policy Sample	
	2003[a]		2020-2021[b]	
	mean	(sd)	mean	(sd)
Avg. Num. Mentally Unhealthy Days	3.475	(0.682)	4.183	(0.594)
County prop. Smoker	0.203	(0.046)	0.175	(0.035)
County prop. Obesity	0.272	(0.0404)	0.33	(0.054)
County prop. Excessive Drink	0.165	(0.04)	0.175	(0.0317)
Primary Care Physicians Rate	0.906	(0.442)	0.543	(0.034)
Preventable Hospitalization Rate	70.7	(19.4)	48.67	(18.28)
Δ unempl (Jun. '03 vs previous month)	0.678	(0.408)		
Δ unempl (Mar. '20 vs previous month)			0.467	(0.934)
Δ unempl (Apr. '20 vs previous month)			7.663	(4.928)

Table 9 (continued).

	Study Sample		Policy Sample	
	2003[a]		2020-2021[b]	
	mean	(sd)	mean	(sd)
Δ unempl (May '20 vs previous month)			-2.119	(2.451)
Δ unempl (Jun. '20 vs previous month)			-1.887	(2.227)
Δ unempl (Jul. '20 vs previous month)			-0.594	(1.523)
Δ unempl (Aug. '20 vs previous month)			-1.179	(1.354)
Δ unempl (Sep. '20 vs previous month)			-0.682	(1.258)
Δ unempl (Oct. '20 vs previous month)			-0.649	(1.092)
Δ unempl (Nov. '20 vs previous month)			0.0454	(1.052)

Table 9 (continued).

	Study Sample		Policy Sample	
	2003[a]		2020-2021[b]	
	mean	(sd)	mean	(sd)
Δ unempl (Dec. '20 vs previous month)			0.2093	(1.024)
Δ unempl (Jan. '21 vs previous month)			0.4107	(1.058)
Δ unempl (Feb. '21 vs previous month)			-0.182	(0.593)
Δ unempl (Mar. '21 vs previous month)			-0.375	(0.570)
Δ unempl (Apr. '21 vs previous month)			-0.5905	(0.573)
Δ unempl (May. '21 vs previous month)				
Observations	1466 respondents		3142 counties	

[a] Descriptive statistics, across respondents, for the counties in which they reside;

[b] Descriptive statistics across 3142 counties or other county FIPS geographic areas.

Month	03/2020 med/mean/sd	04/2020 med/mean/sd	05/2020 med/mean/sd	06/2020 med/mean/sd	07/2020 med/mean/sd
	0	321.12	0	6.82	384.86
WTP(dollars)	111.19	954.69	230.93	255.78	1084.63
	(483.69)	(5902.04)	(989.29)	(1014.05)	(8863.67)
Month	08/2020 med/mean/sd	09/2020 med/mean/sd	10/2020 med/mean/sd	11/2020 med/mean/sd	12/2020 med/mean/sd
	113.33	164.62	204.56	309.94	342.14
WTP(dollars)	377.38	453.63	532.97	636.93	693.35
	(1228.37)	(2068.25)	(1834.24)	(2278.77)	(2445.96)
Month	01/2021 med/mean/sd	02/2021 med/mean/sd	03/2021 med/mean/sd	04/2021 med/mean/sd	05/2021 med/mean/sd
	327.46	232.55	189.10	180.07	163.82
WTP(dollars)	679.62	500.20	432.96	433.46	366.32
	(2830.37)	(2038.80)	(1676.48)	(1691.01)	(1202.98)
Observations	3142	3142	3142	3142	3142

Table 10. County Representative Individual's (monthly) WTP to Reduce COVID-19 Cases and Death through 2020-21

WTP amounts were larger during the first wave of the pandemic spring and summer. The average monthly WTP increased from March 2020 to May 2021.

4.5.3 Scaling to Monthly National Total WTP Amounts to Avoid COVID-19 Cases and Deaths.

Our benefits transfer exercise predicts monthly WTP amounts for a representative adult in each U.S. county over the course of the pandemic from March 2020 through February 2021. It is possible to scale these WTP amounts to a national average for all U.S. adults by weighting

these county averages by the population of adults aged 18 and over in each county. We use county populations aged 18 and over, according to the 2019 5-year ACS estimates, to build a set of weights that sum to the overall number of counties. To get a rough estimate of the national average WTP in each month, we multiply the WTP point estimate for each county in that month by the corresponding weight, sum, and divide by the number of counties to yield average WTP that can be applied for all 251 million adults in the U.S.

The aggregate WTP across the whole adult population of the U.S. adults is then just this national average times 251 million. These totals, by month, are, for 2020: March (123 billion), April (606 billion), May (118 billion), June (125 billion), July (402 billion), August (104 billion), September (130 billion), October (160 billion), November (221 billion), December (253 billion); and for 2021: January (262 billion), February (192 billion), March (174 billion), Apr (179 billion), and May (154 billion). The cumulative U.S. national WTP, for all adults over 18 through March 2020 to May 2021, is about 3 trillion dollars.

It may be tempting to compare this aggregate WTP amount to the sizes of the various "stimulus packages" provided during the pandemic. However, the context for the trade-offs between policy cost and reductions in cases and deaths, in our study sample, did not include an economic shutdown or excessive job losses or business failures. The various stimulus packages during the pandemic were intended to compensate for the collateral economic damages caused by the pandemic, rather than simply to reduce cases and deaths. Our 3 trillion dollar estimate of WTP for March 2020 through Apr 2021 should probably be interpreted as people's *net* WTP to reduce cases and deaths, after the compensation represented by the various stimulus programs for other pandemic costs.
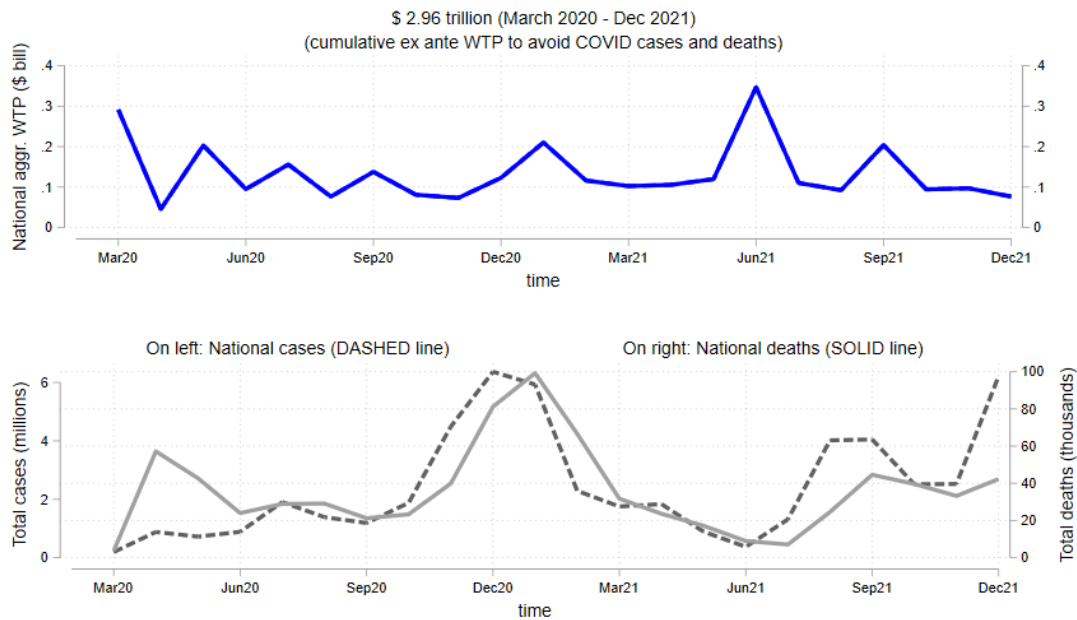
Figure 21. Aggregate WTP to Reduce the Risk of COVID-19 among all U.S.
Counties in 2020-21. The upper graph displays the total U.S. willingness-to-pay
(WTP) for reducing COVID cases and fatalities over time, while the lower graph
presents the actual cases and deaths from COVID during the same period. The
aggregated WTP generally mirrors the trends in cases and deaths, although factors
like unemployment may influence WTP for community health in specific months,
such as June 2021.

115
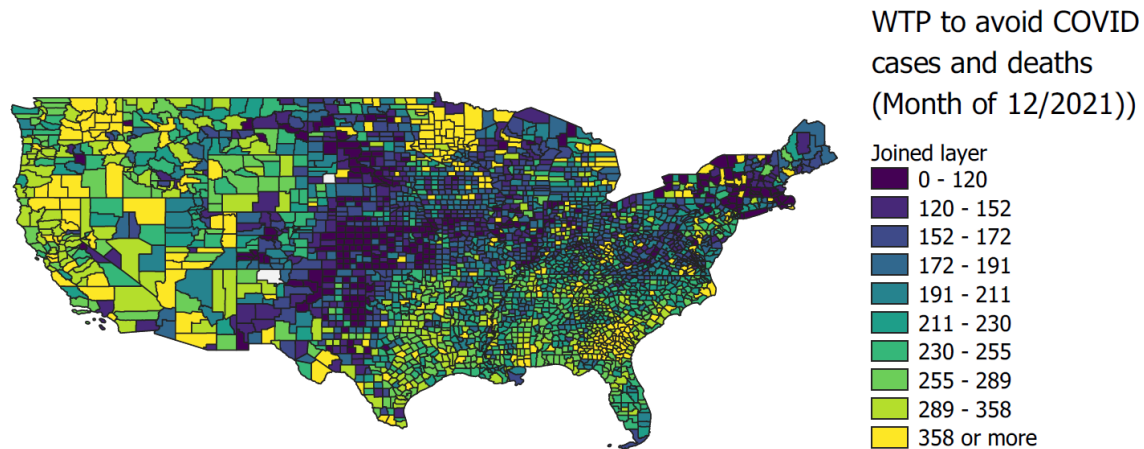
Figure 22. Spatial Distribution of WTP to Reduce the Risk of COVID-19 among all U.S. Counties in December 2021. Estimations of WTP across counties vary over time based on factors such as cases and deaths, unemployment rates, and monthly changes in unemployment rates. Additionally, they differ spatially due to each county's unique sociodemographic characteristics. The spatial distribution of WTPs reveals that counties on the west and east coasts exhibit higher values than those in the Midwest. The WTP for reducing COVID cases and fatalities in counties shows considerable variation.

4.5.4 Systematic Heterogeneity in Predicted WTP to Reduce COVID-19 Cases and Deaths.

We also explore a latent class model that uses only the policy attributes in the utility-difference function, but introduce county-level covariates for each respondent to explain each person's probability of preference-class membership in 2003. In our latent class model, we find three distinct classes of people driven by different features of the preventative public health policies. We label these three preference classes as "cost-conscious," "comprehensive," and "indifferent-or-altruistic."[14] Then, we explore the systematic heterogeneity in predicted WTP to reduce COVID-19 cases and deaths in our 2020-21 simulation. We find that the counties with a population where the proportion of people aged below 45 is lower than the national median have a higher WTP to

---

[14]See Latent class analysis detail in Appendix Table C2.

reduce the risk of COVID-19, especially when entering the winter season (Nov 2020 to Feb 2021). For different ethnic and political groups, we find that for our policy sample in 2020-21, counties with a proportion of Black residents greater than the median have a higher WTP to reduce the risk of COVID-19 than White counties. For political affiliation, we find that Democrat-dominated counties have a higher WTP through March 2020 to April 2021. For the health access level, the higher health-access counties with the primary care physicians rates and preventable hospitalization rates above the median rates among all counties have a higher WTP to reduce the risk of COVID-19 through public health policies. And lastly, for income level, the WTP of higher-income counties is higher than the lower-income counties.

4.6 Conclusions

This paper models people's willingness to bear the costs of public health policies to reduce health risks to their communities. We re-purpose an existing 2003 survey of public health policy preferences, omitting the available individual-level characteristics for the 2003 sample, and expanding the variety of county-level characteristics employed. Almost 18 years passed between the original nationwide survey. However, the U.S. EPA is likewise still making use of a suite of empirical estimates of people's willingness to trade off money for mortality risk reductions—the so-called "value of a statistical life"—from the 1970s, 1980s, and 1990s, after adjusting these numbers to current dollars. This suggests an implicit assumption that people's preferences with respect to mortality risks are highly stable over time.

We have noted several examples of stated-preference choice experiments concerning COVID-19, conducted very early during the recent pandemic. However, none of these contemporaneous studies has elicited such detailed data from its survey respondents.

In our re-analysis of the 2003 survey data, we use a conditional logit model with heterogeneous preferences (where variable selection is based on double LASSO estimation) and a latent class model. In our conditional logit model with heterogeneity in preferences, we allow for heterogeneity only with county-level demographic characteristics and other contextual variables, rather than any individual-specific characteristics. We first use a machine learning algorithm—double LASSO—to winnow down all of the possible interaction terms between the policy attributes and the county-level characteristics that are available for both the 2003 context and the 2020 context. In our latent class model, we identify three distinct preference classes in our sample: "cost-conscious," "comprehensive," and "indifferent-or-altruistic."

Finally, we simulate WTP amounts during the COVID-19 pandemic by transferring our fitted model from our "study" sample in 2003 to our "policy" sample consisting of all U.S. counties in 2020-2021. We replace the "cases prevented" and "premature deaths prevented" attributes for the randomized public health policies described in the original stated-preference choice experiments with the actual county-level monthly COVID-19 cases and deaths during March 2020 through February 2021. We also update all the county-level characteristics from the 2003 era to the 2020-2021 era. We interpret predicted WTP amounts in 2020-21 as WTP for a representative adult in every U.S. county.

Our estimated aggregate WTP across the U.S. population from March 2020 to April 2021 is about 3 trillion dollars. In April 2020, the U.S. had the highest total WTP to reduce cases and deaths of COVID-19 because of the drastic increase in new COVID-19 cases, deaths, and unemployment during the month. The large aggregate WTP persisted for the rest of 2020 and started decreasing in February

2021 as the pandemic become more under control because of vaccinations and stabilized unemployment numbers.

Information about the public's willingness to bear the costs of pandemic control will be important in the event of future pandemics. An understanding of systematic differences in willingness to pay across counties with different sociodemographics can potentially help county-level governments decide upon locally appropriate and acceptable public health interventions.

CHAPTER V

DISSERTATION CONCLUSION

This dissertation has highlighted the significance of recycling and public

health policies through a comprehensive examination of China's waste import

ban and its effects on the international recycling market and environmental

outcomes, and an estimation of people's WTP for public health during a pandemic.

Despite the limited research on these policies, the study uncovers numerous policy

implications that can inform future policy decisions and interventions.

Chapter 2 of this dissertation delved into the impact of China's waste

import ban on the U.S. environment, revealing a substantial increase in U.S.

methane emissions following the policy's implementation. By employing a

synthetic control method, I have determined that several U.S. states, including

California, Virginia, New York, and Texas, experienced significant increases in

emissions from their waste industries. These findings demonstrate that recyclable

wastes, which were once profitable, have become an environmental burden due

to the international policy change. I have demonstrated a direct cause-and-effect

relationship between the export of waste and domestic emissions from the waste

industry. My findings show that for every metric ton of recyclable waste exported,

there is a decrease in domestic CO_2 emissions by 0.89 metric tons.

Chapter 3 investigated the distributional effects of China's waste ban on

local communities in California. I have employed a fixed effects model was utilized

to analyze waste transfers and the socioeconomic and demographic characteristics

of the involved communities. I find that, following China's policy change, lower-

income white communities have received relatively more waste from other locations,

reducing the racial disparity associated with waste transfer. I identify land costs as

the primary mechanism for this pattern change.

120

Chapter 4 assessed the willingness of people to pay for public health policies that benefit both themselves and others. Using survey data from 2003 and applying a benefit transfer-function technique, we estimate that the aggregate willingness to pay for U.S. adults to prevent COVID-19 cases and deaths during March 2020-Feb 2021 was around $3 trillion, similar to the size of COVID-19 stimulus payments in 2020. These findings suggest that public health policies remain relevant and valuable, with potential applications to future pandemics if people's preferences remain constant.

This dissertation emphasizes the crucial role of policy evaluations, particularly in the realms of recycling and public health policies. The findings indicate that China's waste import ban has far-reaching environmental consequences in the U.S. at national, state, and local levels, extending beyond its direct trade impact. Additionally, the study highlights the continuing importance of public health policies, as evidenced by the estimated aggregate willingness to pay of $3 trillion to reduce COVID-19 cases and deaths, even without factoring in the problem of a contagious cause.

A.1 Figures
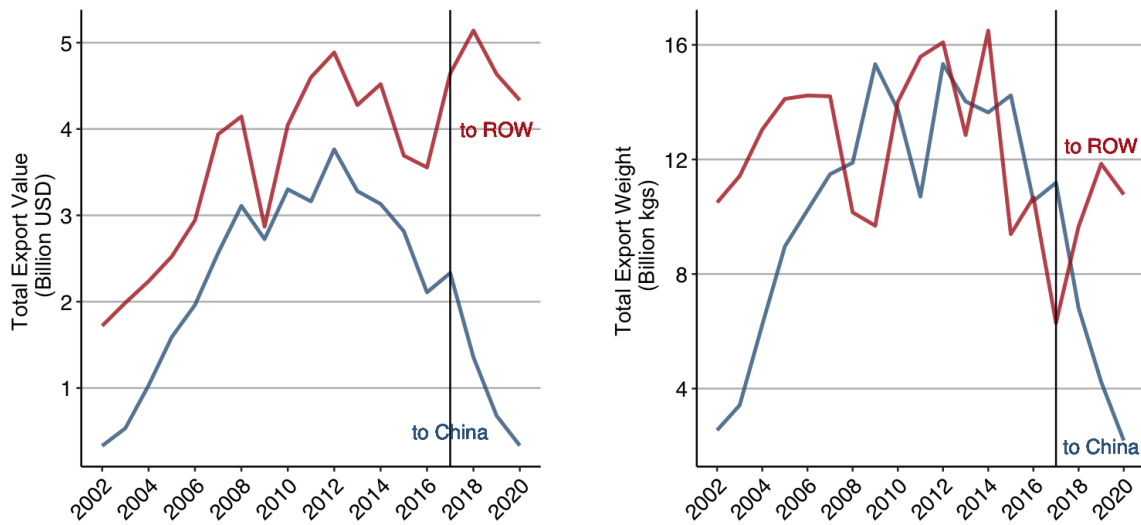
Figure A1. Other Countries' Recyclable Waste Exports to China and the
Rest Of the World (ROW)."Other countries" refers to 11 selected OECD
countries—Australia, Austria, Canada, France, Germany, Portugal, New Zealand,
the United Kingdom, Japan, Spain, and Finland. They all have regular trade with
China in recyclable wastes. Recyclable waste exports from other countries to China
decrease drastically by value and weight. After the GS policy, recyclable waste
exports from other countries to the rest of the world increased temporarily and
fell eventually after the GS policy. These plots show that most of the developed
countries that previously exported a substantial share of their recyclable wastes are
now dealing with these wastes on their own.
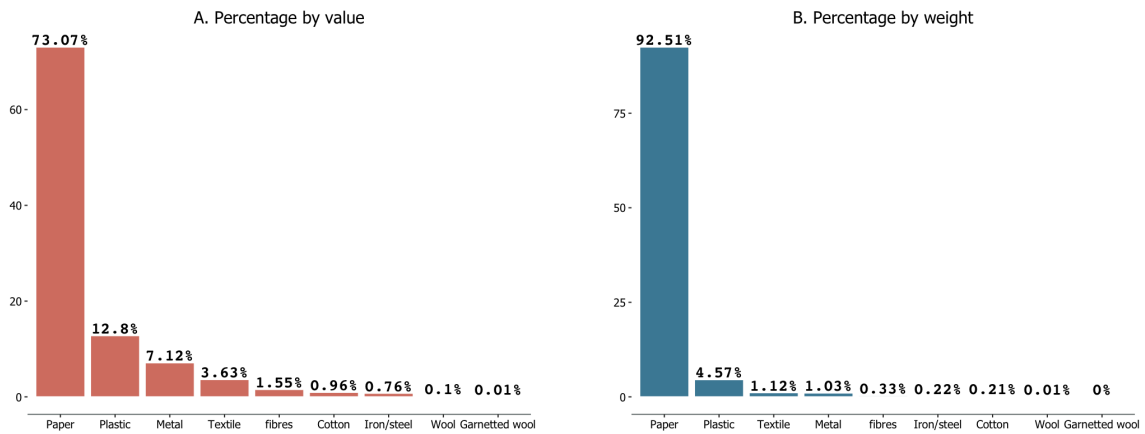
Figure A2. Composition of U.S. Recyclable Waste Exports to the Rest of the World (ROW). This plot shows the composition of recyclable waste materials exported from the U.S. to the rest of the world. Mixed paper/paperboard is still the material that accounts for the greatest percentage of the total exports by value and weight. Plastic scrap is the second most exported recyclable waste. Compared to exports to China, the U.S. exported to the rest of the world lower percentages of plastic scrap and higher percentages of metal, textile, fibers, and cotton scraps.
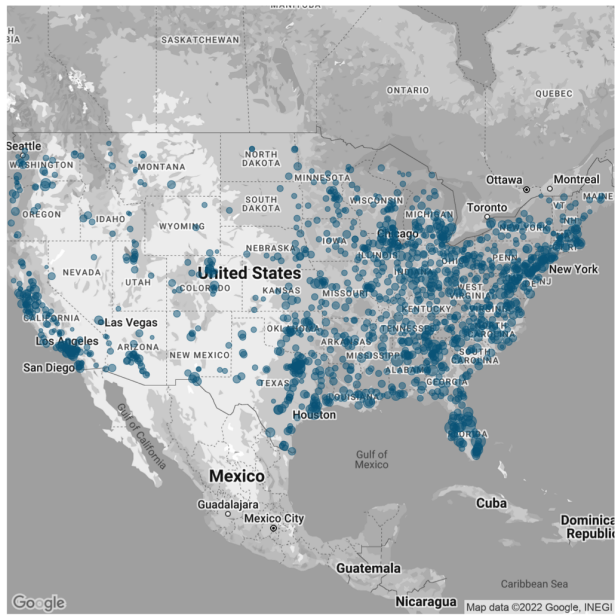
Figure A3. GHGRP: Spatial Distribution of Waste Facilities. This map shows the locations of all landfill facilities in, the U.S., according to the EPA Greenhouse Gas Reporting Program (GHGRP). There are more landfill facilities in states where populations are denser.
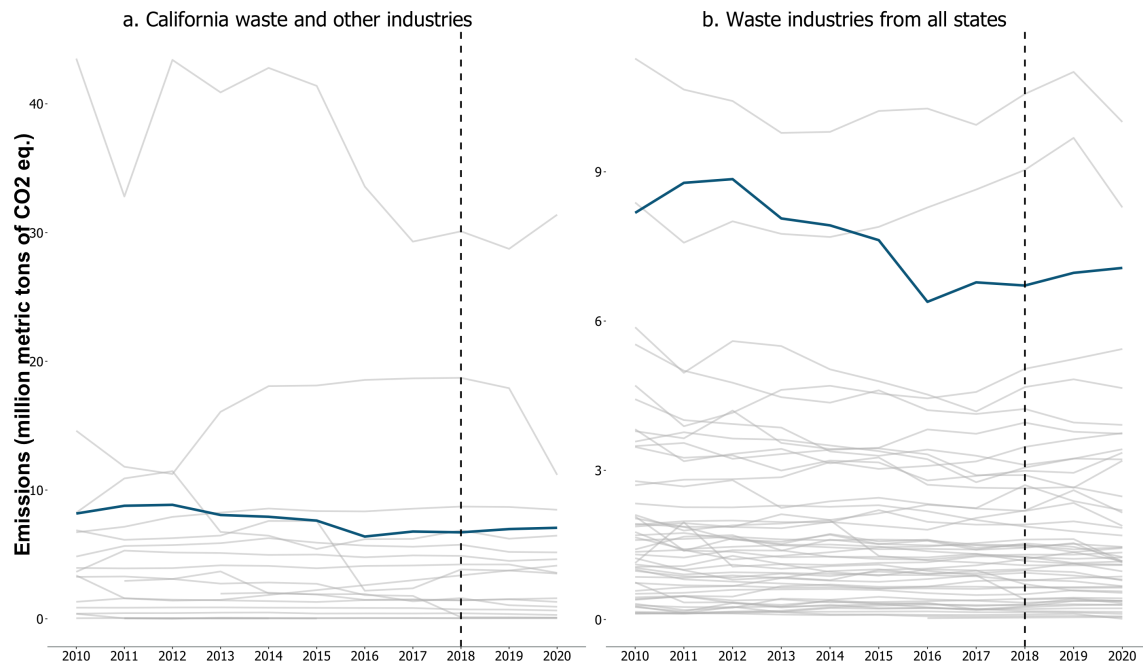
Figure A4. Synthetic Control: Waste Industries and Other Industries. In plot a, the blue line represents methane emissions for California's waste industry; The grey lines represent emissions from non-waste industries in California. In plot b, the blue line again represents methane emissions from California's waste industry, and the grey lines represent methane emissions from waste industries in other states. These plots show that neither "waste industries from other states" nor "other industries within the same state" are separately the most suitable control donor for synthetic controls.
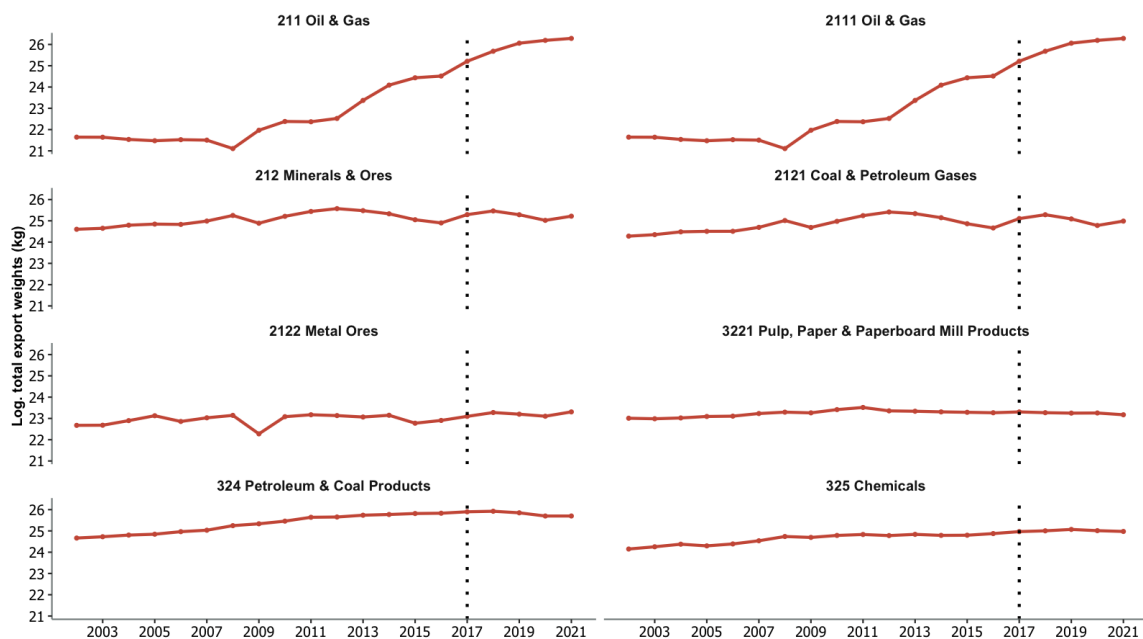
Figure A5. Synthetic Control: Exports of Other Control Industries. These plots show the net export weight by manufacturing industry. The emissions of these manufacturing industries are used as donor groups in the synthetic control method. The plots show no discernible changes in exports of these control manufacturing industries after 2017, which means that the emissions from the control industries are at least not obviously contaminated by changes in their exports.
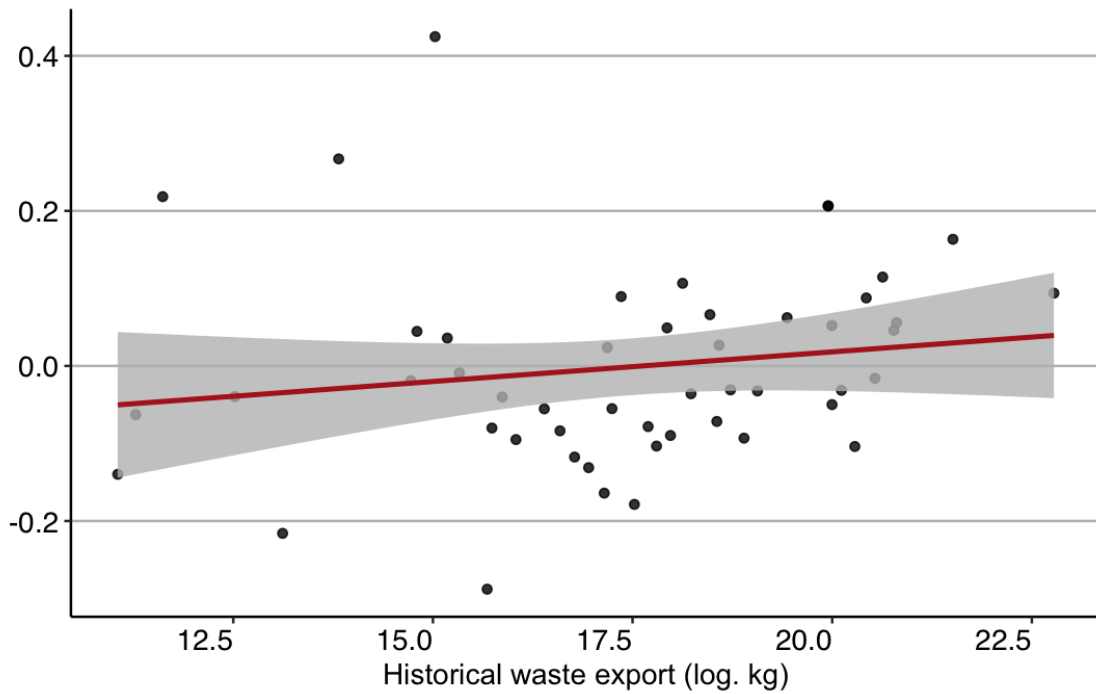
Figure A6. Pairwise Correlations: Heterogeneous Effects of GS Policy on State-level Estimations and Trade Exposures. This figure shows the correlation between the state-level causal estimates of the GS policy and the recyclable waste export exposure. There is a positive correlation between the percentage change in methane emissions and recyclable waste export exposure by state.
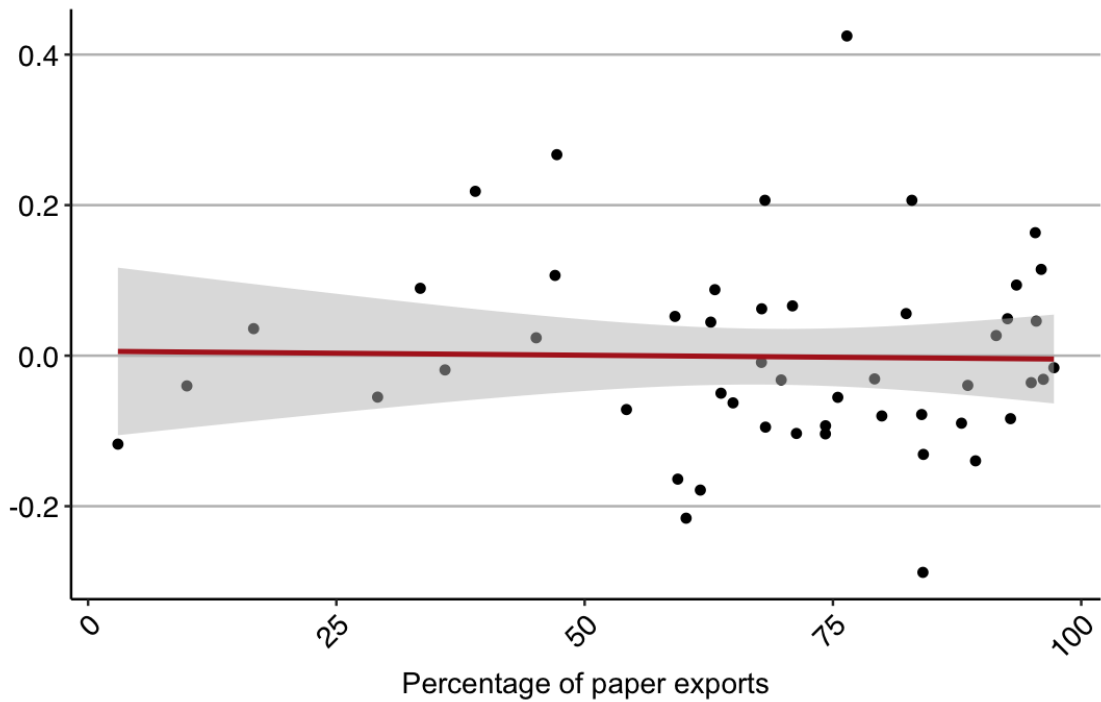
Figure A7. Pairwise Correlations: Heterogeneous Effects of GS policy on State-level Estimations and Paper Exports. This figure shows the correlation between the causal estimates and the percentage of paper exports by each state. There is no apparent correlation between the percentage change in methane emissions and the percentage of paper scrap exports by state.

A.2   Tables

	Total Value $ U.S. million (1)	Total Weight million kg (2)	Percentage of total value (3)	Percentage of total weight (4)
Slag, dross of manufacture of iron or steel	71.9	473	0.15	0.17
Slag, ash, and residues containing metals	292.9	70.2	0.61	0.003
Plastics	15464.1	38756.4	32.4	14.23
Paper and paperboard	31521.9	232466.6	66.11	85.38
Wool and animal hair	4.8	2.3	0.05	0.00008
Wool	0.15	0.02	0.0001	0.0000008
Cotton	116.1	199.5	0.24	0.007
Fibers	150.3	256.9	0.32	0.009
Textile	51.6	51.8	0.11	0.002

Table A1. Summary Statistics: U.S. Recyclable Waste Exports (by Type of Materials). The listed waste materials are all wastes that are directly affected by China's GS policy. Columns (1) and (2) are the total value and weight of recyclable waste exports from the U.S. to China from 2003 to 2020. Columns (3) and (4) are the percentages of each waste material out of all waste materials exported.

	Total Emissions	Methane	CO_2	NO_2
	(1)	(2)	(3)	(4)
Power Plants	20485.96	35.94	20481.52	76.99
Minerals	1193.32	1.22	1198.38	2.39
Waste	**1118.70**	**1000.99**	**311.01**	**3.85**
Chemicals	1053.17	1.92	991.47	64.83
Petroleum and Natural Gas Systems	985.61	88.45	896.96	0.56
Metals	815.38	793.13	1.71	0.29
Pulp and Paper	190.61	560.45	487.80	3.89
Refineries	102.77	102.07	2.87	0.26

Table A2. Summary Statistics: U.S. GHG Emissions (MMT) by Industry. Emissions by industry are calculated by adding up the emissions from all facilities in each industry for 2010-2020. Power plants have the largest total emissions across all industries. The waste industry (in bold) has the highest methane emissions out of all industries.

Year	2010	2011	2012	2013	2014	2015
Number of facilities	1303	1328	1342	1331	1328	1255
Total emissions (MMT.CO_2e)	110.9	104.6	105.3	102.1	101.7	101
Facility emissions, mean (TMT.)	85.1	78.8	78.5	76.7	76.6	80.5
Facility emissions, sd (TMT.)	90.7	83.8	86.3	85.5	85.7	85.6
Emissions by greenhouse gas (CO_2e)						
Carbon dioxide (CO_2)	9.9	10.7	10.8	11.1	11.1	11.4
Methane (CH_4)	101.1	94.1	94.7	91.2	90.8	89.9
Nitrous oxide (N_2O)	0.352	0.352	0.356	0.353	0.352	0.351

Year	2016	2017	2018	2019	2020
Number of facilities	1227	1221	1218	1204	1201
Total emissions (MMT.CO_2e)	98.2	96.8	99.6	101.4	96.9
Facility emissions, mean (TMT.)	80	79.3	81.8	84.2	80.7
Facility emissions, sd (TMT.)	89	90.5	97.6	102.5	92.3
Emissions by greenhouse gas (CO_2e)					
Carbon dioxide (CO_2)	11.7	10.6	11	10.7	10.3
Methane (CH_4)	86.7	86.4	88.8	90.9	86.2
Nitrous oxide (N_2O)	0.358	0.344	0.352	0.345	0.335

Sample size: 12,757

Table A3. EPA: Waste Sector - Greenhouse Gas Emissions Reported to the GHGRP Summary Statistics. Each observation in the sample is a reporting record from a facility from 2010 to 2020. The number of facilities has decreased gradually over the years. However, the total and average emissions of facilities have increased after 2017.

	Power Plants	Minerals	**Waste**	Chemicals	Petroleum and Natural Gas Systems	Metals	Pulp and Paper	Refineries
	(1)	(2)	(3)	(4)	(5)	(6)	(7)	(8)

Panel A. Sum over all states

2010	2295.21	100.97	**110.91**	104.11	65.45	90.79	43.82	27.72
2011	2136.86	100.50	**104.59**	83.93	94.21	82.64	16.88	17.17
2012	1995.041	104.89	**105.35**	80.35	96.16	78.09	16.38	6.81
2013	2006.49	108.39	**102.07**	85.41	93.75	77.11	15.09	6.57
2014	1997.66	113.97	**101.76**	89.87	96.59	77.96	15.69	6.90
2015	1874.29	112.45	**101.03**	93.30	98.15	69.73	15.62	6.69
2016	1771.08	108.15	**98.21**	99.13	76.19	69.10	14.39	6.39
2017	1696.25	111.58	**96.85**	100.97	79.71	69.56	13.48	6.41
2018	1710.59	113.32	**99.59**	104.75	90.67	72.06	13.35	6.46
2019	1577.77	112.02	**101.41**	106.94	97.16	69.17	12.87	6.37
2020	1424.73	107.07	**96.91**	104.41	97.56	59.17	13.01	5.28

Panel B. Average cross all states

2010	42.50	2.24	**2.17**	2.60	1.49	2.67	1.22	1.73
2011	39.57	2.28	**2.05**	2.09	2.00	2.36	4.97	1.07
2012	36.95	2.38	**2.07**	2.06	2.09	2.11	4.82	0.76
2013	37.16	2.46	**2.00**	2.19	2.08	2.14	4.31	0.82
2014	36.99	2.59	**1.99**	2.30	2.15	2.23	4.48	0.99
2015	34.71	2.56	**1.98**	2.39	2.18	1.99	4.34	0.96
2016	33.42	2.46	**1.89**	2.48	1.69	1.97	3.99	1.06
2017	32.00	2.54	**1.86**	2.46	1.81	2.05	3.74	1.07
2018	32.28	2.58	**1.92**	2.62	1.97	2.06	3.71	1.08
2019	29.77	2.55	**1.95**	2.74	2.16	1.98	3.58	1.27
2020	26.88	2.43	**1.86**	2.68	2.12	1.69	3.72	1.06

No. of Facilities	1446	364	**1268**	336	1225	280	143	15

Table A4. Summary Statistics: U.S. GHG Emissions by Industry. The no. of facilities are the average numbers of facilities in each industry during 2010 to 2020. Power plants, waste, and petroleum and natural gas are the industries that have the most facilities in the U.S. on average from 2010 to 2020. The waste industry (in bold) has seen a decrease in methane emissions from 2010 to 2017 and an increase in methane emissions afterwards, both in total and on average.

	Estimate (1)	P-value (2)	No. placebos (3)		Estimate (4)	P-value (5)	No. placebos (6)
Alabama	0.100**	0.040	24	Mississippi	-0.009**	0.020	50
California	0.087*	0.052	57	South Dakota	-0.063	0.500	8
Florida	0.043	0.260	49	Wyoming	-0.139	0.231	39
Georgia	0.050	0.211	37	Utah	-0.036	0.444	45
Hawaii	0.047	0.208	47	Maryland	-0.016	0.520	57
Illinois	0.043**	0.047	42	Delaware	-0.095	0.250	8
Kentucky	0.083**	0.024	40	Oklahoma	-0.019	0.439	82
Louisiana	0.020	0.313	31	Connecticut	-0.055	0.333	66
Missouri	0.023	0.571	6	Massachusetts	-0.031	0.489	47
Montana	0.230	0.333	5	Maine	-0.288	0.111	9
North Dakota	0.190*	0.100	5	Nebraska	-0.084	0.258	217
New Hampshire	0.043*	0.067	29	South Carolina	-0.049	0.352	105
Nevada	0.340*	0.100	9	Idaho	-0.216	0.500	2
New York	0.147**	0.011	87	Pennsylvania	-0.032	0.412	151
Ohio	0.060**	0.015	65	Arizona	-0.078	0.288	59
Oregon	0.063	0.211	37	Michigan	-0.031	0.493	73
Texas	0.083*	0.100	19	Colorado	-0.089	0.222	167
Virginia	0.180*	0.919	87	Iowa	-0.118	0.200	110
Washington	0.107*	0.067	15	Indiana	-0.055	0.353	34
West Virginia	0.033	0.214	14	Minnesota	-0.103	0.222	9
Tennessee	-0.072	0.333	33	Wisconsin	-0.164	0.127	110
Kansas	-0.179	0.428	7	New Jersey	-0.104	0.188	202
North Carolina	-0.093	0.463	41				

Table A5. Synthetic Control Results: Estimates at State Level. Each row (state) is a separate synthetic control and placebo test process. The number of placebos in each case is the number of control state-industry pairs being used in the synthetic control process for each treatment state. Each P-value is calculated by post/pre-Proposition 99 ratios of the MSPE for the "treatment" waste industry of a state and all its control state-industry pairs. Post- and pre-MSPE is calculated by taking the average of the differences between actual emissions and synthetic emissions over the years after and before China's GS policy. *$p < 0.1$, **$p < 0.05$, ***$p < 0.01$.

	Avg. Emissions Before GS Policy 2010-2017	Tot. Emission Increase After GS Policy 2018-2020		Avg. Emissions Before GS Policy 2010-2017	Tot. Emission Increase After GS Policy 2018-2020
	(1)	(2)		(3)	(4)
Alabama	2.957	0.988	Mississippi	4.634	-0.0380
California	7.823	1.797	South Dakota	0.186	-0.043
Florida	8.028	1.141	Wyoming	0.146	-0.068
Georgia	4.453	0.696	Utah	0.667	-0.071
Hawaii	0.561	0.078	Maryland	1.659	-0.079
Illinois	3.534	0.557	Delaware	0.213	-0.086
Kentucky	1.899	0.485	Oklahoma	1.982	-0.112
Louisiana	2.056	0.164	Connecticut	0.926	-0.148
Missouri	1.381	0.096	Massachusetts	1.599	-0.150
Montana	0.339	0.196	Maine	0.301	-0.204
North Dakota	0.294	0.206	Nebraska	0.913	-0.232
New Hampshire	0.390	0.049	South Carolina	1.579	-0.233
Nevada	0.281	0.428	Idaho	0.349	-0.263
New York	3.132	1.370	Pennsylvania	3.701	-0.331
Ohio	5.057	0.845	Arizona	1.430	-0.372
Oregon	1.035	0.194	Michigan	4.634	-0.390
Texas	10.297	2.702	Colorado	1.382	-0.395
Virginia	3.433	1.996	Iowa	1.148	-0.406
Washington	0.972	0.353	Indiana	0.349	-0.442
West Virginia	0.731	0.067	Minnesota	1.464	-0.493
Tennessee	2.485	-0.492	Wisconsin	1.406	-0.627
Kansas	1.666	-0.638	New Jersey	2.234	-0.679
North Carolina	3.501	-1.021			

Table A6. Synthetic Control Results: Emission Increases across States (million metric tons of CO_2 eq.). Average emissions before the GS policy are calculated by taking the mean of total emissions of each state over the years 2010-2017. The total increase in emissions after the GS policy is calculated by summing up the emission increase in each year from 2018 to 2020. The larger states, such as California, Texas, and New York, have seen a greater increase in methane emissions from the waste industry after China's GS policy.

B.1   Figures
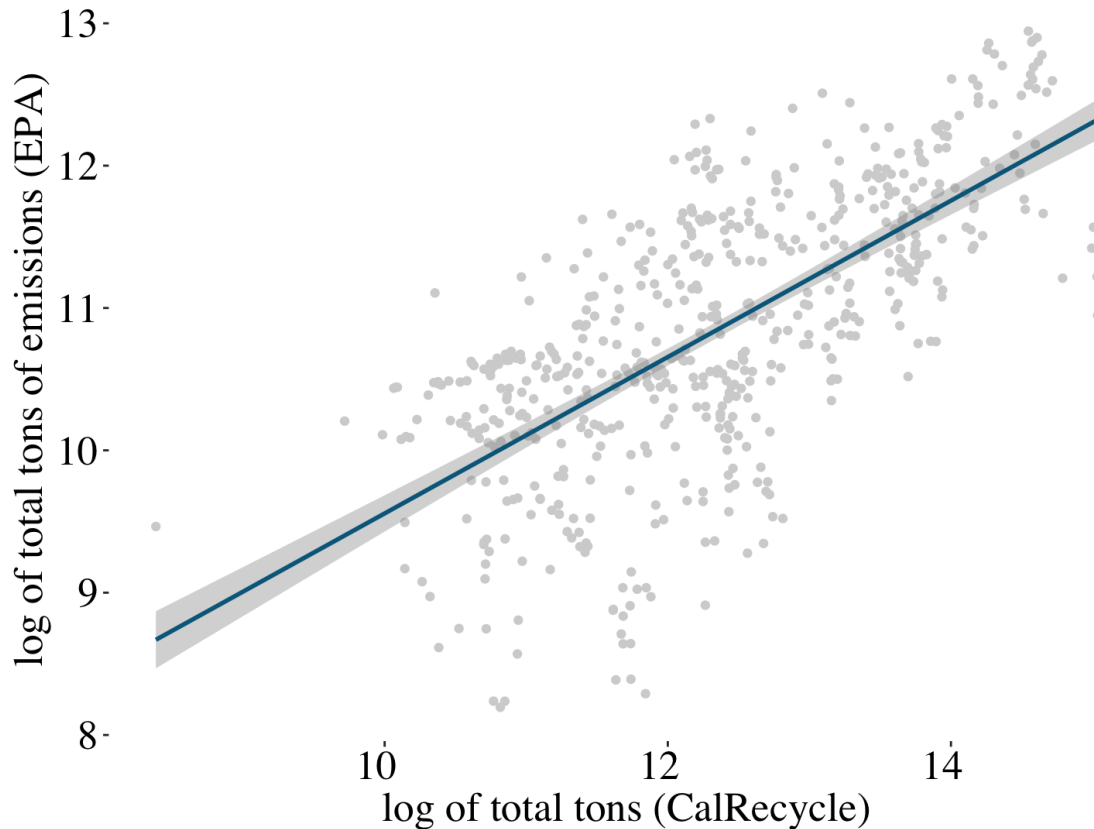
Figure B1. Data Comparison: EPA GHGRP v.s. CalRecycle RDRS. To carry the result from the state-level estimate, I compare the two data sources for state and facility-level analysis. This plot shows that the emissions data in EPA GHGRP and the data for tons of disposal in CalRecycle are highly correlated. This correlation demonstrates that the result I find from the state-level analysis—i.e. that California has seen an increase in methane emissions from the waste industry after China's GS policy—can be used in an analysis of facility-level distributional effects in California. Given that California has seen an overall increase in emissions and pollution from the waste industry due to China's GS policy, I will estimate how local communities have been affected differently by this policy change.

Figure B2. CalRecycle: Recycling and Disposal Reporting System (RDRS) Facility Locations in California by Rural and Urban Areas. This map shows the location of all landfill facilities in the CalRecycle RDRS data. The yellow areas are the urban areas in California. The map shows that most landfill facilities are located in rural regions or suburbs outside the urban areas.

Los Angeles
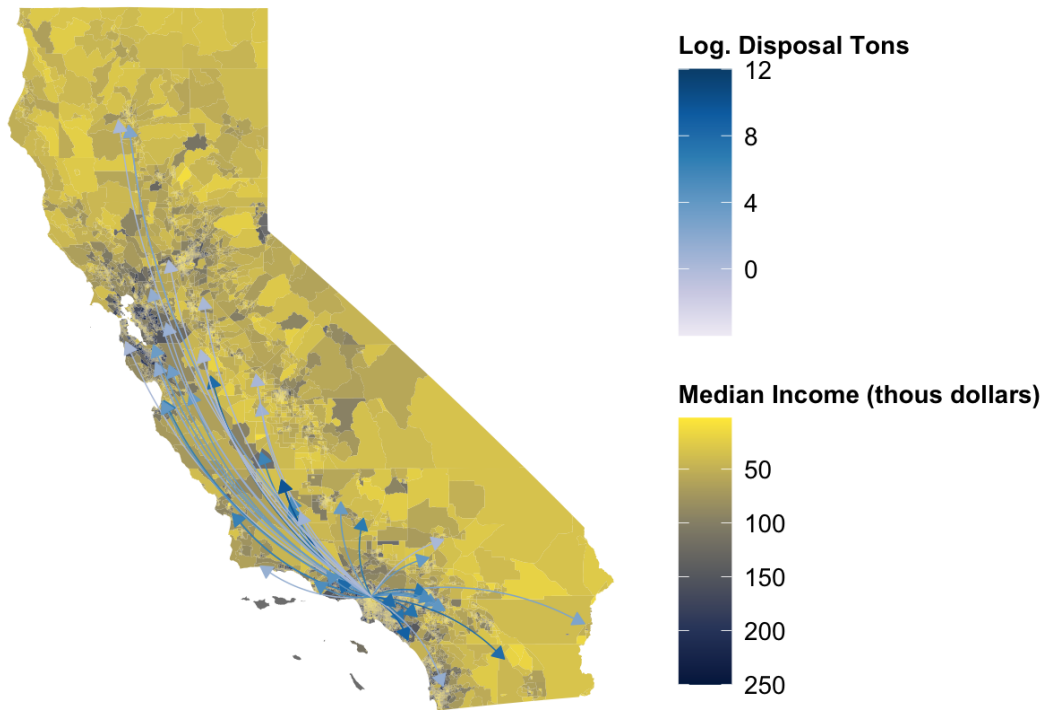
Figure B3. Disposal Flow Map by Median Income. The median income is mapped using 2013 ACS 5-year data at the census block group level. The colors of the arrows show the increase in amount of disposal flows after China's GS policy.
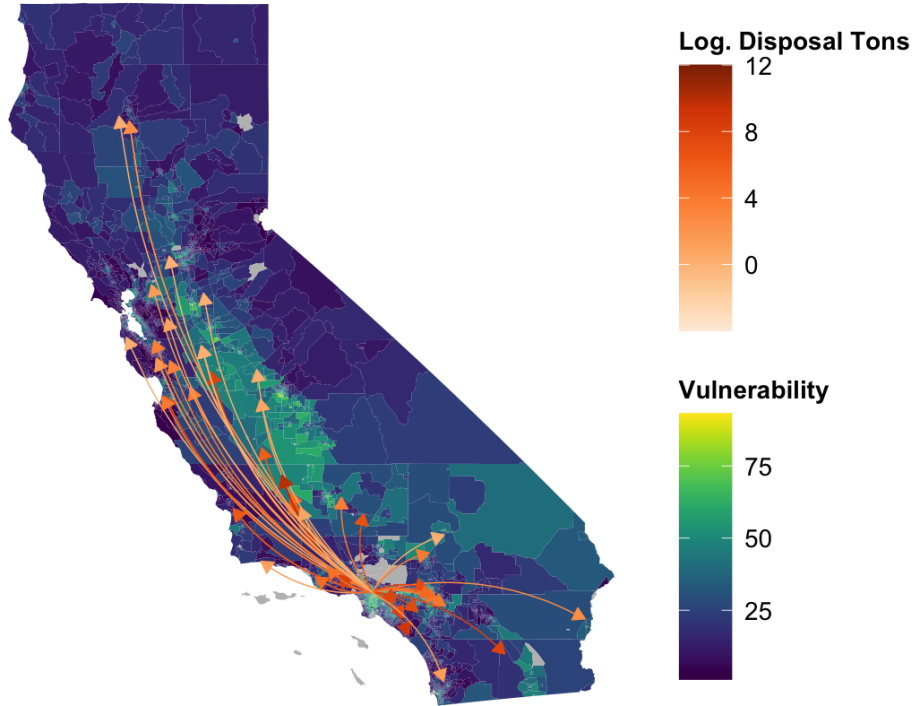
Figure B4. Disposal Flow Map by Environmental Vulnerability. Environmental vulnerability is calculated by the Office of Environmental Health Hazard Assessment (OEHHA). California Communities Environmental Health Screening Tool is a screening methodology that evaluates multiple pollution sources and stressors and measures a community's vulnerability to pollution. The higher the score, the more vulnerable is the community to pollution. The colors of the arrows show the increase in amount of disposal flows after China's GS policy.
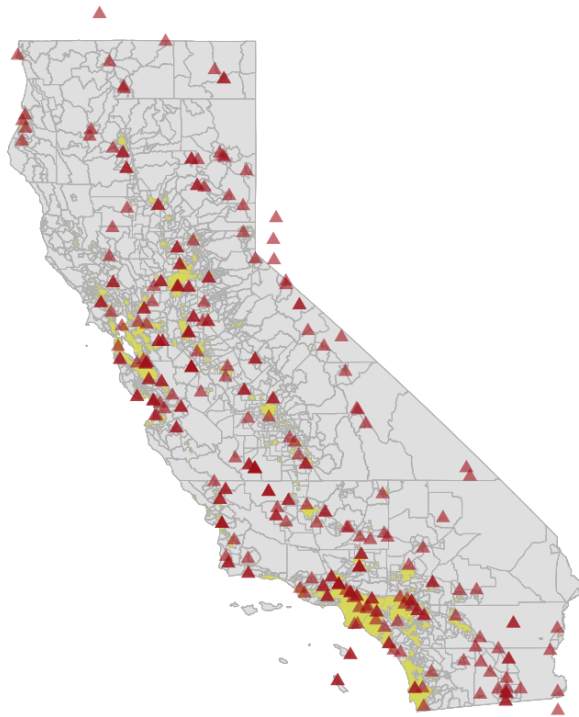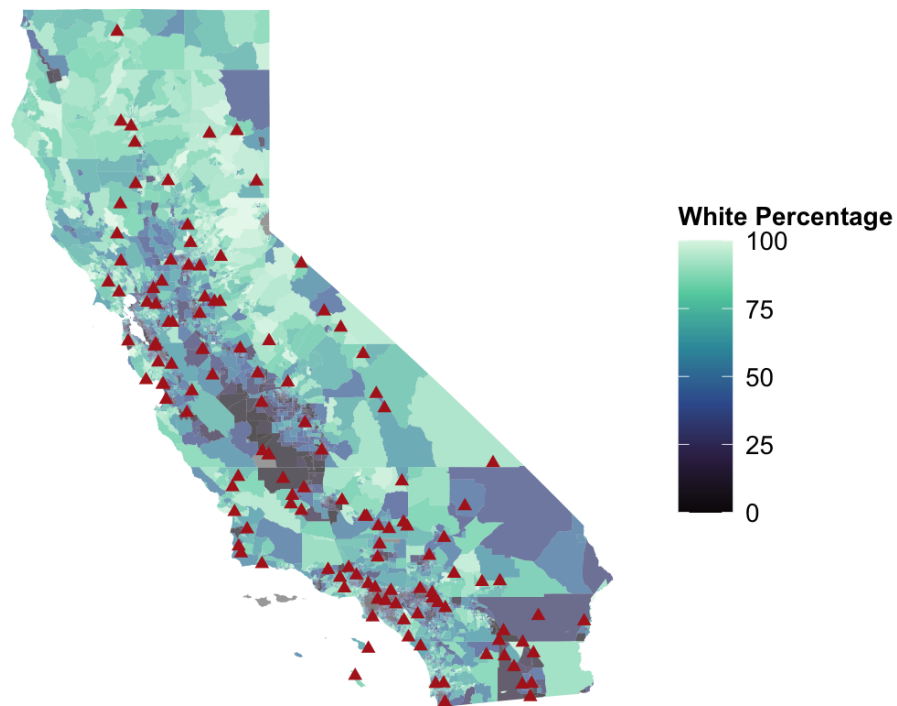
Figure B5. CalRecycle: Recycling and Disposal Reporting System (RDRS) Facility Locations in California by Racial Composition. This map shows the location of all landfill facilities in the CalRecycle RDRS data by racial composition. Racial composition is plotted by census block group level. The map shows that most destination facilities are located in the darker areas where more minority population resides. However, some facilities are still located in the lighter areas where the white population lives.

Los Angeles County
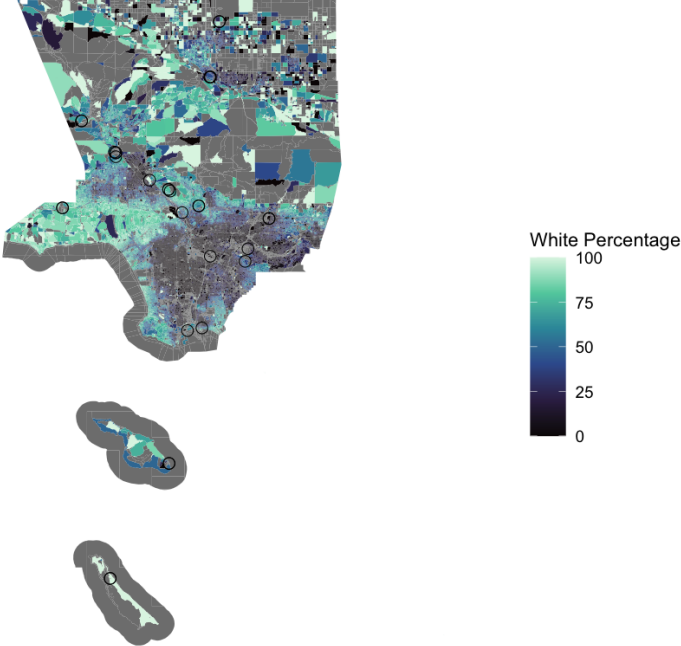
Figure B6. Racial Composition Variation within Los Angeles County. This map
shows the racial composition variations across different communities (the black
circle: within 3 km buffers of the destination facilities) in Los Angeles county.
In the fixed-effects model estimation, the racial composition variable is at the
census block-level, and is time-invariant (as of 2010). Thus, when I add county
fixed effects, the variation in racial composition is the different communities within
a county. Some communities may include multiple census blocks.
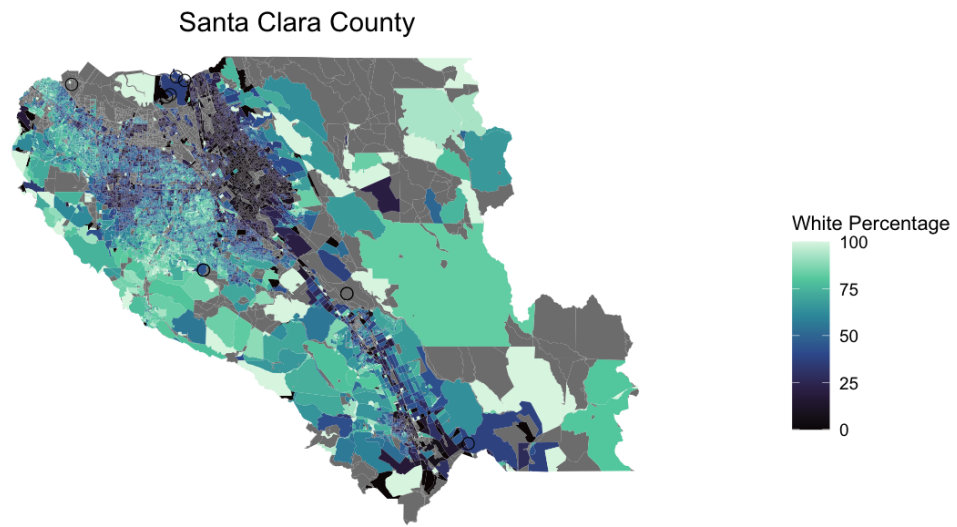
Figure B7. Racial Composition Variation within Santa Clara County. This map
shows the racial composition variations across different communities (the black
circle: within 3 km buffers of the destination facilities) in Santa Clara county.
In the fixed-effects model estimation, the racial composition variable is at the
census block-level, and is time-invariant (as of 2010). Thus, when I add county
fixed effects, the variation in racial composition is the different communities within
a county. Some communities may include multiple census blocks.

Los Angeles County
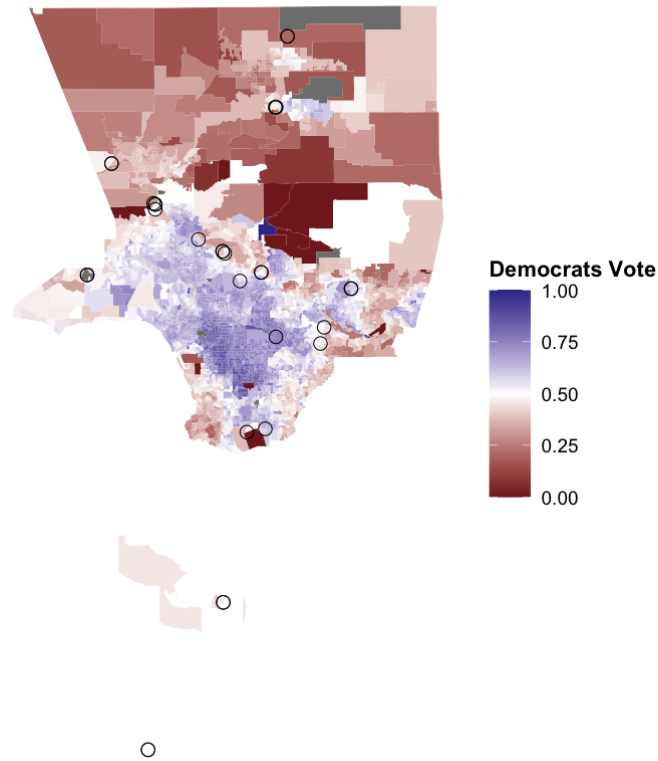
Figure B8. Voting Variation within Los Angeles County. Voting Variation within County. Similar to the racial composition, vote shares of communities (black circle: with 3km buffers of the destination facilities) are also time-invariant (as of 2016) at the precinct level. Thus, when I add county fixed effects, the variation for voting registration share is the different communities within a county. Some communities may include multiple voting precincts.
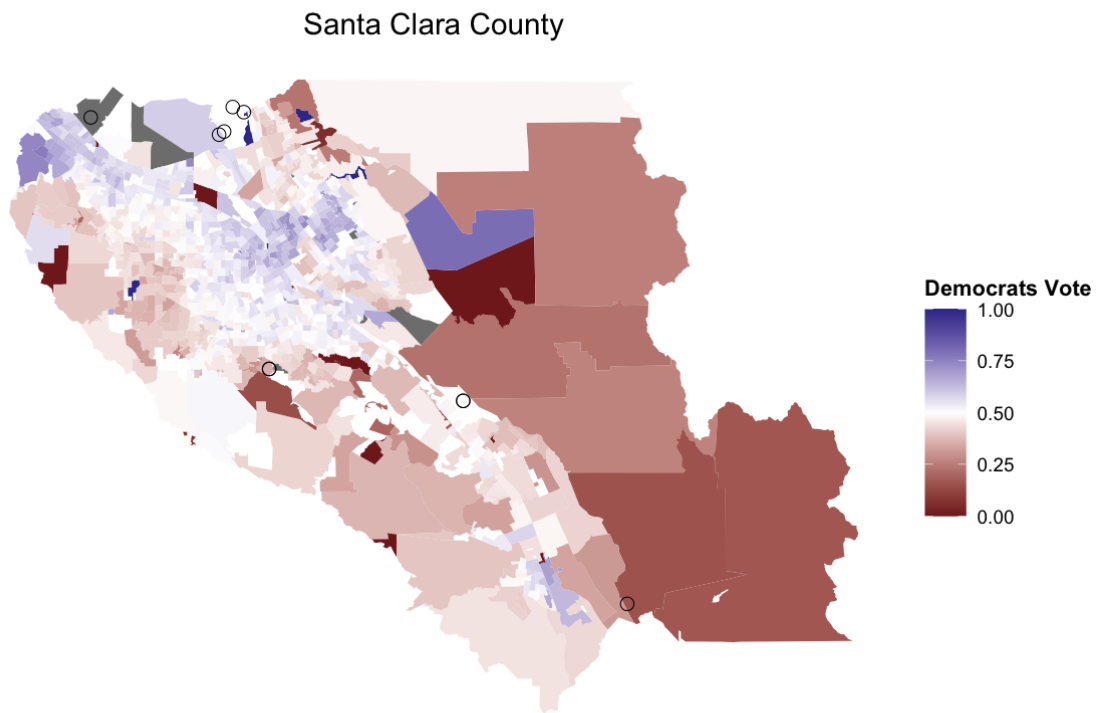
Figure B9. Voting Variation within Santa Clara County. Voting Variation within County. Similar to the racial composition, vote shares of communities (black circle: with 3km buffers of the destination facilities) are also time-invariant (as of 2016) at the precinct level. Thus, when I add county fixed effects, the variation for voting registration share is the different communities within a county. Some communities may include multiple voting precincts.

San Bernardino County

- ● Compost
- ▲ Demolition Landfills
- ■ Landfills
- + Material Recovery Center
- ⊠ Recovery Disposal
- ✳ Recycling & Transfer
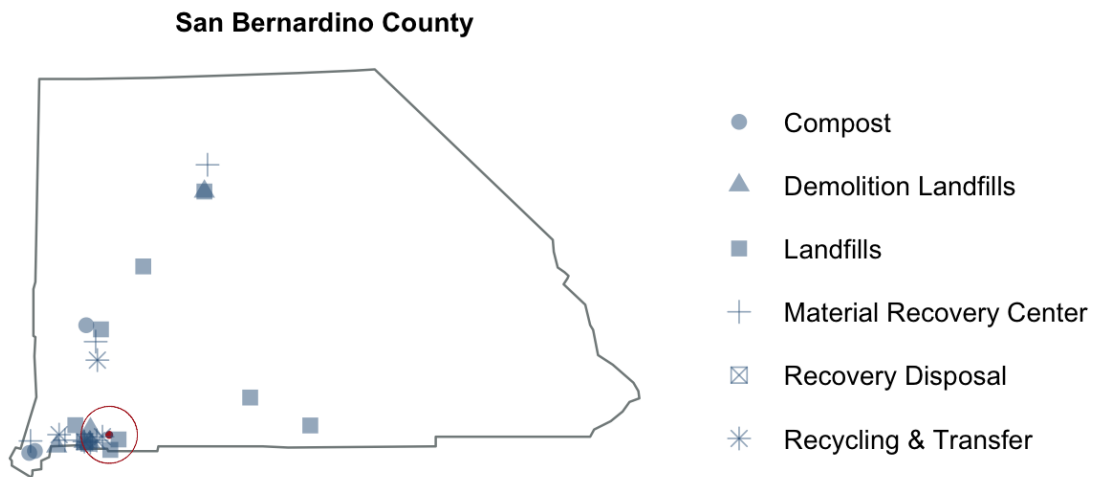
Figure B10. Economies of Scale of Communities Where Destination Facilities are Located. This figure shows how economies of scale are defined. The map shows the number of facilities that are within a 15 km buffer of the destination facility of disposal shipment. The red dot is the destination facility from CalRecycle as a destination for disposal transfer. The blue marks are other types of related facilities within a 15km buffer. They are composts (CO), landfills (LF), recycling centers (MR and MW), and transfer stations (TS). The more facilities around the destination landfill facility, the higher the economy of scale there is in the community where the destination landfill is located.

San Joaquin County
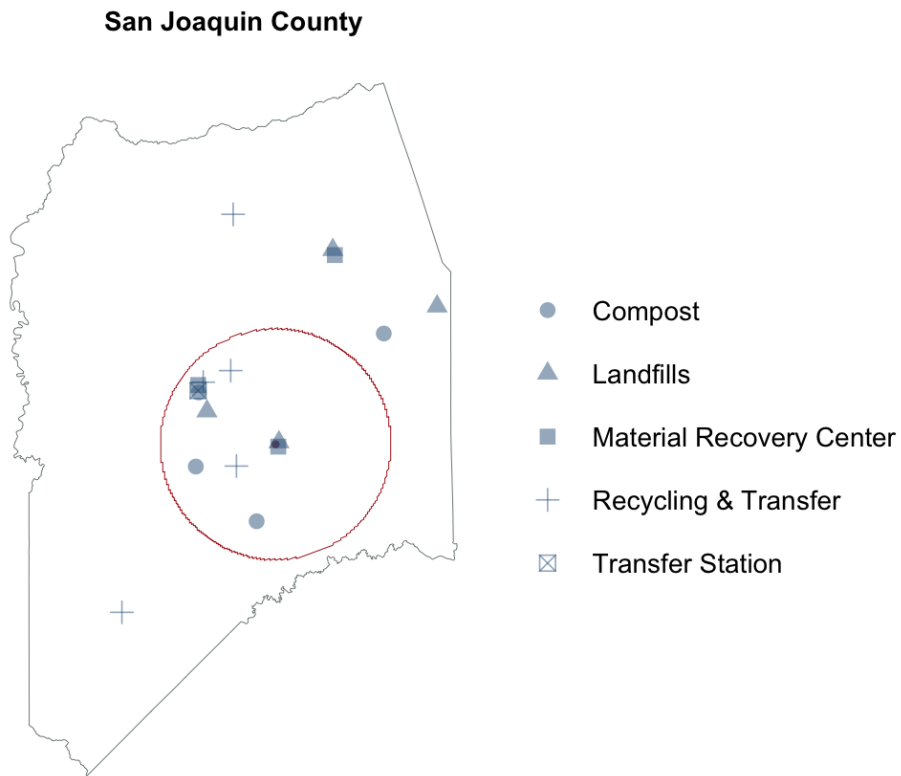
Figure B11. This figure shows how economies of scale are defined. The map shows the number of facilities that are within a 15 km buffer of the destination facility of disposal shipment. The red dot is the destination facility from CalRecycle as a destination for disposal transfer. The blue marks are other types of related facilities within a 15km buffer. They are composts (CO), landfills (LF), recycling centers (MR and MW), and transfer stations (TS). The more facilities around the destination landfill facility, the higher the economy of scale there is in the community where the destination landfill is located.

B.2 Tables

Year	Origin Jurisdiction		Destination Facility		Distance
	(1)	(2)	(3)	(4)	(5)
	no.jurisdictions	mean shipments sent (1000 tons)	no.facilities	mean shipments received (1000 tons)	mean (km)
2002	434	86.6	162	232.0	93.3
		(214.6)		(476.8)	(121.6)
2003	421	94.4	158	251.6	93.9
		(271.5)		(501.4)	(121.0)
2004	424	96.2	152	268.3	96.1.29
		(269.5)		(522.9)	(122.2)
2005	419	100.3	149	281.9	94.6
		(283.9)		(534.5)	(119.5)
2006	412	99.5	148	276.9	89.8
		(271.9)		(517.2)	(109.1)
2007	414	93.6	142	272.9	92.2
		(261.8)		(507.3)	(110.7)
2008	417	84.2	133	264.0	89.4
		(235.0)		(465.9)	(103.0)
2009	412	74.7	134	229.7	98.7
		(211.2)		(431.2)	(120.4)
2010	417	72.0	131	229.4	101.7
		(201.1)		(414.6)	(123.6)
2011	416	71.5	134	221.9	76.4
		(204.2)		(408.5)	(90.9)
2012	414	70.3	131	222.1	71.6
		(203.9)		(405.2)	(71.5)
2013	412	72.7	133	225.2	85.8
		(214.1)		(405.6)	(101.6)
2014	411	75.1	130	237.5	87.1
		(235.4)		(427.2)	(99.1)
2015	410	80.3	128	257.2	89.2
		(250.8)		(456.1)	(104.9)
2016	420	82.9	126	276.3	90.1
		(257.4)		(473.1)	(102.8)
2017	420	89.2	127	294.9	90.3
		(275.3)		(501.5)	(103.4)
2018	417	94.7	128	308.5	90.3
		(284.8)		(519.3)	(98.8)
2019	418	96.5	127	317.6	87.0
		(288.9)		(532.9)	(90.2)
2020	419	96.2	128	314.8	87.8
		(285.3)		(528.8)	(83.7)
Sample Size	281339				

Table B1. CalRecycle: Recycling and Disposal Reporting System (RDRS) Disposal Flows within California, Summary Statistics (Thousands of Tons). Each observation in the sample is a waste shipment from an origin jurisdiction to a destination facility during 2002-2020. The average distance is calculated by taking the mean of origin-destination pairs in each year.

	3 km Buffer	5 km Buffer	10 km Buffer
% White Population	57.12	53.67	52.37
	(27.07)	(25.91)	(24.01)
% Black Population	2.78	3.24	4.07
	(4.98)	(4.83)	(4.93)
% Hispanic Population	32.79	35.19	35.50
	(25.65)	(24.91)	(22.48)
Median Income ($Thousand)	63.156	61.137	59.921
	(24.616)	(21.974)	(20.503)
	5 km Buffer	10 km Buffer	15 km Buffer
Economies of Scale (no. of facilities)	1.96	4.04	6.42
	(1.79)	(3.95)	(6.39)
# of destination facilities	264		

Table B2. Summary Statistics for Community Characteristics around each Destination Facility. # of facilities are all destination facilities from 2002 to 2020 in the CalRecycle RDRS data. Racial composition is from the U.S. Census decennial data 2010 at census block level. Median income is from the U.S. Census American Community Survey (ACS) 5-year survey in 2013 at census block group level. Economies of scale are calculated using Waste Business Journal (WBJ) data at the facility level. See Appendix, Figure 4, for a detailed definition of economies of scale. I choose 15km distance buffers for economies of scale since there are normally no other facilities within a 3 km buffer of destination landfill facilities.

Dep.Variable: Disposal shipments received (tons)	(1)	(2)	(3)	(4)
Distance (log km)	-0.300***	-0.233***	-0.216***	-0.029
	(0.078)	(0.078)	(0.084)	(0.113)
Distance (log)×1(*post*)	0.070*	0.068	0.061	0.059
	(0.041)	(0.048)	(0.045)	(0.048)
White share (log %)	-0.459***	-0.620***	-0.599***	-1.197***
	(0.184)	(0.027)	(0.183)	(0.163)
White share (log %)×1(*post*)	0.269*	0.267*	0.271*	0.496**
	(0.144)	(0.161)	(0.156)	(0.195)
Black share (log %)	0.152***	0.178***	0.200***	0.340***
	(0.047)	(0.063)	(0.078)	(0.091)
Black share (log %)×1(*post*)	0.069	0.092	0.083*	0.084**
	(0.045)	(0.057)	(0.049)	(0.039)
Hispanic share (log %)	-0.315	-0.203	-0.204	-0.635
	(0.214)	(0.211)	(0.199)	(0.111)
Hispanic share (log %)×1(*post*)	-0.061***	-0.065*	-0.044	-0.072
	(0.022)	(0.028)	(0.032)	(0.085)
Median income (log $)		1.702***	1.806***	1.969***
		(0.279)	(0.352)	(0.351)
Median income (log $)×1(*post*)		-0.097	-0.165**	-0.151***
		(0.062)	(0.069)	(0.048)
Economies of scale			0.121	0.531***
			(0.161)	(0.184)
Economies of scale×1(*post*)			-0.110	-0.354***
			(0.074)	(0.089)
Republican votes (log %)				1.000***
				(0.344)
Republican votes (log %)×1(*post*)				-0.667**
				(0.300)
County FE	✓	✓	✓	✓
Year FE	✓	✓	✓	✓
Quarter FE	✓	✓	✓	✓
Observations	226,128	226,128	226,188	217,212

Table B3. Altered Distributional Effects: Fixed-effects Model for Waste Flows from Origin Jurisdiction to Receiving Facilities and their Local Communities, before/after China's GS Policy. Economies of scale are the numbers of related facilities, such as transfer station, landfills, and recycling centers, that are within 5 km buffers of the destination facilities in CalRecycle RDRS data. Data for Republican votes is from California Statewide Database (SWDB) election data at the precinct level. It is defined as the percentage of the population that registered as Republicans in the 2016 election year among all voting registrations.

C.1   Figures

	Policy A	**Policy B**
(1)	reduces air pollutants that cause heart disease	reduces pesticides in foods that cause adult leukemia
(2) Policy in effect	over 20 years	over 25 years
(3) Without policy / With policy	1,100 get sick / only 100 get sick	30 get sick / only 5 get sick
(4) **Cases Prevented**	**1,000 fewer cases**	**25 fewer cases**
(5) Without policy / With policy	220 will die / only 20 will die	6 will die / only 1 will die
(6) **Deaths Prevented**	**200 fewer deaths over 20 years**	**5 fewer deaths over 25 years**
(7) **Cost to you**	$90 per month (= $1,080 per year for 20 years)	$25 per month (= $300 per year for 25 years)
(8) **Your choice**	○ Policy A reduces air pollutants that cause heart disease	○ Policy B reduces pesticides in foods that cause adult leukemia
	○ Neither Policy	

Recall that these two policies will be implemented for the 50,000 people living around you.

Would you be most willing to pay for policy A, policy B, or neither of them?

Figure C1. One Example of a Choice Set in the Original 2003 Survey. Each respondent faces a choice between either of two different health policies and the status quo.

C.2 Tables

Table C1. Sources of county-level data for estimation and simulation

Variable	Sources for ca. 2003 data (estimation)	Sources for ca. 2020 data (simulation)
County population	2000 Census	2018 5-yr ACS
Population affected	"People living around you" in choice scenario, as a proportion of the population in the respondent's county	1.0 (i.e. county population as a proportion of county population)
Median household income	2000 Census STF3 Table P53, P053001	2018 5-yr ACS
Unemployment rate, county-level, current month	BLS monthly for May, June 2003	for Feb-May for 2020

Table C1 (continued).

Variable	Sources for ca. 2003 data (estimation)	Sources for ca. 2020 data (simulation)
Change in unemployment rate since last month, county level	BLS May-June 2003	Feb-Mar, Mar-Apr, Apr-May, May-June for 2020
Ethnic mix. Proportion of county population: pblack, pasian, phispanic, pother	2000 Census	2018 5-yr ACS
Ethnic fractionalization. For 7 racial groups: white, black, asian, amerind, hawaii-pacisl, other, multi-race	calculated from 2000 Census	calculated from 2018 5-yr ACS
Age distribution. Proportions of population in each age group: 0-17, 18-24, 65 plus	2000 Census	2018 5-yr ACS

Variable	Sources for ca. 2003 data (estimation)	Sources for ca. 2020 data (simulation)
Last Presidential election vote shares: Democratic, Republican, Green, Libertarian, Other	David Leip's US Election atlas for 2000	David Leip's US Election atlas for 2016
Hospitals per 100,000 population.	CDC Open Data	same
Health insurance coverage, county level	(US Census Bureau, 2008 - 2018 Small Area Health Insurance Estimates (SAHIE) using the American Community Survey (ACS)[a])	same

Table C1 (continued).

Variable	Sources for ca. 2003 data (estimation)	Sources for ca. 2020 data (simulation)
Air quality[1]	Van Donkelaaret al.	same
Health indicators[2]	Robert Wood Johnson Foundation Program County Health Rankings and Roadmaps	same

---

[1]Given that COVID-19 is primarily a respiratory disease, baseline airquality may be important. We have only one environmental variable in this research– particular matter (PM2.5). PM2.5 pollution consist of tiny particles in the air ofdiameter less than 2.5 micrometres. These particles of dust or soot can be inhaled andhave the potential to cause long-term health problems.

[2]The variableswe employ in our re-estimation and simulation models include the percentage of adultswho report smoking, obesity, and excessive drinking. For seniors in each county, we alsouse clinical care data for "access to care", and "quality of care" from Medicare claims.

Table C2. Homogeneous Preferences versus Model with Three Latent Classes

Description		Three Latent Classes of Preferences		
		Class 1	Class 2	Class 3
	Homog.	Cost-	Compre-	Indiff./
	Pref.	Consc.	hensive	Altruist.
Latent classes of preferences (marginal utilities of policy attributes)				
Monthly cost of policy	-0.004***	-0.01***	-0.003*	0.1
Policy duration	-0.01***	-0.02**	-0.01***	-0.5
Base. cases of illness	-	-	-	0.028
Reduction in cases	0.00008***	-	0.0001**	0.06
Base. prem. deaths	-	-	0.0003*	0.022
Reduction in deaths	0.000098.	-	0.0004	0.33
Private benefit	0.6***	-0.53***	2.1***	0.74
Status quo alternative	1.54***	-0.77**	3.9***	13.53
Class membership propensities (relative to Class 1)				

Table C2 (continued).

Description		Three Latent Classes of Preferences		
		Class 1	Class 2	Class 3
	Homog.	Cost-	Compre-	Indiff./
	Pref.	Consc.	hensive	Altruist.
log(County population)	n/a	0		1.91***
Cnty pr. Repub. vote	n/a	0	1.18*	3.49*
Proportions of county population in different age brackets				
% pop. age 0-17	n/a	0		
% pop. age 25-44	n/a	0	-8.31*	-22.52*
% pop. age 45-64	n/a	0	9.36*	20.39*
% pop. age 65-84	n/a	0	-8.15*	
Proportions of county population in different racial/ethnic groups				
% pop. White	n/a	0	-5.86*	

Table C2 (continued).

Description		Three Latent Classes of Preferences		
		Class 1	Class 2	Class 3
	Homog.	Cost-	Compre-	Indiff./
	Pref.	Consc.	hensive	Altruist.
% pop. Black	n/a	0		
% pop. Native Amer.	n/a	0	-27.57***	
% pop. Asian	n/a	0	-10.89**	-37.32*
% pop. multi-race	n/a	0		
% pop. Hispanic	n/a	0		
log(Med. income/100K)	n/a	0	-1.69***	
Hospitals per 10K pop.	n/a	0		
County unempl (current)	n/a	0		
Δ unempl (v last month)	n/a	0		
Health insurance coverage	n/a	0	0.13.	

Description		Three Latent Classes of Preferences		
		Class 1	Class 2	Class 3
	Homog.	Cost-	Compre-	Indiff./
	Pref.	Consc.	hensive	Altruist.
% adults completing college or bachelor degree	n/a	0		8.05*
Poverty percent, all ages	n/a	0	-0.089**	
Average PM2.5	n/a	0		
% Fair or Poor Health	n/a	0		
Average Number of Physically Unhealthy Days	n/a	0		
Average Number of Mentally Unhealthy Days	n/a	0		
% Smokers	n/a	0		
% Adults with Obesity	n/a	0		

Description		Three Latent Classes of Preferences		
		Class 1	Class 2	Class 3
	Homog.	Cost-	Compre-	Indiff./
	Pref.	Consc.	hensive	Altruist.
% Excessive Drinking	n/a	0	-0.032	0.23***
Prim. Care Physic. Rate	n/a	0	-0.003	
Preventable Hosp. Rate	n/a	0		
Observ.	1466	1466	1466	

REFERENCES CITED

Aadland, D., & Caplan, A. J. (2006). Curbside Recycling: Waste Resource or Waste of Resources? *Journal of Policy Analysis and Management*, *25*(4), 855–74.

Abadie, A., Diamond, A., & Hainmueller, J. (2012). Synthetic Control Methods for Comparative Case Studies: Estimating the Effect of California's Tobacco Control Program. *Journal of the American Statistical Association*, *105*(490), 493-505.

Abel, T. D., & White, J. (2011). Skewed Riskscapes and Gentrified Inequities: Environmental Exposure Disparities in Seattle, Washington. *American Journal of Public Health*, *101*, 246-254.

Abernethy, S., O'Connor, F., Jones, C., & Jackson, R. (2021). Methane removal and the proportional reductions in surface temperature and ozone. *Philosophical Transactions of the Royal Society*(379).

Adeel, B. A., Catalano, M., Catalano, O., Gibson, G., Muftuoglu, E., Riggs, T., Sezgin, H. M., Shvetsova, O., Tahir, N., VanDusky, J., Zhao, T., & Zhirnov, A. (2020). COVID-19 Policy Response and the Rise of the Sub-National Governments. *Canadian Public Policy*, *46*, 565-584. doi: 10.3138/cpp.2020-101

Aizer, A., Currie, J., Simon, P., & Vivier, P. (2018). Do low levels of blood lead reduce children's future test scores? *American Economic Journal: Applied Economics*, *10*(1), 307-41.

Autor, D., Dorn, D., & Hanson, G. (2013). The China Syndrome: Local Labor Market Effects of Import Competition in the United States. *America Economic Review*, *103(6)*, 2121-2168.

Baden, B. M., & Coursey, D. L. (2002). The Locality of Waste Sites within the City of Chicago: a Demographic, Social, and Economic Analysis. *Resource and Energy Economics*, *24*(1-2), 53-93.

Banzhaf, S., Ma, L., & Timmins, C. (2019). Environmental Justice: The Economics of Race, Place, and Pollution. *Journal of Economic Perspectives*, *33*(1), 185-208.

Banzhaf, S. H., & Walsh, R. P. (1994). Environmental Equity: the Demographics of Dumping. *Demography*, *31*(2), 229-248.

Banzhaf, S. H., & Walsh, R. P. (2008). Do People Vote with Their Feet? An Empirical Test of Tiebout's Mechanism. *American Economic Review*, *93*(3), 843-63.

Banzhaf, S. H., & Walsh, R. P. (2013). Segregation and Tiebout Sorting: The Link between Place-based Investments and Neighborhood Tipping. *Journal of Urban Economics*, *74*, 83-98.

Bartik, T. J. (1991). Who Benefits from State and Local Economic Development Policies? *W.E. Upjohn Institute for Employment Research*.

Becker, R., & Henderson, V. (2000). Effects of Air Quality Regulations on Polluting Industries. *Journal of Political Economy*, *2*(108), 379-421.

Black, S. E., Devereux, P. J., & Salvanes, K. G. (2007). From the cradle to the labor market? the effect of birth weight on adult outcomes. *Quarterly Journal of Economics*, *122*(1), 409-39.

Bohm, R., Folz, D. H., Kinnaman, T. C., & Podolsky, M. J. (2010). The Costs of Municipal Waste and Recycling Programs. *Resources, Conservation and Recycling*, *54*(8), 64–71.

Bosworth, R., Cameron, T. A., & DeShazo, J. R. (2009). Demand for environmental policies to improve health: Evaluating community-level policy scenarios. *Journal of Environmental Economics and Management*, *57*(3), 293–308. doi: 10.1016/j.jeem.2008.07.009

Brander, L., Beukering, P. V., & Cesar, H. S. (2007). The recreational value of coral reefs: A meta-analysis. *Land Economics*, *63*, 209-218. doi: 10.1016/j.ecolecon.2006.11.002

Brandt, L., Biesebroeck, J. V., & Zhang, Y. (2012). Creative Accounting or Creative Destruction? Firm-level Productivity Growth in Chinese Manufacturing. *Journal of Development Economics*, *2*(97), 339-351.

Bransetter, L., & Lardy, N. (2006). China's Embrace of Globalization. *NBER Working Paper*(12373).

Bullard, R. D. (1983). Solid waste sites and the black houston community. *Sociological Inquiry*, *53*(2-3), 273-88.

Cameron, T. A. (2010). Euthanizing the value of a statistical life. *Review of Environmental Economics and Policy*, *4*(2), 161–178. doi: 10.1093/reep/req010

Cameron, T. A., & McConnaha, I. T. (2006). Evidence of Environmental Migration. *Land Economics*, *82*(2), 273-90.

Cattapan, A., Ackerverney, J. M., Dobrowolsky, A., Findlay, T., & Mandrona, A. (2020). Community Engagement in a Time of Confinement. *Canadian Public Policy*, *14*, 288-298. doi: IO.3138/cpp.2020-064

Chavis, B. F., & Lee, C. (1987). Toxic Wastes and Race in the United States: A National Report on the Racial and Socio-Economic Characteristics of Communities with Hazardous Waste Sites. *New York: Commission for Racial Justice, United Church of Christ.*.

Chay, K. Y., & Greenstone, M. (2003). The impact of air pollution on infant mortality: Evidence from geographic variation in pollution shocks induced by a recession. *Quarterly Journal of Economics*, *118*(3), 1121-67.

Cherniwchan, J. (2017). Trade liberalization and the environment: Evidence from NAFTA and U.S. manufacturing. *Journal of International Economics*, *C*(105), 130-149.

Chorus, C., Sandorf, E. D., & Mouter, N. (2020). Diabolical dilemmas of COVID-19: An empirical study into Dutch society's trade-offs between health impacts and other effects of the lockdown. *PLoS ONE*, *15*, 1-19. doi: 10.1371/journal.pone.0238683

Cook, A. R., Zhao, X., Chen, M. I., & Finkelstein, E. A. (2018). Public preferences for interventions to prevent emerging infectious disease threats: A discrete choice experiment. *BMJ Open*, *8*, 1-12. doi: 10.1136/bmjopen-2017-017355

Copeland, B., Shapiro, J., & Taylor, S. (1994). North-south Trade and the Environment. *The Quarterly Journal of Economics*, *3*(109), 755-87.

Copeland, B., Shapiro, J., & Taylor, S. (2021). Globalization and the Environment. *NBER Working Papers*(28797).

Currie, J., Davis, L., Greenstone, M., & Walker, R. (2015). Environmental health risks and housing values: Evidence from 1,600 toxic plant openings and closings. *American Economic Review*, *105*(2), 678-709.

Currie, J., Greenstone, M., & Moretti, E. (2011). Superfund cleanups and infant health. *American Economic Review*, *101*(3), 435-41.

Currie, J., & Moretti, E. (2007). Biology as destiny? short-and long-run determinants of intergenerational transmission of birth weight. *Journal of Labor Economics*, *25*(2), 231-64.

Currie, J., & Neidell, M. (2007). Getting inside the 'black box' of head start quality: What matters and what doesn't. *Economics of Education Review*, *26*(1), 83-99.

Currie, J., Voorheis, J., & Walker, R. (2023). What Caused Racial Disparities in Particulate Exposure to Fall? New Evidence from the Clean Air Act and Satellite-Based Measures of Air Quality. *American Economic Review*, *113*, 71-97.

Currie, J., & Walker, R. (2011). Traffic congestion and infant health: Evidence from e-zpass. *American Economic Journal: Applied Economics*, *3*(1), 65-90.

Depro, B., Timmins, C., & O'Neil, M. (2011). Hazardous Waste Cleanup, Neighborhood Gentrification, and Environmental Justice: Evidence from Restricted Access Census Block Data. *American Economic Review*, *101*(3), 620-24.

Depro, B., Timmins, C., & O'Neil, M. (2015). White Flight and Coming to the Nuisance: Can Residential Mobility Explain Environmental Injustice? *Journal of the Association of Environmental and Resource Economists*, *2*(3), 439-468.

Dorantes, C. A., Kaushal, N., & Muchow, A. N. (2020). Is the Cure Worse than the Disease? County-Level Evidence from the COVID-19 Pandemic in the United States. *NBER Working Paper No. 27759*, 1-35. Retrieved from `https://www.nber.org/papers/w27759` doi: 10.3386/w27759

Echazu, L., & Nocetti, D. C. (2020). Willingness to pay for morbidity and mortality risk reductions during an epidemic. Theory and preliminary evidence from COVID-19. *GENEVA Risk and Insurance Review*, *45*(2), 114–133. doi: 10.1057/s10713-020-00053-0

Figlio, D., Guryan, J., Karbownik, K., & Roth, J. (2014). The effects of poor neonatal health on children's cognitive development. *American Economic Review*, *104*(12), 3921-55.

GAO. (1983). Siting of Hazardous Waste Landfills and their Correlation with Racial and Economic Status of Surrounding Communities. *Washington, DC: General Accounting Office (GAO)*.

Greenstone, M. (2002). The Impacts of Environmental Regulations on Industrial Activity: Evidence from the 1970 and 1977 Clean Air Act Amendments and the Census of Manufactures. *Journal of Political Economy*, *6*(110), 1175-1219.

Greenstone, M., He, G., Li, S., & Zou, E. (2021). China's War on Pollution: Evidence from the First Five Years. *Review of Environmental Economics and Policy*, *2*(15), 281-299.

Gregson, N., & Crang, M. (2015). From waste to resource: The trade in wastes and global recycling economies. *Annual Review of Environment and Resources*, *1*(40), 151-176.

Henderson, V. J. (1996). Effects of Air Quality Regulation. *American Economic Review*, *4*(84), 789-813.

Hernandez-Cortes, D., & Meng, K. C. (2020). Do Environmental Markets Cause Environmental Injustice? Evidence from California's Carbon Market. *NBER Working Paper*(27205).

Higashida, K., & Managi, S. (2014). Determinants of Trade in Recyclable Wastes: Evidence from Commodity-based Trade of Waste and Scrap. *Environment and Development Economics*, *19*(2), 250-270.

Hipp, J. R., & Lakon, C. M. (2010). Bringing Satellite-Based Air Quality Estimates Down to Earth. *Health and Place*, *16*, 674-683.

Ho, P. (2023). The Costs and Environmental Justice Concerns of NIMBY in Solid Waste Disposal. *Journal of the Association of Environmental and Resource Economists*, *3*(10), 607-654.

Hoek, G., Krishnan, R. M., Beelen, R., Peters, A., Ostro, B., Brunekreef, B., & Kaufman, J. D. (2013). Long-term air pollution exposure and cardio-respiratory mortality: A review. *Environmental Health*, *12*(43).

Johnston, R. J., Boyle, K. J., Vic Adamowicz, W., Bennett, J., Brouwer, R., Ann Cameron, T., Michael Hanemann, W., Hanley, N., Ryan, M., Scarpa, R., Tourangeau, R., & Vossler, C. A. (2017). Contemporary guidance for stated preference studies. *Journal of the Association of Environmental and Resource Economists*, *4*(2), 319–405. doi: 10.1086/691697

Kellenberg, D. (2012). Trading Wastes. *Journal of Environmental Economics and Management*, *1*(64), 68-87.

Kellenberg, D. (2015). The Economics of the International Trade of Waste. *Annual Review of Resource Economics*, *1*(7), 109-125.

Kinnaman, T. C. (2014). Effects of Norms and Opportunity Cost of Time on Household Recycling. *Resources, Conservation and Recycling*, *85*, 5–10.

Kinnaman, T. C., Shinkuma, T., & Yamamoto, M. (2014). The Socially Optimal Recycling Rate: Evidence from Japan. *Journal of Environmental Economics and Management*, *68*, 54–70.

Lee, J., Wei, S.-J., & Xu, J. (2020). The welfare Cost of a Current Account Imbalance: A "Clean" Effect. *Research Collection School Of Economics*, 1-57.

Li, J., & Takeuchi, K. (2021). Import Ban and Clean Air: Estimating the Effect of China's Waste Import Ban on the Ozone Pollution. *Kobe University Discussion Paper*.

Li, L., Long, D., & Rad, M. R. (2020). Stay-at-Home Orders and the Willingness to Stay Home During the COVID-19 Pandemic: A Stated-Preference Discrete Choice Experiment. *SSRN*.

Lincoln, K. D., Abdou, C. M., & Lloyd, D. (2014). Race and socioeconomic differences in obesity and depression among black and non-hispanic White Americans. *Journal of Health Care for the Poor and Underserved*, *25*(1), 257–275. doi: 10.1353/hpu.2014.0038

Lindhjelm, H., & Navrud, S. (2008). How Reliable Are Meta-Analyses for International Benefit Transfer? *Ecological Economics*, *66*, 425-435. doi: 10.1016/j.ecolecon.2007.10.005

Miles, D., Stedman, M., & Heald, A. (2020). LIVING with COVID-19: BALANCING COSTS against BENEFITS in the FACE of the VIRUS. *National Institute Economic Review*, *253*, 60-76. doi: 10.1017/nie.2020.30

Morehouse, J., & Rubin, E. (2021). Downwind and out: The Strategic Dispersion of Power Plants and their Pollution. *Working paper*.

Mühlbacher, A., & Johnson, R. F. (2016). Choice Experiments to Quantify Preferences for Health and Healthcare: State of the Practice. *Applied Health Economics and Health Policy*, *14*, 253-266. doi: 10.1007/s40258-016-0232-7

Olivia, G. (2014). Determinants of European Fright Rates: The Role of Market Power and Trade Imbalance. *Transportation Research Part E: Logistics and Transportation Review*(62), 23-33.

Oreopoulos, P., Stabile, M., Walld, R., & Roos, L. L. (2008). Short-, medium-, and long-term consequences of poor infant health, an analysis using siblings and twins. *Journal of Human Resources*, *43*(1), 88-138.

Pais, J., Crowder, K., & Downey, L. (2013). Unequal Trajectories: Racial and Class Differ- ences in Residential Exposure to Industrial Hazard. *Social Forces*, *92*, 1189-1215.

Palma, A., Lindsey, R., Quinet, E., & Vickerman, R. (2011). China's Embrace of Globalization. *A Handbook of Transport Economics*.

164

Persico, C., Figlio, D., & Roth, J. (2016). Inequality before birth: The developmental consequences of environmental toxicants. *NBER Working Paper*, *22263*.

Price, J., Dupont, D., & Adamowicz, W. (2017). Willingness to accept tradeoffs among Covid-19 cases, social-distancing restrictions, and economic impact: A nationwide US study. *Environmental and Resource Economics*, *68*, 643-662. doi: 10.1007/s10640-016-0039-x

Ready, R., & Navrud, S. (2006). International benefit transfer: Methods and validity tests. *Ecological Economics*, *60*, 429-434. doi: 10.1016/j.ecolecon.2006.05.008

Reed, S., Gonzalez, J. M., & Johnson, F. R. (2020). Willingness to accept tradeoffs among Covid-19 cases, social-distancing restrictions, and economic impact: A nationwide US study. *medRxiv*, *11*, 1438-1443. doi: 10.1101/2020.06.01.20119180

Rees-Jones, A., Attoma, J., Piolatto, A., & Salvadori, L. (2020). COVID-19 Changed Tastes for Safety-Net Programs. *NBER Working Paper No. 27865*, 1-20. Retrieved from `http://www.nber.org/papers/w27865.pdf`

Repa, E. W. (2005). Interstate movement of municipal solid waste. bulletin report. *National Solid Waste Management Association.*.

Richardson, L., Loomis, J., Kroeger, T., & Casey, F. (2015). The role of benefit transfer in ecosystem service valuation. *Ecological Economics*, *115*, 51-58. doi: 10.1016/j.ecolecon.2014.02.018

Royer, S., Ferron, S., Wilson, S., & Karl, D. (2018). Production of Methane and Ethylene from Plastic in the Environment. *PLOS ONE*.

Sanders, N. J. (2012). What doesn't kill you makes you weaker: Prenatal pollution exposure and educational outcomes. *Journal of Human Resources*, *47*(3), 826-50.

Schlenker, W., & Walker, R. W. (2016). Airports, air pollution, and contemporaneous health. *Review of Economic Studies*, *83*(2), 768-809.

Shapiro, J. S. (2016). Trade Costs, CO2, and the Environment. *American Economic Journal: Economic Policy*, *8*(4), 220-54.

Shapiro, J. S. (2021). The Environmental Bias of Trade Policy. *Quarterly Journal of Economics*, *136*(2), 831-886.

Shapiro, J. S., & Walker, R. (2021). Where is Pollution Moving? Environmental Markets and Environmental Justice. *AEA Papers and Proceedings*, *111*, 410-14.

Shapiro, R., Joseph S.and Walker. (2018). Why is Pollution from U.S. Manufacturing Declining? The Roles of Environmental Regulation, Productivity, and Trade. *American Economic Review*, *108*(12), 3814-54.

Smith, V. K., Van Houtven, G., & Pattanayak, S. K. (2002). Benefit transfer via preference calibration: "Prudential Algebra" for policy. *Land Economics*, *78*, 132-152. doi: 10.1007/s10640-016-0039-x

Tanaka, S., Teshima, K., & Verhoogen, E. (2021). North-South Displacement Effects of Environmental Regulation: The Case of Battery Recycling. *American Economics Journal: Insights (Forthcoming)*.

Unfried, K., & Wang, F. (2022). Importing Air Pollution? Evidence from China's Plastic Waste Import. *IZA Institute of Labor Economics*(15218).

Viscusi, W. K. (2020). Pricing the global health risks of the COVID-19 pandemic. *Journal of Risk and Uncertainty*, *61*, 101-128. doi: 10.1007/s11166-020-09337-2

Wong, W. (2021). The Round Trip Effect: Endogenous Transport Costs and International Trade. *American Economics Journal: Applied Economics (Forthcoming)*.

Yancy, C. W. (2020). COVID-19 and African Americans. *JAMA - Journal of the American Medical Association*, *323*(19), 1891–1892. doi: 10.1001/jama.2020.6548